

The Islamic University – Gaza
Higher Education Deanship
Faculty of Engineering
Civil Engineering Department
Infrastructure



الجامعة الإسلامية- غزة
عمادة الدراسات العليا
كلية الهندسة-قسم مدني
البنى التحتية

Evaluation of Ground Movement and Pressure Distribution at Gabion Retaining Wall by Field Testing

Rafiq M. Abed

Supervised by

Professor Dr. Mohamed Awad

**A Thesis Submitted in Partial Fulfillment of the Requirements for the
Degree of Master in Infrastructure**

محرم 1425- مارس 2004

March 2004

ACKNOWLEDGEMENTS

The author expresses his special thanks, gratitude and appreciation to his supervisor Professor Dr. Mohamed Awad for his efforts, encouragement and advice, which were extended to him during the course of this study.

Special thanks for the Special Environmental Health Programme's staff for their support and assistance during carrying out the experiments. High appreciation and gratitude are extended particularly to the supervisory team of Beach Camp Shore Protection Project as well as the staff helped in typing, organizing and finalizing the Thesis document.

The author extends his gratitude to Dr. Jihad Hamad and Dr. Mamoun El Qidra for their encouragement and follow up during the study. Many thanks for the Material Testing Laboratory staff at the Islamic University, headed by Mr. Ahmad El Kurd, for their cooperation during the study.

ABSTRACT

The classical theoretical assumption of Rankine's or Coulomb's theory has been widely used for retaining wall analysis. Although the assumption is based on sufficient lateral movement that should take place to mobilize fully active conditions behind the wall, the effects of deformation parameters of backfill, wall flexibility and other construction conditions, were not taken into consideration.

This case study describes the results from an experimental program where the factors affecting the behavior of gabion retaining wall, constructed within Beach Camp Shore Protection Project, have been investigated. The analyses show that the wall and soil movements have considerable effects on prediction of lateral earth pressures.

Based on the experimental results, the coefficient of earth pressure K is determined for a practical design. The tests were carried out on three different conditions of the backfill sand behind a gabion retaining wall, loose, medium and dense cases. A comparison with previous methods is presented in our case study. It was difficult to compare the actual results obtained in both medium and dense cases with the theoretical assumptions since the active condition has not been reached in these two cases. However, this comparison could be made successfully in the loose case where the active condition has been reached. The displacement was within the limited theoretical values to create an active condition.

According to the results achieved, it is clear that the value of Rankine coefficient of earth pressure K is overestimated compared with the K value computed from actual results of earth pressure.

Key words: active earth pressure; surcharge; inclined surface slope, coefficient of earth pressures K , pressure cells, deformation meter.

بسم الله الرحمن الرحيم

المخلص

دراسة موقعية لتأثير الضغوط والحركات الأفقية على الحائط الاستنادي الصخري

ما زالت الفرضيات النظرية القديمة لكل من رانكن و كولومب تستخدم بشكل واسع في جميع انحاء العالم وعلى الرغم ان الفرضيات مبنية على أساس حركة جانبية للحائط الساند الى الخارج تكفي لتوليد حالة من الضغط الجانبي إلا ان تأثير عوامل التشكل للردم خلف الحائط، ومرونة الحائط نفسه بالإضافة الى عوامل اخرى مثل الظروف المحيطة بالإنشاء لم تأخذ في الاعتبار.

إن هذه الحالة الدراسية تصف نتائج تم الحصول عليها من برنامج تجارب تم تنفيذه على حائط صخري استنادي في مشروع حماية الشاطئ المقابل لمعسكر الشاطئ. لقد تمت دراسة العوامل المؤثرة على تصرف الحائط الاستنادي الصخري. ولقد دلت نتائج تحليل التجارب ان حركة الحائط الاستنادي والتربة خلف الحائط لها تأثير ملحوظ على حساب الضغط الجانبي للتربة.

لقد تم تعيين معامل ضغط التربة (K) للتصميم العملي من التجارب، حيث تم عمل التجارب على ثلاث حالات مختلفة لتربة الرمل خلف الحائط الاستنادي الصخري وهي الحالة السائبة والمتوسطة الدمك والحالة المدموكة جيدا. لقد تم عمل مقارنة بين هذه الحالات والطرق السابق دراستها، من هذه المقارنة تم استنتاج ان المقارنة كانت صعبة بين النتائج الفعلية في حالي المتوسطة الدمك والمدموكة جيدا مع الفرضيات النظرية وذلك لعدم التمكن من الوصول لحالة حركة الحائط الاستنادي للخارج ($Active$) في كلتا الحالتين ولكن هذه المقارنة يمكن عملها بنجاح في الحالة السائبة للرمل خلف الحائط الاستنادي حيث تم حصول حركة الحائط الاستنادي للخارج ($Active$). ولقد كانت قيمة حركة الحائط في حدود القيمة المنصوص عليها في النظريات السابقة لحصول الحركة للخارج.

بناء على التجارب التي تم تحقيقها فإن قيمة معامل رانكن (K) كانت قيمة أكبر من القيمة التي تم حسابها من نتائج ضغط التربة حيث كانت قيمة رانكن مبالغ فيها.

TABLE OF CONTENTS

Chapter 1	1
Introduction	1
1.1 Background	1
1.2 General Objective	2
1.3 Specific Objectives	2
1.4 Methodology of the Research.....	3
Chapter 2	4
Literature Review	4
2.1 Background	4
2.2 Gabions, Description and Use.....	4
2.3 Gabions Advantages	6
2.4 Lateral Earth Pressures.....	7
2.4.1 Surcharge Applied on Ground Surface.....	10
2.4.2 Coefficient of Lateral Earth Pressures (K)	10
Chapter 3	16
Tests Description and Procedures	16
3.1 General.....	16
3.2 Instruments Used in the Experiments	16
3.2.1 <i>Vibrating Wire Earth Pressure Cell (Model 4810)</i>	16
3.2.1.1 Applications	16
3.2.1.2 Operating Principle.....	17
3.2.1.3 Advantages & Limitations	17
3.2.1.4 Technical Specifications	19
3.2.1.5 Theory of Operation	20
3.2.1.6 Earth Pressure Cell Design	22
3.2.1.7 Earth Pressure Cell Construction.....	23
3.2.1.8 Preliminary Tests.....	25
3.2.1.9 Earth Pressure Cell Installation.....	26
3.2.1.10 Cable Installation.....	28
3.2.1.11 Electrical Noise	28
3.2.1.12 Initial Readings.....	28
3.2.1.13 Taking Readings, Operation of the GK-401 Readout Box	29
3.2.1.14 Data Reduction	30
3.2.1.15 Calibration.....	32
3.2.1.16 Earth Pressure Cells Specifications.....	32
3.2.2 <i>Vibrating Wire Deformation Meter (Model 4430)</i>	34
3.2.2.1 Applications	34
3.2.2.2 Operating Principle.....	34
3.2.2.3 Advantages and Limitations	35
3.2.2.4 Model 4430 Deformation Meter	35
3.2.2.5 Technical Specifications	36
3.2.2.6 Theory of Operation	36
3.2.2.7 Preliminary Tests.....	37
3.2.2.8 Deformation Meter Installation in Fills & Embankments	37
3.2.2.9 Cable Protection and Termination.....	39
3.2.2.10 Initial Readings.....	39

3.2.2.11	Electrical Noise	40
3.1.3.12	Taking Readings, Operation of the GK-401 Readout Box	40
3.2.3.13	Deformation Calculation.....	40
3.2.2.14	Temperature Correction.....	41
3.2.2.15	Environmental Factors	43
3.2.2.16	Specifications	43
3.2.3	<i>Vibrating Wire Readout (Model GK-401)</i>	44
3.2.3.1	Applications	44
3.2.3.2	Operating Principle.....	44
3.2.3.3	Advantages and Limitations	45
3.2.3.4	Technical Specifications	45
3.2.3.5	Theory of Operation	45
3.2.3.6	Taking Readings.....	46
3.2.3.7	Data Reduction	46
3.2.3.8	Maintenance and Trouble Shooting	47
3.2.3.9	Readout System.....	47
3.2.3.10	Specifications	48
3.2.3.11	Reading Other Manufactures Instruments.....	48
3.3	Field Testing Programme	49
3.3.1	<i>Method of Project Construction</i>	49
3.3.2	<i>Site Preparation for Tests</i>	50
3.3.3	<i>Test Procedures:</i>	50
3.3.3.1	For Loose Case:.....	50
3.3.3.2	For Medium Case	52
3.3.3.3	For Dense Case	52
3.3.3.4	Other Tests	52
Chapter 4	57
Test Results	57
4.1	Introduction	57
4.2	Soil Investigation Results during Design Stage.....	57
4.3	Backfill Sand Test Results During Construction Stage	58
4.4	Rocks Test Results during Construction Stage.....	58
4.4.1	<i>Stone Fill Material in Apron</i>	59
4.4.2	<i>Stone Fill Material in Gaboin Boxes</i>	60
4.5	Test Results of Base Course Filter for Apron	61
4.6	Test Results of Base Course Surface Apron	61
4.7	Test Results of Geotextile Material during Construction Stage.....	61
4.8	Test Results of Experimental Case Study	61
4.8.1	<i>Backfill Sand Results</i>	61
4.8.2	<i>Lateral Earth Pressure Results</i>	62
4.8.2.1	Results of Loose case experiment, Tests No.1	62
4.8.2.2	Results of all Tests.....	65
Chapter 5	69
Data Analysis and Discussion	69
5.1	Introduction	69
5.2	Measured Vertical and Horizontal Pressures.....	69
5.3	Additional Lateral Earth Pressures.....	70
5.4	Coefficient of Earth Pressure (K)	74

5.5 Displacement Analysis	77
5.6 Comparison between Coulomb and Measured Value of k	79
Chapter 6	81
Conclusions and Recommendations	81
6.1 General Conclusions	81
6.2 Conclusions Related to Beach Camp Shore Protection Project	81
6.3 Recommendations	82
LIST OF REFERENCES.....	83
APPENDICES	85

Appendix A	Lateral Earth Pressure Results
Appendix B	Sand Laboratory Test Results, Field Study
Appendix C	Instruments Calibration Certificates
Appendix D	Experiments Photos
Appendix E	Photos of Equipment used in Geotextile Tests
Appendix F	Project Implementation Photos

LIST OF FIGURES

<u>Figure</u>		<u>Page No.</u>
Figure 1.1	Location of Beach Camp Shore Protection Project	1
Figure 2.1	Gabion Mattress Channel Lining	5
Figure 2.2	Gabion Walls for Flood Control and Bank Protection	5
Figure 2.3	Rankine Earth Pressures	9
Figure 2.4	Earth Pressure Evaluation	11
Figure 2.5	Value of Earth Pressure Coefficient $K_{a,\gamma,q}$ versus the Dimensionless Parameter λ	15
Figure 2.6	Limits of Boundary Conditions	15
Figure 3.1	Model 4810 Earth Pressure Cell and Contact Pressure Cell	17
Figure 3.2	Model 4800 Earth Pressure Cells installed in fill for soil pressure measurement in three directions.	18
Figure 3.3	Modified Pressure Cell, with two thick plates, for use in granular materials.	19
Figure 3.4	Stress Redistribution, weak soil with stiff cell	21
Figure 3.5	Stress Redistribution, strong soil with stiff cell	21
Figure 3.6	Stress Redistribution, stiff soil with weak cell	21
Figure 3.7	Model 4800 Rectangular Earth Pressure Cell	23
Figure 3.8	Model 4800 Circular Earth Pressure Cell	24
Figure 3.9	Model 4810 Contact Pressure Cell	24
Figure 3.10	Model 4820 Jack-Out Pressure Cell	25
Figure 3.11	Attachment of Model 4810 to Concrete Form	26
Figure 3.12	Model 4810 Contact Pressure Cell Installation	27
Figure 3.13	Sample Model 4810 calibration sheet	33
Figure 3.14	Three models of 4400 series Deformation Meters	34
Figure 3.15	Model 4430 Deformation Meter	35
Figure 3.16	Model 4430 Deformation Meter, detailed view	37
Figure 3.17	Installation Along Crest of Dam	38
Figure 3.18	Borehole Installation in Embankment	39

<u>Figure</u>		<u>Page No.</u>
Figure 3.19	Model GK-401 Vibrating Wire Readout Box	44
Figure 3.20	Gabion Wall Cross Section (General View)	55
Figure 3.21	Position of Devices	56
Figure 4.1	Horizontal Earth Pressure versus Depth	63
Figure 4.2	Vertical Earth Pressure versus Depth	64
Figure 4.3	Values of Earth Pressure Coefficient (k) versus Depth	64
Figure 5.1	Depth versus Vertical Pressure for Horizontal Soil Surface	70
Figure 5.2	Depth versus Horizontal Pressure for Horizontal Soil Surface	71
Figure 5.3	Depth versus Increment of Horizontal Pressure due to Soil Surface Inclinations (Dense Case)	71
Figure 5.4	Depth versus Loading Increment at 25 cm from the Gabion Face (Loose Case)	72
Figure 5.5	Depth versus Increment Load due to Square footing at 25 cm (Medium Sand Filling)	72
Figure 5.6	Depth versus Increment Loading (25 cm, Dens Case)	73
Figure 5.7	Depth versus Pressure Increment due to 6 kPa Loading at Different Surface Distances (Loose Case)	74
Figure 5.8	Depth versus Increment Load due to 6 kPa with Different Surface Distances (Medium Case)	75
Figure 5.9	Depth versus Increment Load due to 6 kPa with Different Surface Distances (Dense Case)	75
Figure 5.10	Depth versus Increment due to 12 kPa Loading at Different Surface Distances (Loose Case)	76
Figure 5.11	Depth versus Horizontal Increment due to 12 kPa, (Medium Case)	76
Figure 5.12	Earth Pressure Coefficients versus Depth for three Sand Cases	77
Figure 5.13	Comparison between the Measured and Calculated K Values	78
Figure 5.14	K versus Internal Friction Angle	78
Figure 5.15	Measured Deformation versus Depth (Loose Case)	79
Figure E-1	Preparation of Geotextile Sample in the Laboratory	E-1
Figure E-2	Geotextile Testing of Tensile Strength	E-1
Figure E-3	Geotextile Sample Before Failure	E-2
Figure E-4	Geotextile CBR Static Puncture Test	E-2

LIST OF TABLES

<u>Table</u>		<u>Page No.</u>
Table 3-1	Technical Specifications of Vibrating Wire Earth pressure Cell	19
Table 3-2	Earth Pressure Cell Specifications	22
Table 3-3	GK-401 Display Position vs. Geokon Model Number	29
Table 3-4	Engineering Units Multiplication Factors	30
Table 3-5	Technical Specifications of Vibration Wire Deformation Meter	36
Table 3-6	Engineering Units Conversion Multipliers	41
Table 3-7	Thermal Coefficient Calculation Constants	42
Table 3-8	Model 4430 Specifications	43
Table 3-9	Technical Specifications of Vibrating Wire Readout Box	45
Table 3-10	GK-401 Readout Box Specifications	48
Table 3-11	Vibrating Wire Length vs. Frequency Range	49
Table 3-12	Placement of Devices at different levels believed the gabion wall	53
Table 4-1	Test Results of Backfill Sand During Experiments	62
Table 4-2	Lateral Earth Pressure, K value and Deformation for Loose Case	63
Table 4-3	Lateral Earth Pressure K value and Deformation, All Cases	65
Table 5-1	Summary of Safe Horizontal Distance (d) in (m)	73
Table 5-2	Motta Quantities and the Author Verification	79
Table 5-3	Calculated Coulomb K_a values using Motta Procedures for Sand Loose Case	80
Table 5-4	Calculated Coulomb K_a Versus Motta Procedures for Sand Medium Case	80
Table 5-5	Calculated Coulomb K_a values using Motta Procedures for Sand Dense Case	80

LIST OF ABBREVIATIONS

AC	Alternative Current (Electricity)
ASCE	American Society of Civil Engineers
ASTM	American Society for Testing and Materials
BS	British Standards
GLE	General Limit Equilibrium
f	Frequency = $\frac{1}{\text{period (Second)}}$
Hz	Hertz (Frequency Unit)
IECA	International Erosion Control Association
ISO	International Organization for Standardization
K	Earth Pressure Coefficient
K_a	Active Earth Pressure Coefficient
K_p	Passive Earth Pressure Coefficient
LCD	Liquid Crystal Display
MSL	Mean Sea Level
SEHP	Special Environmental Health Programme
UNRWA	United Nations Relief and Works Agency For Palestine Refugees
VS	Versus
W	Weight of the Failure Wedge
W_t	Total Weight of Soil Mass and Surcharge
S_a	Active Earth Pressure
β	Contact Angle between the Back Face of the Wall with the Soil
γ	Bulk Unit Weight of Soil
q	Uniformly Distributed Load (Surcharge)
C	Cohesion
φ	Angle of Internal Friction
f	Soil-to-Soil Friction Coefficient
δ	Soil Wall Friction Angle
AWG	American Wire Gauge (System)
μ	Micro (μ second = 0.001 second)

Chapter 1

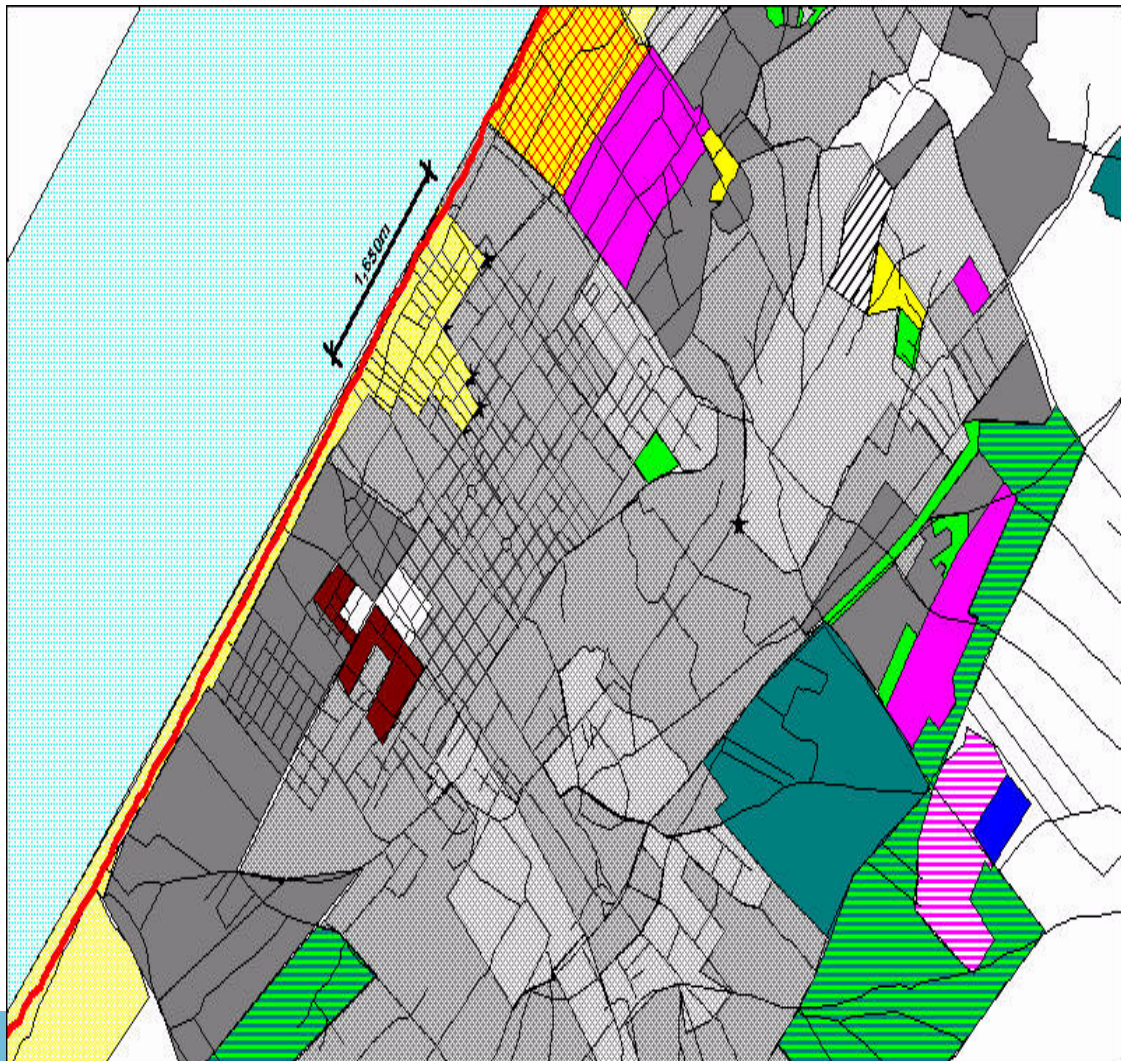
Introduction

1.1 Background

Gabions and mattresses are wire baskets filled with rocks and wired together to form a retaining wall or lining. They are fastened together and used for retaining walls, revetments, slope protection, bank protection, channel linings and other structures.

Basic infrastructure has been provided by UNRWA for the Beach Camp, a refugee camp in the northern part of Gaza City. Both on-land and along the coastline, amongst others, a coastal road and drainage and sewerage systems were implemented. The facilities near the coastline are particularly exposed to hydraulic and morphological actions and threat of the sea. In order to protect these facilities UNRWA sought funding to construct the Shore Protection Project at Beach Camp. The project area stretches all along the shoreline of the camp with a total length of approximately 1,650 m as shown in figure (1) below.

Figure 1.1 – Location of Beach Camp Shore Protection Project



The project consists of two major components, construction of a gabion retaining wall and construction of groynes inside the sea. Construction of the gabion retaining wall, the component which has been completed recently, provides protection for the cliff against erosion over the length as shown in figure (1) above. The other component will be implemented at later stage when comprehensive and integrated shore development being realized. In general, gabion construction could be a versatile construction technique for the civil engineer, with good design, quality materials, high standard of work quality and proper supervision. An increasing number of gabion retaining walls have been constructed, recently in Gaza strip.

A considerable attention has been given to developing efficient methods for prediction of pressure distribution behind the gabion retaining wall. However, a major problem is that determining the coefficient of lateral earth pressure (K) related to gabions movement is difficult since it depends on the quality of stones and the way of handling. The engineer, therefore, has to develop designs which take account of the likelihood of rather poor quality stones in order to keep the gabion retaining wall in a safe position. The gabion retaining wall as a semi- flexible element will be affected by movement as a result of several external forces.

1.2 General Objective

The main goal of this study is to evaluate the lateral earth pressures and movement of the gabion retaining wall and to estimate the coefficient of lateral earth pressure (K).

1.3 Specific Objectives

- To specify theoretically the type of forces affecting the gabions whether active, passive or at rest.
- To measure earth pressure and movement of the gabion retaining wall through devices, such as strain gauges, load cells or other alternative devices.
- To determine the coefficient of lateral earth pressure (K).
- To determine effect of the adjacent structures, such as buildings or the coastal road on pressure distribution and movement of the gabion retaining wall.

The above mentioned gabion retaining wall at Beach Camp has been taken as a case study to measure the lateral forces affecting the wall and the coefficient of lateral earth pressure K. This will enable us checking the stability of the wall. A comparison has been made between the estimated K and the value obtained

from experimental tests. The study described the results of testing of the construction materials used and method of construction of the gabion retaining wall because the type of materials and method of construction have an effect on the resistance and sustainability of the gabion retaining wall.

1.4 Methodology of the Research

Previous studies, though they are limited has been reviewed with emphasis on lateral earth pressure and coefficient of lateral earth pressure(K) for gabion retaining wall; the specifications of the existing soil surrounding the gabions as well as gabion contents were defined through laboratory tests; method of construction of the gabion wall was described, certain points within the project area were selected to fix the required measuring devices; readings for pressure and movement at different levels; analysis of these readings and results were carried out; summary of the research including conclusions and recommendations for future studies were described.

Chapter 2

Literature Review

2.1 Background

Soil erosion is an ever present problem and gabions have proved to be the best solution around the world. The earliest known use of gabion- type structures was for bank protection along the Nile River during the era of the Pharaoh. (C. E. Shepherd company Lp.)

The gabions initially used by the Egyptians about 7,000 years ago. The gabion system has developed from baskets of woven reeds to engineered containers manufactured from wire mesh. The most important and last appeal of gabions lies in their inherent flexibility. Gabion structures are flexible when subjected to earth movements but they maintain high efficiency and remain structurally sound. (C. E. Shepherd company Lp.)

Gabions have been used largely in Europe over the last 100 years. Today, gabions are used more frequently for stopping erosion and in lining of channels especially in streams running through parks in urban areas. (Burroughs, 1979)

2.2 Gabions, Description and Use

Gabions are used in channel lining and bank protection, as shown in Figure 2.1 and 2.2, because they are economical, permeable and flexible. The widely used dimensions of a gabion are 1 m high x 1m deep x (1 to 4 m) long. Individual units are wired together to form larger structures. The dimensions of meshes wire is 2 to 3 mm diameter, with opening from 60 to 100 mm. The meshes may be galvanized or coated with (PVC) for the purpose of protection against corrosion in marine environment. (Burroughs, 1979; Hausmann, 1990; IECA, 2004)



Figure 2.1: Gabion Mattress Channel Lining



Figure 2.2: Gabion Walls for Flood Control and Bank Protection

Gabion is defined as a corrosion resistant wire container filled with stone used for structural purposes. The material filling the meshes consists of durable rock fragments or river cobbles, larger than the mesh size but not exceeding half the depth of the individual basket to produce a neat front of the structure. In order to minimize deformation during construction, meshes should be stretched or tensioned prior to filling with rocks. (Hausmann, 1990).

To reduce the danger of washing out of soil particles through rock fill, a filter layer, a geotextile material for example, is fixed between the gabions and the adjacent backfill as well as between the foundation of the gabion wall and gabions. (Haskoning, 1998).

2.3 Gabions Advantages

Gabions and mattresses are widely used as erosion-resistant lining and for building gravity structures. They have many advantages, such as flexibility where gabions conform to difficult site geometry and can adjust to lateral movement; permeability where gabions prevent the creation of water pressure; high capacity drainage system could be constructed easily; low level of work skill is required; unskilled labor could be trained quickly and easily; low cost of transportation where local rock fill can be used; easy and quick construction could be achieved. (Hausmann, 1990)

Gabions are unlike rigid or semi-rigid structures which may be exposed to failure when slight changes occur in their foundations. Gabions form a semi-flexible retaining gravity structure where rocks retain the fill behind this structure. Slight deformations are possible and allowable due to external influences. The purpose of this type of structure is to avoid damage due to its flexibility; it will rearrange itself to the new position without a significant damage. Highly permeable, the gabion structures act as self-draining units which pass the ground waters, relieving hydrostatic heads and the spaces in the rock fill dissipate the energy of wave action and flood currents. By itself a gabion structure offers a good, clear and tidy look in its environment. Without loss of its functional requirements, gabions can be formed and integrated with existing structures. (Haskoning, 1998)

During heavy storm conditions the gabions may be attacked by waves. Therefore, the designer should take into consideration that the top level of the gabion wall should be chosen at a level that the slope will not be affected by splash of sea waves attacking the toe-line. The height of gabion wall should be more than any expected wave height, so gabions may be affected alone and the structure above the first gabion level will be safe against wave attack and splash. (Haskoning, 1998)

Gabion efficiency, rather than decreasing with age, actually increases. After construction, silt and vegetation together with the rock fill form a naturally

permanent structure as shown in Figure 2.1 and may be used to remove solid pollutants or floatable from the water. They are stable product which assembles quickly and easily. (Maccaferri company, UK)

The gabions solution for various problems controls and stops erosion without encroaching on private property. It also eliminates the safety hazards, and visually is pleasing in addition to low cost and easy construction of the gabion structures. (Burroughs, 1979)

2.4 Lateral Earth Pressures

Lateral earth pressure problems are of high importance and great interest in geotechnical engineering. In many earth retaining problems, it is necessary to study the exact distribution of the earth pressure behind the retaining wall. Many researchers have studied this distribution using laboratory and field experimental studies. (Motta, 1994)

Knowledge of lateral earth pressures is very crucial to design a retaining wall. The lateral earth pressures are the pressures developed by the backfill retained by the wall. Several soil parameters should be known by the designer in order to assess the wall design and its overall stability. Among others, these parameters are:

- angle of internal friction;
- soil unit weight;
- water table location; and
- cohesion and plasticity indices for cohesive soils such as clayey soil.

Once the lateral earth pressures are determined, the wall is checked against stability which includes checks for overturning, base sliding and soil bearing capacity failures. Failure of the retaining wall is attributed mainly, among other reasons, to improper design and construction. Therefore, understanding of how a wall works and how it can fail, it is possible for engineer to design a retaining structure that meets all environmental, structural and construction requirements. (Concrete network, 2003)

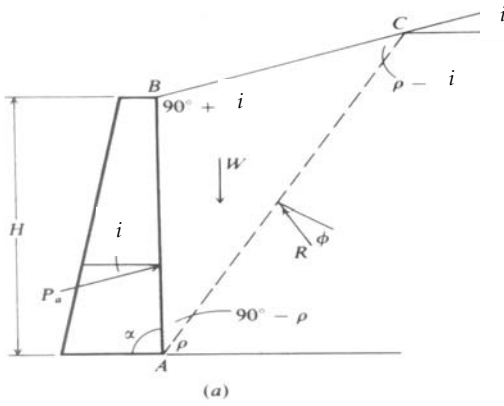
The theoretical formulations of Coulomb (1776) and Rankine (1857) are still the fundamental approaches to the analysis of majority of gravity- type retaining walls. These conventional design methods as well as other ones, assume that adequate lateral displacement will occur to create fully active condition behind the retaining wall. Despite the researches conducted on this subject, there is almost no trustful information on the validity of assuming active earth pressure conditions in the field. (Goh, 1993)

Conventional design methods take no account of the deformation parameters of the backfill or foundation subsoil or the method of construction. These methods also ignore the influence of wall flexibility and interaction between materials. Many of these factors are taken into consideration in detailed studies using theory of mechanics or the finite element method. The finite element method used by Goh, 1993 has the advantage of being able to provide predictions of stresses and displacements under working load conditions, where limit equilibrium solutions generally provide information related to the ultimate failure condition. (Goh, 1993)

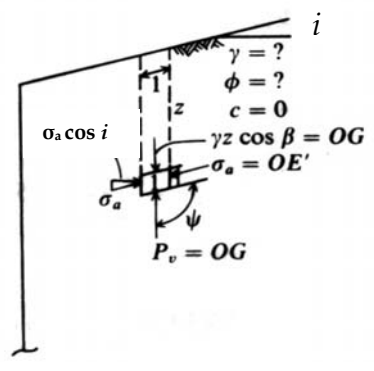
The recent developments in calculating the lateral earth pressures involve the use of methods of slices and limit equilibrium concept. Zaker Zadeh et al, 1999 used the force equilibrium solution of the general limit equilibrium (GLE) to compute the active and passive earth pressures. The most important issue taken in this solution is the selection of a proper interslice force function that the normal and shear stresses between the slices of the sliding mass. (Zaker Zadeh et al, 1999)

Coulomb's theory (1776) is one of the earliest methods for computing earth pressures against walls. The main assumptions of this theory, among others, include: the soil should be isotropic; homogeneous; has internal friction and cohesion; the rupture surface is a plane surface; the friction resistance is uniformly distributed along the rupture surface; there is wall friction, i.e. a friction force is developed between soil and the wall, the soil -to-soil friction coefficient $f = \tan \Phi$. (Bowles, 1988)

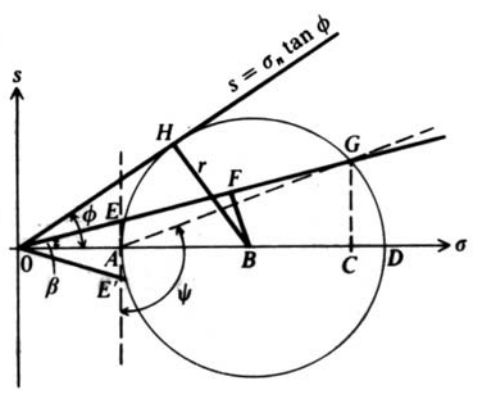
Rankine's theory (1857) considered the soil in a plastic equilibrium state and used the same assumptions as Coulomb except that he assumed no wall friction or soil cohesion. The Rankine case as shown in Figure 2-3(a) with a Mohr's construction for the general case as shown in Figure 2-3(b) & (c). The Mohr circle representing the state of stress at failure in a two- dimensional element as shown in Figure 2.3. The angle of internal friction (Φ) and cohesion (C), as denoted in Figure 2.3(d), are the relevant shear parameters. The shear failure occurs along a plane at angle of $(45 + \Phi/2)$ to the horizontal plane as shown in Figure 2-3(e). In the case that the whole soil mass is stressed such that the stresses at each point are in the same directions then, theoretically, there will be a network of failure planes, known as a slip line field, equally inclined to the horizontal planes as shown in Figure 2.3(e). (Bowles, 1988 and Craig, 1992)



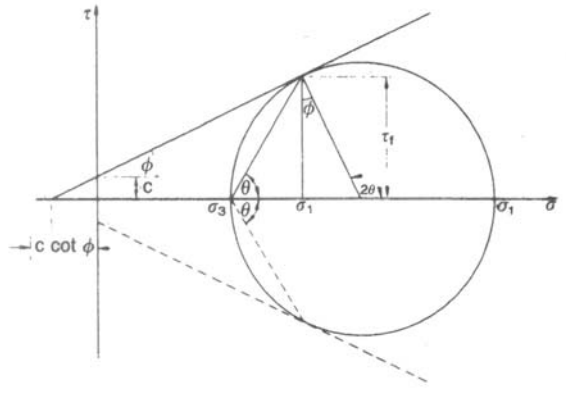
(a)



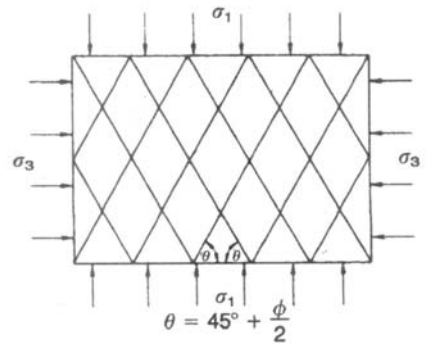
(b)



(c)



(d)



(e)

Figure 2.3: Rankine Earth Pressures

Lateral earth pressures obtained theoretically by Rankine and Coulomb methods have significant differences. The difference between these methods and test results was found to be less than 20 percent as mentioned by Georgiadis and Anagnostopoulos, 1998. This was conducted for a special case of strip load located with a specified distance from deep excavation retained with a sheet pile. (Georgiadis and Anagnostopoulos, 1998)

2.4.1 Surcharge Applied on Ground Surface

Different solutions are widely used for measuring active earth pressure coefficient in the design of retaining structures. These solutions attribute the earth pressure active coefficient to the soil weight. In different practical problems, the earth pressure could be attributed due to soil weight as well as due to surcharge applied on the ground surface of the soil retained. (Motta, 1994)

In most cases, the surcharge is applied at a certain distance from the wall. Therefore, Motta, 1994 derived a graphical solution that took into account the distance at which the load is applied. Evaluation of the lateral earth pressure due to a surcharge revealed that the pressure is referred to the elastic solutions based on Boussinesq's equations. However Motta, 1994 stated that "the theory of elasticity does not take into account the effect of soil strength on lateral earth pressures against a wall, which is in contrast with evidence."

Additional earth pressure resulted from surcharge strip loads applied on the soil surface behind a retaining wall is necessary to be considered in majority of earth retaining structures. (Georgiadis and Anagnostopoulos, 1998)

An experimental program on model cantilever sheet pile wall subjected to surcharge strip loads was carried out by Georgiadis and Anagnostopoulos, 1998. The results of this program were compared to predictions made by using different methods of calculating lateral earth pressures. The most accurate results of earth pressures computed through the model were those obtained using coulomb and the simple 45° distribution methods. By using elastic analysis theory in calculations made by the above two researchers, a significant large values of lateral earth pressures and bending moments were found. (Georgiadis and Anagnostopoulos, 1998)

2.4.2 Coefficient of Lateral Earth Pressures (K)

The Rankine case as shown in Figure 2.3(a) with a Mohr's construction for the general case as shown in Figure 2.3 (b) & (c), we can develop the Rankine active and passive pressure cases by making substitution of the equation for r into the equations for E F. At the end of series of equations, active and passive earth pressure coefficient values are obtained according to (Bowles, 1988):

$$k_a = \frac{\cos i - \sqrt{\cos^2 i - \cos^2 \phi}}{\cos i + \sqrt{\cos^2 i - \cos^2 \phi}} \dots\dots\dots(2-1)$$

$$k_p = \frac{\cos i + \sqrt{\cos^2 i - \cos^2 \phi}}{\cos i - \sqrt{\cos^2 i - \cos^2 \phi}} \dots\dots\dots(2-2)$$

The basic assumptions made for determination of the active earth pressure coefficient are that the soil should be dry, homogeneous, cohesionless, the failure surface of the wedge is plane, the uniformly distributed load q should be sufficiently large to ensure that the load q is intersected by the failure plane as shown in Figure 2.4 (Motta, 1994).

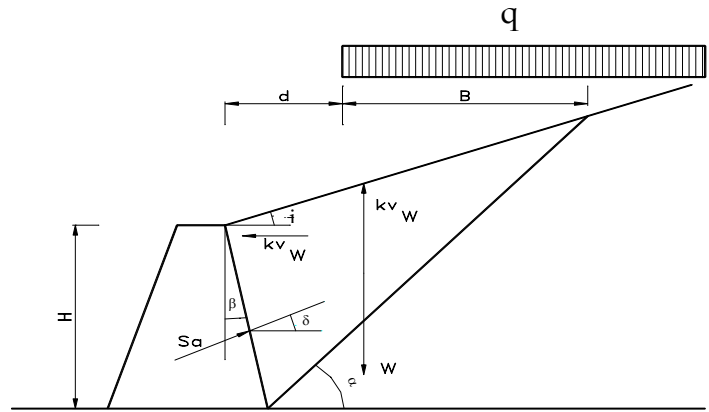


Figure 2.4: Earth-Pressure Evaluation

As shown in Figure 2-4 and assuming a failure plane inclined at an angle α with respect to the horizontal, it is possible to show that the weight of the failure wedge W and the extension B of the effective-applied load on the wedge can be expressed as follows:

$$W = \frac{1}{2} \gamma H^2 \left[(1 + \tan \beta \tan i) \tan \beta + \frac{(1 + \tan \beta \tan i)^2}{\tan \alpha - \tan i} \right] \dots \dots \dots (2-3)$$

and

$$B = H \left(\frac{1 + \tan \alpha \tan \beta}{\tan \alpha - \tan i} - \frac{d}{H} \right) \dots \dots \dots (2-4)$$

Thus the total weight of the failure wedge, due to the soil mass and surcharge is:

$$W_t = W + qB \dots \dots \dots (2-5)$$

In majority of practical cases, the back face of the wall, in contact with the soil is vertical, i-e $\beta=0$, then the expressions for W and B can be simplified as follows:

$$W = \frac{1}{2} \gamma H^2 \left(\frac{1}{\tan \alpha - \tan i} \right) \dots \dots \dots (2-6)$$

and

$$B = H \left(\frac{1}{\tan \alpha - \tan i} - \lambda \right) \dots \dots \dots (2-7)$$

Where λ = ratio between the horizontal distance of the surcharge from the head of the wall and the height of the wall. That is

$$\lambda = d/H \dots\dots\dots(2-8)$$

If k_h, k_v denote the horizontal and vertical seismic coefficient, respectively, by applying equilibrium conditions in the vertical and horizontal direction, the following expression can be derived for the active earth pressure S_a

$$S_a = \frac{1}{2} \gamma (1 - k_v) H^2 \frac{\tan(\alpha - \phi') + k_h / (1 - k_v)}{(\tan \alpha - \tan i) [\cos \delta + \sin \delta \tan(\alpha - \phi')]} + q(1 - k_v) H \frac{\tan(\alpha - \phi') + k_h / (1 - k_v)}{(\tan \alpha - \tan i) [\cos \delta + \sin \delta \tan(\alpha - \phi')]} \cdot [1 - \lambda(\tan \alpha - \tan i)] \dots\dots\dots(2-9)$$

where γ = bulk unit weight of soil; ϕ' = soil friction angle; δ = soil-wall friction angle; H = height of wall; and q = intensity of distributed load behind wall. In (2-9), the contribution of the surcharge q to the seismic loading has been evaluated assuming horizontal and vertical forces:

$$F_{hq} = k_h q B \dots\dots\dots(2-10)$$

and

$$F_{vq} = k_v q B \dots\dots\dots(2-11)$$

Equation (2-9) can be written in the classical form:

$$S_a = \frac{1}{2} \gamma (1 - k_v) H^2 K_{a,\gamma} + q(1 - k_v) H K_{a,q} \dots\dots\dots(2-12)$$

where

$$K_{a,\gamma} = \frac{\tan(\alpha - \phi') + k_h / (1 - k_v)}{(\tan \alpha - \tan i) [\cos \delta + \sin \delta \tan(\alpha - \phi')]} \dots\dots\dots(2-13)$$

and

$$K_{a,q} = r K_{a,\gamma} \dots\dots\dots(2-14)$$

where

$$r = [1 - \lambda(\tan \alpha - \tan i)] \dots\dots\dots(2-15)$$

It follows that the earth-pressure coefficient $K_{a,q}$, due to the surcharge, will be equal to the earth-pressure coefficient $K_{a,\gamma}$, due to the soil weight, only if $\lambda = 0$; i.e., only if the surcharge is applied close to the wall, otherwise $K_{a,q}$, will be somewhat less than $K_{a,\gamma}$, depending on the value of λ . Assuming

$$\theta = \tan^{-1}[k_h / (1 - k_v)] \dots \dots \dots (2-16)$$

and introducing the dimensionless parameter n_q

$$n_q = \frac{2q}{\gamma H} \dots \dots \dots (2-17)$$

Equation (2-12) can be re-written in the following form:

$$S_a = \frac{1}{2} \gamma (1 - k_v) H^2 K_{a,\gamma q} \dots \dots \dots (2-18)$$

Where $K_{a,\gamma q}$ = a coefficient, which takes into consideration the effects of soil weight and the surcharge load, and after some manipulations, can be expressed as

$$K_{a,\gamma q} = \frac{[1 + n_q - \lambda n_q (\tan \alpha - \tan i)] \sin(\alpha + \theta - \phi')}{\cos \theta \cos(\alpha - \phi' + \delta) (\tan \alpha - \tan i)} \dots \dots \dots (2-19)$$

To find the solution for S_a it must be imposed that the derivative of S_a with respect to α must be equal to zero; that is:

$$\frac{dS_a}{d\alpha} = 0 \dots \dots \dots (2-20)$$

Applying (2-20) allows finding the critical angle α_c for the failure plane, i.e, the angle that gives the maximum earth pressure by means of the following expression:

$$\tan(\alpha_c - i) = \frac{\sin a \sin b + (\sin^2 a \sin^2 b + \sin a \cos a \sin b \cos b + A \cos c \cos a \sin b)^{0.5}}{A \cos c + \sin a \cos b} \dots (2-21)$$

where $a = \phi' + \delta - i$; $b = \phi' - i - 0$; $c = 0 + \delta$; and

$$A = [(1 + n_q) \sin i \cos i + \lambda n_q] / (1 + n_q) \cos^2 i \dots \dots \dots (2-22a)$$

By utilizing (2-21) the active earth pressure coefficient $K_{a,\gamma q}$ can be written as follows:

$$K_{a,\gamma q} = \frac{(1 + n_q) \cos^2 i [1 - A \tan(\alpha_a - i)] [\cos b - \sin b / \tan(\alpha_c - i)]}{\cos \theta [\cos a + \tan(\alpha_c - i) \sin a]} \dots\dots\dots(2-22b)$$

As an example, in Figure 2.5 the coefficient $K_{a,\gamma q}$ is plotted versus λ and for different values of n_q . Also utilized parameters were $\theta = 0$ (seismic-horizontal coefficient $k_h = 0$); $i = 0$ (horizontal ground surface behind wall); $\phi' = 30^\circ$; and $\delta/\phi' = 1/2$.

Obviously, the curve for $n_q = 0$ in Figure 2.5 coincides with the classical solution when no surcharge is present on the ground surface and for this particular case, $K_{a,\gamma q} = K_{a,\gamma} = 0.301$.

According to Figure 2.6, limits for boundary conditions, it should be pointed out that (2-21) & (2-22) apply only if $\alpha_c < \alpha_1$, that is

$$\tan \alpha_c < \tan i + \frac{1}{\lambda} \dots\dots\dots(2-23)$$

Equation (2-23) ensures that the boundary conditions are compatible with basic assumptions, that is the critical failure plane intersects the surcharge at the ground surface. For example, curves for $n_q > 0$ in Figure 2.5 are truncated when (2-23) is no longer valid.

To find the maximum earth pressure coefficient, even if (2-23) is valid, one should also compare the solutions given by (2-21) & (2-22) for the two cases $n_q = 0$ and $n_q > 0$, respectively. Indeed, in some particular circumstances the conditions $n_q = 0$ may be more critical than the condition $n_q > 0$, as shown in Figure 2.5. This happens because the failure planes associated with the two conditions are quite different. Generally, however, the case $n_q > 0$ is the most critical condition.

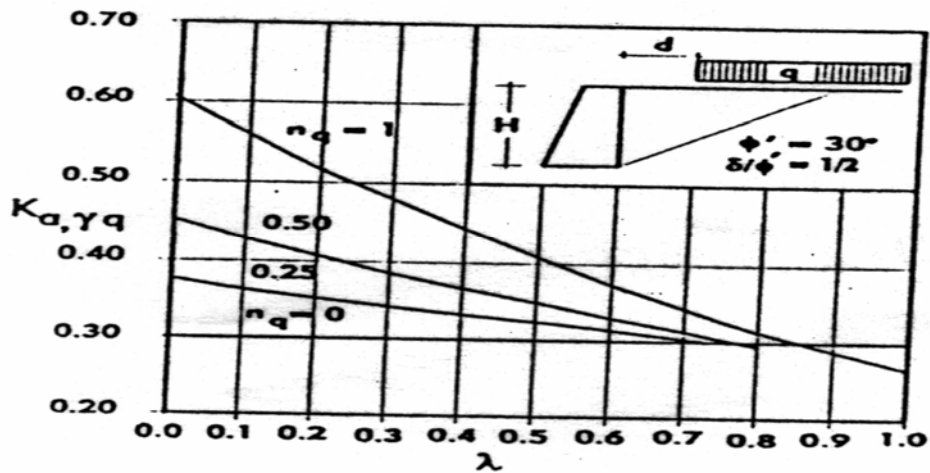


Figure 2.5 Values of Earth-Pressure Coefficient $K_{a,\gamma q}$ versus the Dimensionless Parameter λ

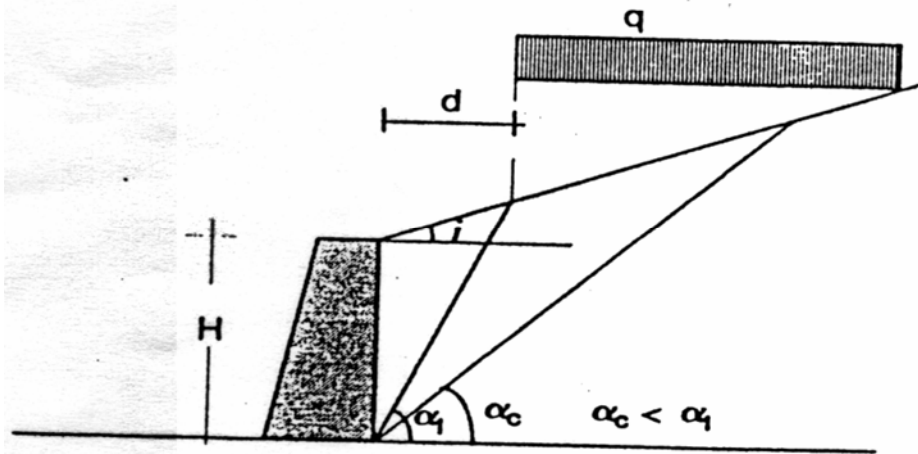


Figure 2.6 Limits for Boundary Conditions

In particular, values for coefficient of earth pressure (K) appear to be uncertain for sand since consideration was not given to the actual behavior occurring in the sand mass. However, values of earth pressure coefficient have been evaluated using experimental findings (Seok, et al., 2001 and Shields and Tolunay, 1974).

Unfortunately, the recent theories have not introduced special values of the coefficient of earth pressure for the gabion retaining wall. Therefore, it is found valuable that the experimental study has to be conducted to find the coefficient of earth pressure related to gabion retaining wall behavior. The above equations (Motta, 1994) are applied in our case study on the gabion retaining wall as described in details in Chapter 5.

Chapter 3

Tests Description and Procedures

3.1 General

The devices used in the experiments of our case study are manufactured in Geokon Company for Geotechnical Instrumentation in USA. The majority of technical specifications and methods of operation of these instruments are summarized from the Instruction Manuals provided by the manufacturer. Other devices were used at the Islamic University Material Testing laboratory where tests on backfill sand, such as gradation, specifications and degree of compaction were carried out during the course of this study. Shear box instrument is one of these devices.

During implementation, construction materials were tested in different material testing laboratories to make sure that they are matching the specifications of the project. Rocks and geotextile materials as well as backfill soil were tested. Some of these tests were conducted in local testing laboratories at the Islamic University and Arab Center Laboratories and others particularly the tests related to geotextile material were conducted by UNRWA in the Netherlands where they need special equipment and expertise.

3.2 Instruments Used in the Experiments

Four vibrating wire devices were used in the experiments. Two devices of the same category for measuring vertical and horizontal earth pressure and one for measuring deformation while the fourth one is the readout box. Details on these devices are described in this chapter.

3.2.1 Vibrating Wire Earth Pressure Cell (Model 4810)

Two units of this device were used to measure lateral earth pressures behind the gabion retaining wall. Horizontal and vertical earth pressures were measured using these devices. One device was placed vertically adjacent to the wall to measure the horizontal earth pressure and the other one was placed horizontally in the soil and adjacent to the wall to measure the vertical earth pressure.

3.2.1.1 Applications

Earth Pressure Cells provide a direct means of measuring total pressures, i.e. the combination of effective soil stress and pore water pressure, in the following cases:

- Bridge abutments;
- Diaphragm walls;
- Fills and embankments;
- Retaining walls surfaces;
- Sheet piling;
- Slurry walls and
- Tunnel linings.

They may also be used to measure earth bearing pressures on foundation slabs and footings and at the tips of piles. Figure 3.1 shows model 4800 and 4810 earth pressure cells, model 4810 is the type used in measurement of horizontal and vertical earth pressures in our case study.

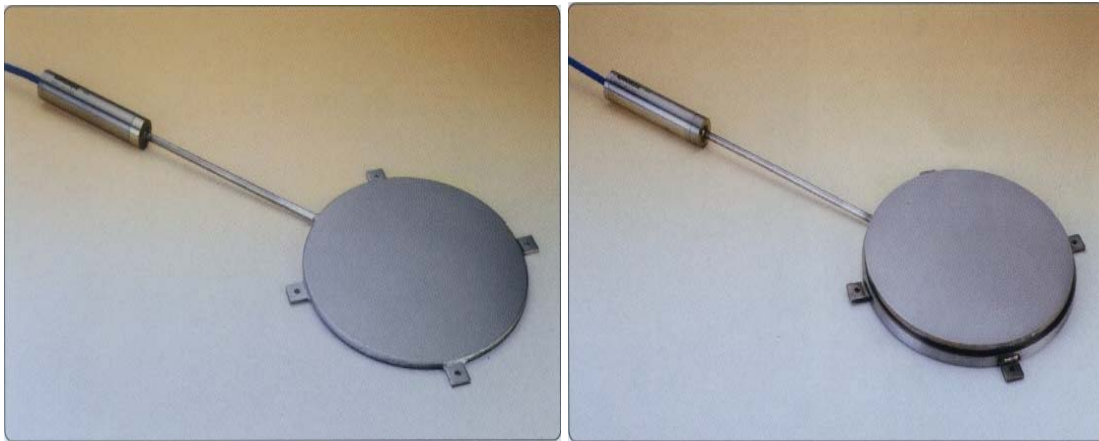


Figure 3.1 - Model 4800 Earth Pressure Cell (left) and model 4810 Contact Pressure Cell for attachment to existing surfaces(right).

3.2.1.2 Operating Principle

Earth Pressure Cells are constructed from two stainless steel plates welded together around their periphery and separated by a narrow gap filled with hydraulic fluid. External pressures squeeze the two plates together creating an equal pressure in the internal fluid. A length of stainless steel tubing connects the fluid filled cavity to a pressure transducer that converts the fluid pressure into an electrical signal transmitted by cable to the readout location.

3.2.1.3 Advantages & Limitations

The 4800 Series Earth Pressure Cells use vibrating wire pressure transducers and thus have the advantages of long term stability, reliable performance with long cables and insensitivity to moisture intrusion. All models also include a thermistor for temperature measurements and a gas discharge tube

for lightning protection. Where dynamic stress changes are to be measured a semi-conductor type pressure transducer is substituted.

Cell performance depends strongly on the surrounding soil properties. It would be prohibitively expensive to calibrate a cell in the soil type specific to the application being conducted. However, studies have shown that the most consistent cell performance is achieved using cells of maximum stiffness with ratios $D/t > 10$ (D is the diameter of the cell, t the thickness). Maximum stiffness is achieved by using hydraulic oil with less than 2 ppm of dissolved gas and aspect ratios generally greater than 20 to 30. Tests on cells in various types of soil have shown that the cells over-register the soil pressure by less than 5 percent. This is probably no greater than the inherent variability of the soil pressure distribution in the ground. Typical photos of model 4800 and 4810 are shown in Figure 3.1.

Typical of all closed hydraulic systems, earth pressure cells are sensitive to temperature changes which cause the internal fluid to expand at a different rate than the surrounding soil giving rise to spurious fluid pressure changes. The magnitude of the effect depends to a greater extent on the elasticity of the surrounding soil, i.e., on the degree of compaction and confinement, and is difficult to predict and correct for. The built-in thermistor is helpful in separating these spurious effects from real earth pressure changes.

Cells are constructed from two thin pressure sensitive plates. They can be positioned in the fill at different orientations so that soil pressures can be measured in two or three directions. Special armored cables are recommended in earth dam applications. Small diameter cells (50 mm) are also available for laboratory studies as shown in Figure 3.2.

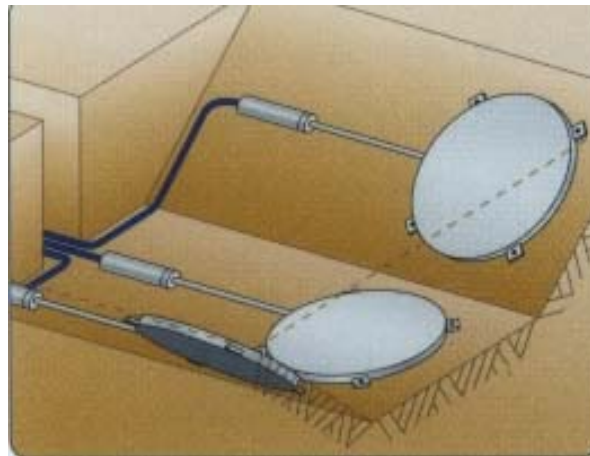


Figure 3.2 - Model 4800 Earth Pressure Cells installed in fill for soil pressure measurement in three directions.

A special cell modification that effectively reduces the severity of point loading is available for cells when used in granular materials. The modification uses two thick plates welded together at a flexible hinge that

helps provide more uniform pressure distribution. This type of modified cell is shown in Figure 3.3

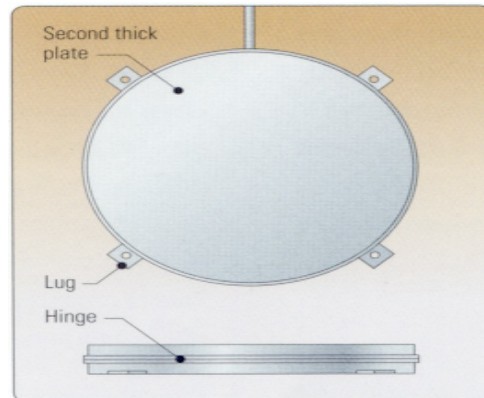


Figure 3.3 - Modified pressure cell, with two thick plates, for use in granular materials.

The model 4810 Contact Pressure Cell, shown in Figure 3.1- right, is designed to measure soil pressures on structures. The backplate of the cell which bears against the external surface of the structure is thick enough to prevent the cell from warping. The other plate is thin and is welded to the backplate in a manner which creates a flexible hinge to provide maximum sensitivity to changing soil pressures.

3.2.1.4 Technical Specifications

Table 3-1 shows the technical specifications of model 4810, the device used in our case study.

Table 3-1, Technical Specifications of Vibrating Wire Earth Pressure Cell

Model 4810	
Transducer Type	Vibrating Wire
Output	2000-3000Hz
Standard Ranges	0.35,0.7,107,3.5,5 Mpa (50,100,250,500,750psi)
Standard Cell Dimensions (HXD)	12x230mm
Transducer Dimensions (LXD)	150x25mm
Excitation Voltage	2.5-12v swept square wave
Material	304 Stainless Steel
Temperature Range	-20°C to +80°C

3.2.1.5 Theory of Operation

Earth Pressure Cells, sometimes called Total Pressure Cells or Total Stress Cells are designed to measure stresses in soil or the pressure of soil on structures. Cells will respond not only to soil pressures but also to ground water pressures or to pore water pressure, hence the term total pressure or total stress. A simultaneous measurement of pore water pressure (μ), using a piezometer, is necessary to separate the effective stress (σ) from the total stress (σ') as defined by Terzaghi's principle of effective stresses where;

$$\sigma = \sigma' + \mu \quad \dots\dots\dots (3-1)$$

These parameters coupled with the soil strength characteristics will determine soil behavior under loads.

Earth pressure cells of the type described here are the hydraulic type; two flat plates are welded together at their periphery and are separated by a small gap filled with a hydraulic fluid. The earth pressure acts to squeeze the two plates together thus building up a pressure inside the fluid. If the plates are flexible enough, i.e. if they are thin enough relative to their lateral extent, then at the center of the plate the supporting effect of the welded periphery is negligible and it can be stated that at the center of the cell the external soil pressure is exactly balanced by the internal fluid pressure.

This is true only if the deflection of the plates is kept to a minimum and thus it is important that the cell be stiff. This in a practical sense means that the fluid inside the cell should be as incompressible as possible and that the pressure transducer required to measure the fluid pressure should also be stiff having very little volume change under increasing pressure.

Tests conducted by various researchers have shown that the introduction of a flat stress cell into a soil mass will alter the stress field in a way dependent on the relative stiffness of the cell with respect to the soil and also with respect to the aspect ratio of the cell, i.e. the ratio of the width of the cell to its thickness. A thick cell will alter the stress more than a thin cell. Hence, for these reasons, a thin, stiff cell is best and studies have shown an aspect ratio of at least 20 to 1 to be desirable.

Ideally, the cell ought to be as stiff (compressible) as the soil. But in practice this is difficult to achieve. If the cell is stiffer (less compressible) than the soil then it will over-register the soil pressure because of a zone of soil immediately around the cell which is "sheltered" by the cell so that it does not experience the full soil pressure. This can be represented schematically as shown in Figure 3.4.

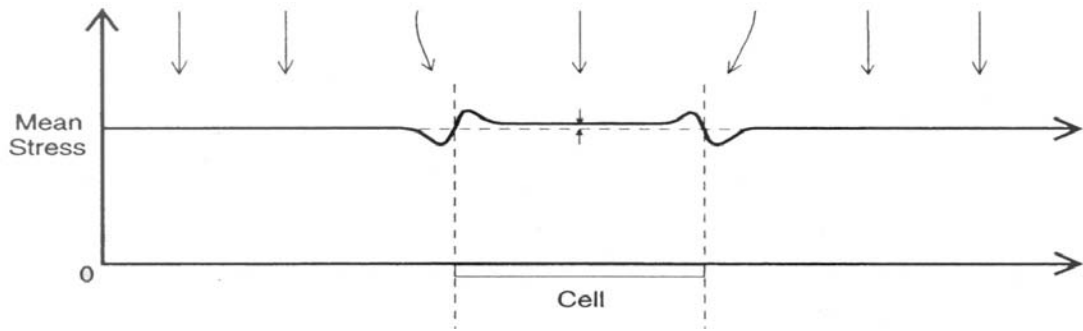


Figure 3.4 - Stress Redistribution, Weak Soil with Stiff Cell

As can be seen there is a stress concentration at the rigid rim but in the center of the cell the soil stress is only slightly higher than the mean soil stress, i.e. only slightly higher than the stress which would obtain were the cell not present.

In a stronger soil the de-stressed zone around the edge of the cell is more extensive and hence at the center of the cell the degree of *over-registration* of the mean stress is greater. This is represented schematically in Figure 3.5

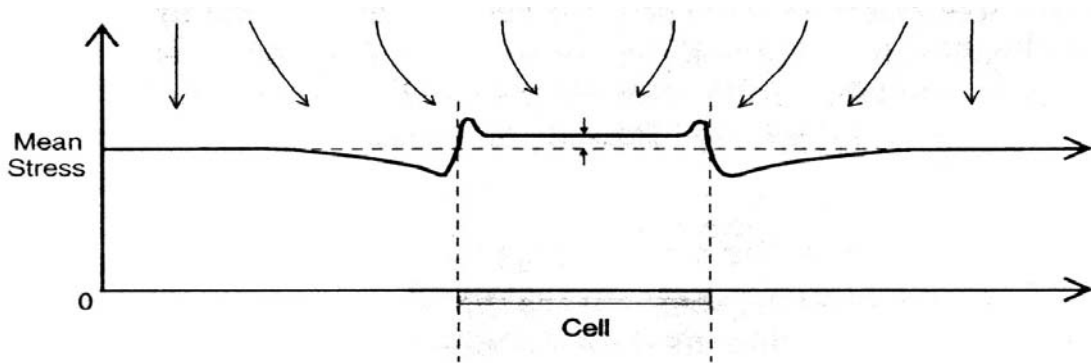


Figure 3.5 - Stress Redistribution, Strong Soil with Stiff Cell

Space in a stiff soil the cell may be less stiff (more compressible) than the soil, in which case the cell *will under-register* the mean soil stress as the stresses in the soil tend to "bridge" around the cell. This is represented schematically in Figure 3.6.

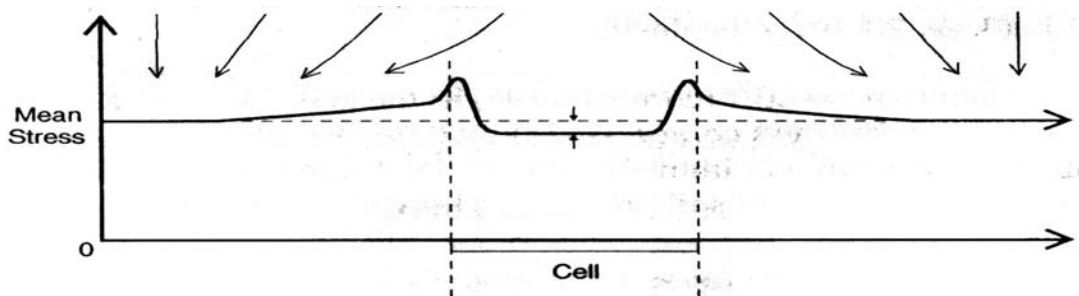


Figure 3.6 - Stress Redistribution, Stiff Soil with Weak Cell

Tests conducted at the University of Ohio (Ohio, USA) with several different soil types have shown that the maximum degree of over or under-registration amounts to 15% of the mean soil stress.

Other factors should be kept in mind; the inherent variability of soil properties which give rise to varying soil stresses at different locations and a corresponding difficulty in getting a good sample of the mean stress from a limited number of cell locations. Also, the response of the cell to its immediate surroundings depends very largely on how closely the soil mass immediately around the cell has the same stiffness or compressibility or the same degree of compaction as the undisturbed soil mass. Installation methods will need to pay particular attention to this detail.

3.2.1.6 Earth Pressure Cell Design

Earth Pressure Cells are constructed from two stainless steel plates welded together around the periphery so as to leave a narrow space between them. This space is completely filled with hydraulic oil which is connected hydraulically to a pressure transducer where the oil pressure is converted to an electrical signal which is transmitted through a signal cable to the readout location.

In general, Earth Pressure Cells use an all welded construction so that the space confining the oil is entirely metal not requiring 'O' rings which tend to trap air and reduce the cell stiffness. The pressure transducer normally employed is the Geokon Model 4500H which is available in several different pressure ranges as described in Table 3-2. The cable is attached to the transducer in a sealed, water-resistant manner. For earth pressure cells located inside a soil mass the cable may be armored and provided with strain relief at the cell to reduce the possibility of pull-out.

Table 3-2 , Earth Pressure Cell Specifications

Model:	4800 Earth Pressure Cell (rectangular)	4800 Earth Pressure Cell (circular)	4810 Contact Pressure Cell	4820 Jack-Out Pressure Cell
Ranges	350 kPa (50 psi) 700 kPa (100 psi) 1.5 MPa (250 psi) 3.5 MPa (500 psi) 5 MPa (750 psi) 7 MPa (1000 psi) 20 MPa 3000 psi)	350 kPa (50 psi) 700 kPa (100 psi) 1.5 MPa (250 psi) 2.5 MPa (500 psi) 5 MPa (750 psi) 7 MPa (1000 psi) 20 MPa (3000 psi)	2 MPa (300 psi) 3.5 MPa (500 psi) 5 MPa (750 psi)	0.3 MPa (50 psi) 0.7 MPa (100 psi) 1.5 MPa (200 psi)

Table 3-2 , Earth Pressure Cell Specifications(continued)

Operating Temperature:	-30 to +70° C			
Cell Dimensions (active area)	100 x 200 mm 4 x 8"	230 mm OD 9" OD	230 mm OD 9" OD	125 mm OD 5" OD
Coil Resistance:	150 Ω			
Cell Material:	304 Stainless Steel			
Transducer Material:	303 & 304 Stainless Steel			
Weight:	2.3 kg.	2.3 kg.	4.7 kg.	2.7 kg.
Electrical Cable	2 twisted pair (4 stranded conductor), 22 AWG Foil shield (with drain wire), PVC jacket, nominal OD=6.3 mm (0.250")			

3.2.1.7 Earth Pressure Cell Construction

Major components of the Model 4800 (rectangular and circular), 4810 and 4820 Earth Pressure Cells are shown in Figures 3.7 through 3.10, respectively.

The model 4800 Earth Pressure Cells may be rectangular or circular in shape. The standard size for the rectangular Model 4800 is 150 mm x 250 mm (8" x 10") as shown in Figure 3.7, for the circular it is 230 mm (9") in diameter as shown in Figure 3.8. Standard thickness for both styles is 6 mm (aspect ratio > 20). For laboratory tests smaller, thinner cells can be manufactured.

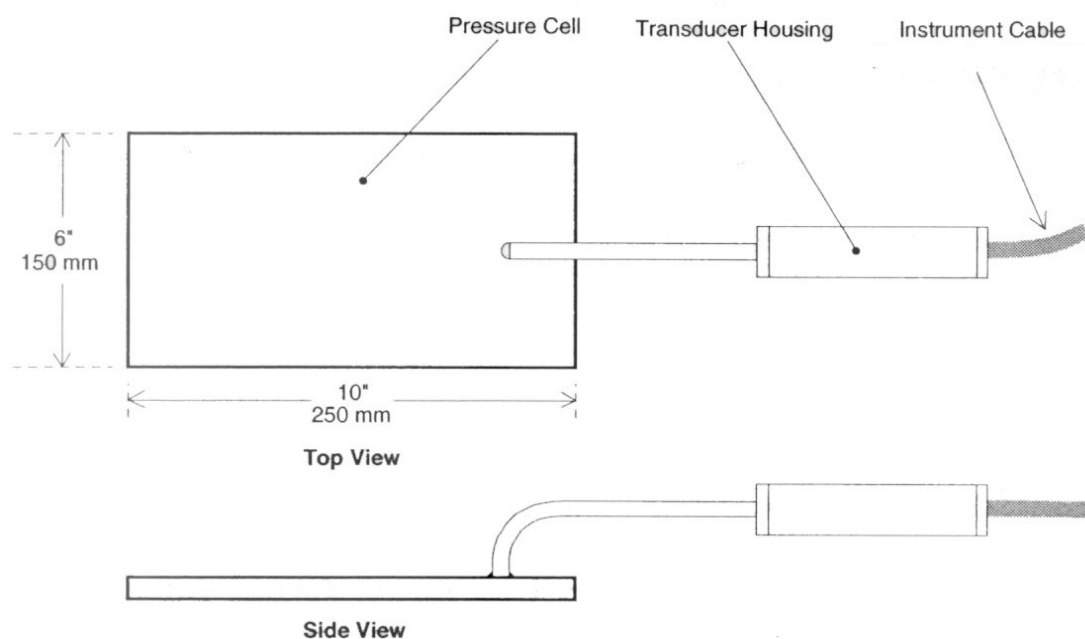


Figure 3.7 - Model 4800 Rectangular Earth Pressure Cell

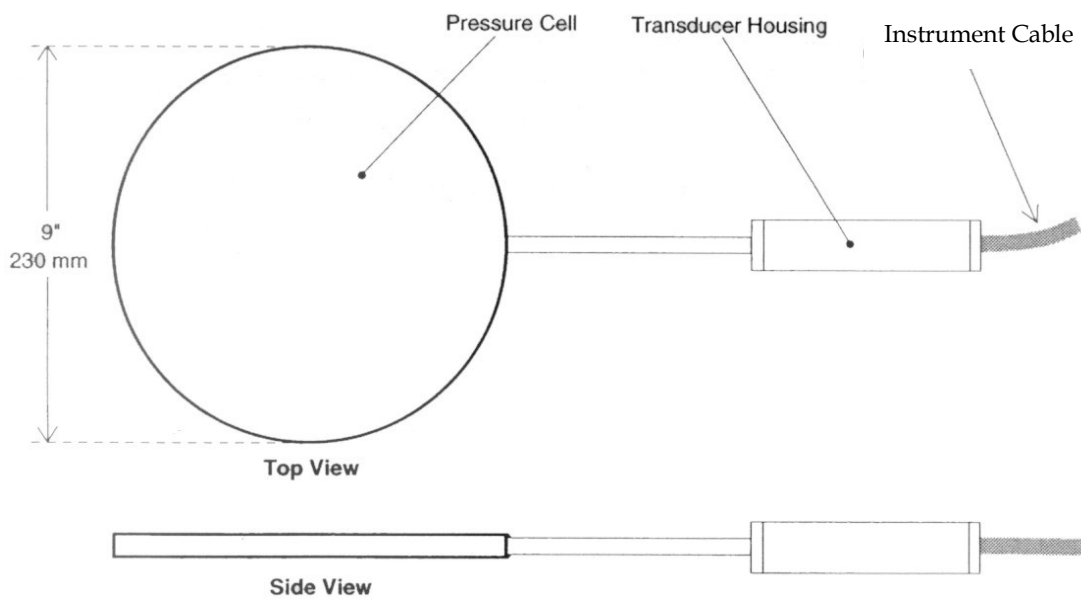


Figure 3.8 - Model 4800 Circular Earth Pressure Cell

The model 4810 Earth Pressure Cell, or "contact" cell as shown in Figure 3.9 is designed for measuring soil pressures on structures, similar to our case study.

One of the plates is thick and designed to bear against the external surface of the structure in a way that will prevent flexure of the cell. The other plate is thin and reacts to the soil pressure.

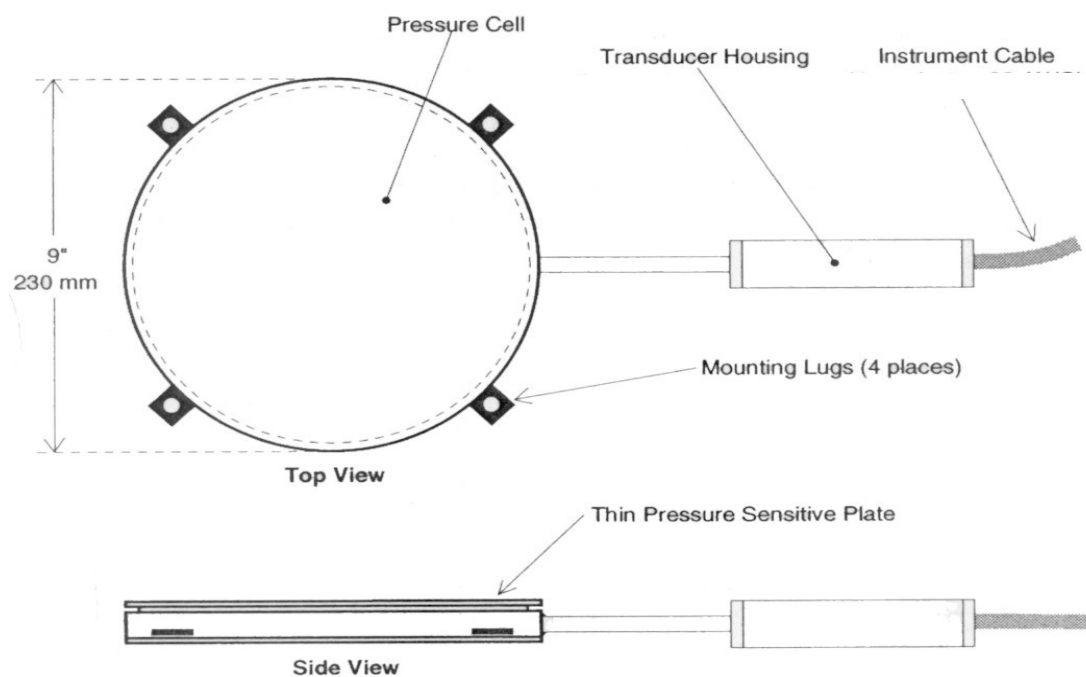


Figure 3.9 - Model 4810 Contact Pressure Cell

The model 4820 Earth Pressure Cell or "jack-out" cell, as shown in Figure 3.10, is designed specifically for the measurement of soil pressures on the back side of slurry walls. The pressure transducer housing is connected directly and perpendicular to the thick back plate.

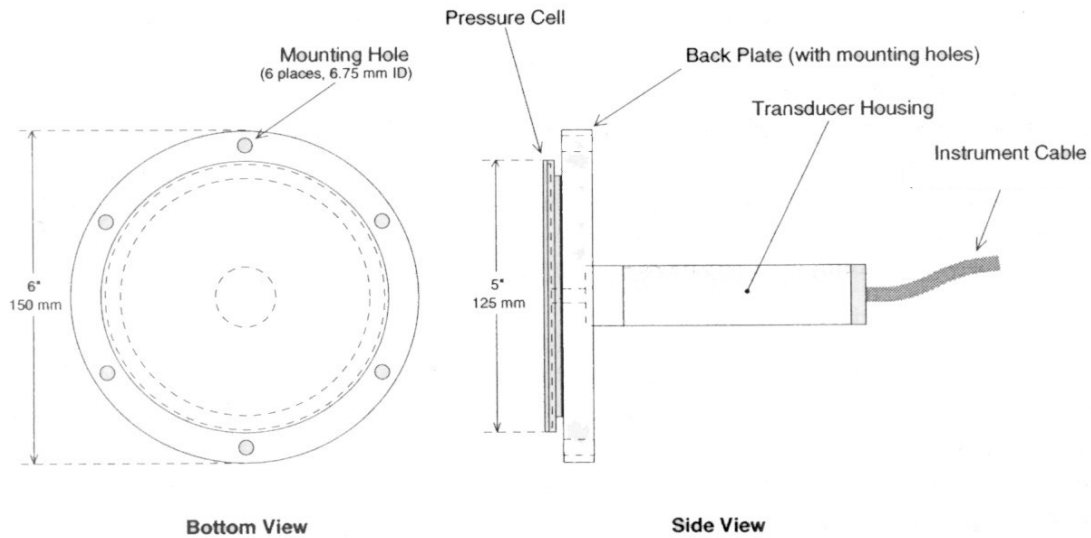


Figure 3.10 - Model 4820 Jack-Out Pressure Cell

3.2.1.8 Preliminary Tests

It is always wise, before installation commences, to check the cells for proper functioning. Each cell is supplied with a calibration sheet as shown in Figure 3.13 which shows the relationship between readout digits and pressure and also shows the initial no load zero reading.

The cell electrical leads (usually the red and black leads) are connected to a readout box as described in section 3.2.1.13 and the zero reading given on the sheet is now compared to a current zero reading. The two readings should not differ by more than ≈ 50 digits after due regard to corrections made for different temperatures, barometric pressures and height above sea level and actual cell position (whether standing up or laying down).

By pressing on the cell it should be possible to change the readout digits, causing them to fall as the pressure is increased.

Checks of electrical continuity can also be made using an ohmmeter. Resistance between the gage leads should be approximately 150 ohms, ± 20 ohms. Remember to add cable resistance when checking (22 AWG stranded copper leads are approximately 14.70/1000' or 48.50/km, multiply by 2 for

both directions). Between the green and white should be approximately 3000 ohms at 25° and between any conductor and the shield should exceed 20 megohm.

3.2.1.9 Earth Pressure Cell Installation

- **Installation of Model 4810 Contact ("fat-back") Pressure Cell**

This section details installation instructions for the model 4810 Earth Pressure Cells which are used for the measurement of earth pressures on structures. In backfills for piers, piles, bridge abutments, retaining walls, culverts and other structures the cells may be installed either inside a concrete structure being poured or directly on the surface of an existing structure as shown in Figure 3.11

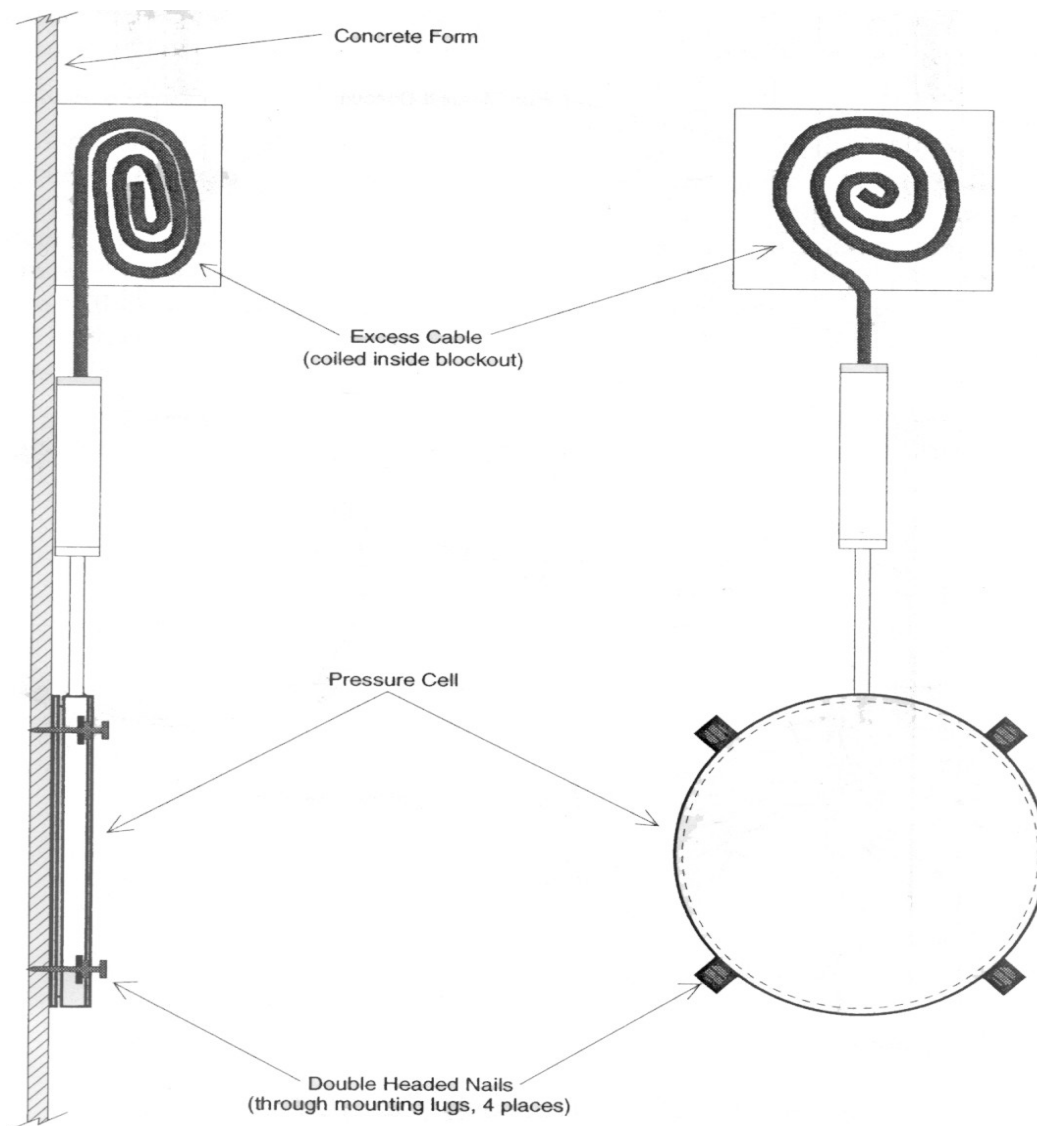


Figure 3.11 - Attachment of Model 4810 to Concrete Form

- **Installation on Existing Structures**

Again the lugs welded to the edge of the cell can be used to hold the cell against the structure using nails, lag bolts, tie wire, etc.

Even if the surface is smooth, but especially where the surface is rough or irregular a mortar pad between the cell and the structure is required as shown in Figure 3.12.

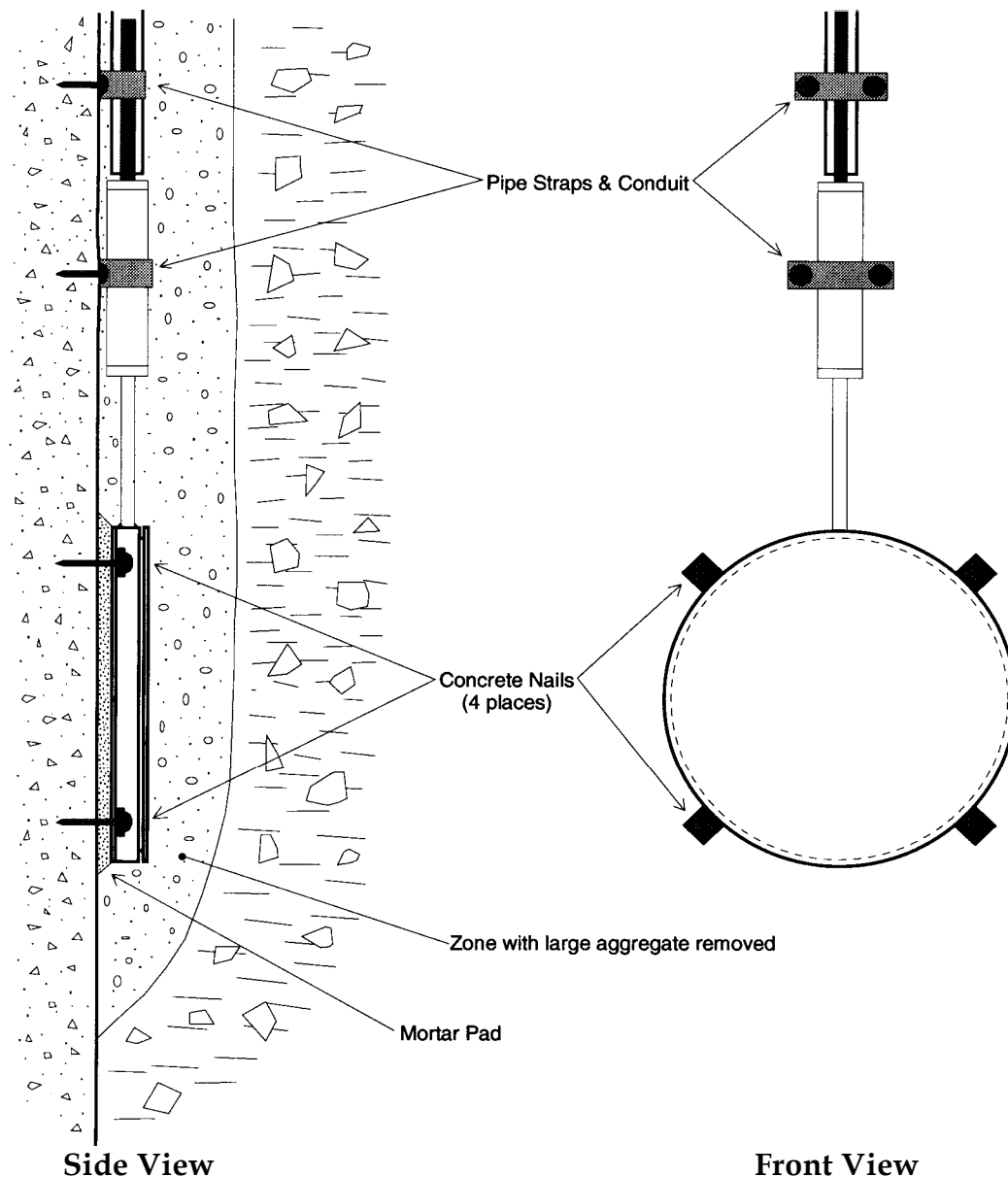


Figure 3.12 - Model 4810 Contact Pressure Cell Installation

Use the lugs on the cell as a template to locate the position for drilling holes for the installation of expanding anchors or install the anchors nearby and use wire to hold the cells in place.

Alternately the cell may be nailed in place using the lugs as a guide. First mix up some quick setting cement mortar or epoxy cement. Trowel this onto the surface then push the cell into the cement so that the excess cement extrudes out from the edges of the cell.

Hold the cell in place while the cement sets up, then complete the installation by adding the lag bolts (using the expansion anchors) and tightening or nailing the cell in place. Protect the cell, transducer housing and cable from direct contact with large pieces of rock by covering them with fine grained fill material from which all pieces larger than about 10 mm (0.5") have been removed. This fine material is kept next to the cell and cable as the fill is placed. Additional cable protection can be achieved by using metal conduit strapped to the surface of the structure.

3.2.1.10 Cable Installation

Cable placement procedures vary with individual installations. In general, however, all installations have in common the requirements that; 1) the cable must be protected from damage by angular particles of the material in which the cable is embedded, 2) the cable must be protected from damage by compaction equipment, 3) in earth and rock embankments and backfills, the cable must be protected from stretching as a result of differential compaction of the embankment, 4) in concrete structures, the cable must be protected from damage during placement and vibration of the concrete.

Cables may be spliced, without affecting gage readings, nevertheless splicing should be avoided wherever possible. If necessary, waterproof the splice completely.

3.2.1.11 Electrical Noise

Care should be exercised when installing instrument cables to keep them as far away as possible from sources of electrical interference such as power lines, generators, motors, transformers, arc welders, etc. Cables should never be buried or run with AC power lines. The instrument cables will pick up the 50 or 60 Hz (or other frequency) noise from the power cable and this will likely cause a problem obtaining a stable reading.

3.2.1.12 Initial Readings

Initial readings must be taken and carefully recorded along with the barometric pressure and temperature at the time of installation. Take the initial readings while the cell is in position, just prior to it being covered by fill and pouring of concrete. Again, it is imperative that initial readings at zero load are taken!

3.2.1.13 Taking Readings, Operation of the GK-401 Readout Box

The GK-401 is a basic readout for all Vibrating Wire Pressure Cells.

Connect the Readout using the flying leads or in the case of a terminal station, with a connector. The red and black clips are for the vibrating wire gage, the green or blue clip for the shield drain wire. The GK-401 cannot read the thermistor.

1. Turn on the Readout. Turn the display selector to position "B" as shown in Table 3-3. Readout is in "digits" as described in section 3.2.1.14, Equation 3-2.
2. Turn the unit on and a reading will appear in the front display window. The last digit may change one or two digits while reading. Record the value displayed
3. The unit will automatically turn itself off after approximately 4 minutes to conserve power.

Table 3-3 GK-401 Display Position vs. Geokon Model Number

Display Position	Model No.	Display Units	Excitation Range	Gage Factor
A	All	Period in	450-6000 Hz	None
B	4210 4300BX 4400 4500 4600 4700 4800 4900	$f^2 \times 10^{-3}$ (digits)	1500-3500 Hz	1.000
C	4000	μ strain	450-1200 Hz	4.062
D	4200	μ strain	450-1200 Hz	3.304
E	4100	μ strain	1500-3500 Hz	0.391
F	4300EX	$f^2 \times 10^{-3}$ (digits)	2500-6000 Hz	1.000

Notes:

- General position for all gages; possibility of harmonics in 4000 and 4200 gages at very low strain levels.
- The period readings can be very useful for greater resolution of strain measurements. Also, measurements as low as 0.1 μ strain can be made.
- Factor multiplies digits ($f^2 \times 10^{-3}$).

3.2.1.14 Data Reduction

- **Pressure Calculation**

The basic units utilized by Geokon for measurement and reduction of data from Vibrating Wire Earth Pressure Cells are "digits".

The GK-401, GK-402 and GK-403 Readouts all display "digits" in the Earth Pressure Cell reading position. Calculation of digits is based on the following Equation;

$$\text{Digits} = (1/\text{period}(\text{second}))^2 \times 10^{-3} \text{ or } \text{Digits} = \text{Hz}^2/1000 \dots\dots\dots (3-2)$$

To convert digits to pressure the following Equation applies;

Pressure = (Initial Reading - Current Reading) x Calibration Factor or

$$P = (R_o - R_1) \times C \dots\dots\dots(3-3)$$

The Initial Reading (Ro) is normally obtained during installation (usually the zero reading). The Calibration Factor (C, usually in terms of psi or MPa per digit) comes from the supplied Calibration Sheet as shown in Figure 3.13. To convert the output to other engineering units, multiply the Calibration Factor by the conversion multiplier listed in Table 3-4.

Table 3-4, Engineering Units Multiplication Factors

From To	psi	"H ₂ O	'H ₂ O	mm H ₂ O	m H ₂ O	"HG
psi	1	.036127	.43275	.0014223	1.4223	.49116
"H ₂ O	27.730	1	12	.039372	39.372	13.596
'H ₂ O	2.3108	.08333	1	.003281	3.281	1.133
mm H ₂ O	704.32	25.399	304.788	1	1000	345.32
m H ₂ O	.70432	.025399	.304788	.001	1	.34532
"HG	2.036	.073552	.882624	.0028959	2.8959	1
mm HG	51.706	1.8683	22.4196	.073558	73.558	25.4
atm	.06805		.0024583.0294996	.0000968	.0968	.03342
mbar	68.947	2.4908	29.8896	.098068	98.068	33.863
bar	.068947		.0024908.0298896	.0000981	.098068	.033863
kPa	6.8947	.24908	2.98896	.0098068	9.8068	3.3863
MPa	.006895	.000249	.002988	.00000981	.009807	.003386

Continuation to Table 3-4, Engineering Units Multiplication Factors

From To → ↓	mm HG	atm	mbar	bar	kPa	MPa
psi	.019337	14.696	.014503	14.5039	.14503	145.03
"H ₂ O	.53525	406.78	.40147	401.47	4.0147	4016.1
'H ₂ O	.044604	33.8983	.033456	33.4558	.3346	334.6
mm H ₂ O	13.595	10332	10.197	10197	101.97	101970
m H ₂ O	.013595	10.332	.010197	10.197	.10197	101.97
"HG	.03937	29.920	.029529	29.529	.2953	295.3
mm HG	1	760	.75008	750.08	7.5008	7500.8
atm	.0013158	1	.0009869	.98692	.009869	9.869
mbar	1.3332	1013.2	1	1000	10	10000
bar	.001333	1.0132	.001	1	.01	10
kPa	.13332	101.320	.1	100	1	1000
MPa	.000133	.000101320	.0001	.1	.001	1

For example, assume an initial reading of 9101, a present reading of 7380 and a Calibration Factor of 0.06943 psi/digit. The calculated pressure is;

$$119.5 \text{ psi} = (9101 - 7380) \times 0.06943 = 823.9 \text{ kPa}$$

• Temperature Correction

The vibrating wire sensor is relatively insensitive to temperature fluctuations and often temperature changes in the ground are minor and can be ignored. But, if desired, correction for temperature effects on the sensor can be made using the Thermal Factor (K) supplied on the calibration sheet as shown in Figure 3.13 along with an Equation for its proper use as shown in Equation 3-4.

Temperature Correction = (Current Temperature - Initial Temperature) x Thermal Factor or

$$P_{\text{correction}} = (T_1 - T_0) \times K \dots \dots \dots (3-4)$$

The Temperature Correction value is then added to the pressure calculated using Equation 3-3. For example, assume an initial temperature of 25° C, a temperature at the time of measurement of 12° C and a Thermal Factor of -0.02814 psi/° C. The thermally corrected pressure is:

$$119.9 \text{ psi} = 119.5 + ((12 - 25) \times -0.02814) = 826.7 \text{ kPa}$$

Hence, the thermally corrected pressure calculation is shown in Equation 3-5.

$$P_{\text{corrected}} = ((R_0 - R_1) \times C) + ((T_1 - T_0) \times K) \dots \dots \dots (3-5)$$

Note that the correction for temperature applies only to the pressure transducer itself and not to the entire cell surrounded by soil or soil and concrete each with its own (different) temperature coefficient of expansion. Commercially it is not practical to measure this effect without incurring huge expenses. It is enough to say that the effect is usually small, especially at depths where the temperature is fairly constant.

• **Barometric Correction**

The pressure transducer used in Geokon Vibrating Wire Earth Pressure Cells is evacuated and hermetically sealed and will respond to barometric pressure fluctuation. However, since the magnitudes are on the order of ±3.45 kPa (±0.5 psi), correction is generally not required.

If a correction for these fluctuations is required then it is necessary to record the barometric pressure at the time of each reading.

3.2.1.15 Calibration

Each device should be provided with a calibration sheet showing details on the calibration factor, date of calibration and other data. The calibration sheet of one of the Vibrating Wire Pressure cells is shown as a sample in Figure 3.13. The calibration sheets provided by the manufacturer are shown in Appendix “C”.

3.2.1.16 Earth Pressure Cells Specifications

Table 3-2 describes the Earth Pressure Cells Specifications for different types of cells.

Vibrating Wire Pressure Transducer Calibration Report

Type: S Date of Calibration: May 28, 2003
 Serial Number: 03-3666 Temperature: 23.4 °C
 Pressure Range: 350 kPa †Barometric Pressure: 985.7 mbar
 Cal. Std. Cntrl. #(s): 511, 506, 216, 468, 524, 529, 25167, 018 Technician: KOB

Applied Pressure (kPa)	Gage Reading 1st Cycle	Gage Reading 2nd Cycle	Average Gage Reading	Calculated Pressure (Linear)	Error Linear (%FS)	Calculated Pressure (Polynomial)	Error Polynomial (%FS)
0.000	9064	9064	9064	0.235	0.07	0.042	0.01
70.00	8528	8527	8528	69.93	-0.02	69.90	-0.03
140.0	7990	7990	7990	139.8	-0.07	139.9	-0.03
210.0	7450	7450	7450	209.9	-0.03	210.1	0.02
280.0	6910	6910	6910	280.0	0.01	280.1	0.03
350.0	6371	6370	6371	350.1	0.04	349.9	-0.04

(kPa) Linear Gage Factor (G): 0.1299 (kPa/ digit) Regression Zero: 9066
 Polynomial Gage Factors: A: -1.998E-07 B: -0.1268 C: 1166.0
 Thermal Factor (K): -0.11554 (kPa/ °C)

(psi) Linear Gage Factor (G): 0.01884 (psi/ digit)
 Polynomial Gage Factors: A: -2.89722E-08 B: -0.01839 C: 169.11
 Thermal Factor (K): -0.016758 (psi/ °C)

Calculated Pressures: Linear, $P = G(R_0 - R_1) + K(T_1 - T_0) - (S_1 - S_0)**$
 Polynomial, $P = AR_1^2 + BR_1 + C + K(T_1 - T_0) - (S_1 - S_0)**$
 **Barometric compensation is not required with vented and differential pressure transducers.

Factory Zero Reading:
 GK-401 Pos. B or F(R₀): 9007 Temp(T₀): 23.2 °C †Baro(S₀): 989.9 mbar Date: June 05, 2003

*Initial zero readings must be established in the field following the procedures described in the Instruction Manual. If the Polynomial equation is used the field value of C must be calculated by plugging the initial zero reading into the polynomial equation with the value of P set to zero.

The above instrument was found to be in tolerance in all operating ranges.
 The above named instrument has been calibrated by comparison with standards traceable to the NIST, in compliance with ANSI Z540-1.
 This report shall not be reproduced except in full without written permission of Geokon Inc.

Figure 3.13 - Sample Model 4810 Calibration Sheet

3.2.2 Vibrating Wire Deformation Meter (Model 4430)

Figure 3.14 shows three different types of vibrating wire deformation meters related to 4400 Series.



Figure 3.14 - Model 4410 Strandsmeter (front), Model 4400 Embedment Jointmeter (center) and model 4420 Crackmeter (rear)

3.2.2.1 Applications

The 4400 Series shown in Figure 3.14 are designed to measure or monitor the following:

- Expansion or contraction of a joint;
- Strains in tendons and steel cables;
- Movement across surface cracks and joints;
- Closures in underground excavations, tunnels, etc.;
- Displacements associated with landslides and
- Movement of boulders, snow, ...etc. on unstable slopes.

3.2.2.2 Operating Principle

Vibrating wire displacement transducers are designed to measure displacements across joints and cracks in concrete, rock, soil and structural members.

The transducer consists of a vibrating wire in series with a tension spring. Displacements are accommodated by a stretching of the tension spring, which produces a considerable increase in wire tension.

The wire and spring are connected to a free-sliding rod which is free to slide inside a protective outer tube. An o-ring seal prevents water from entering.

The frequency signal is transmitted through the cable to the readout location, conditioned, and displayed on portable readouts or dataloggers.

3.2.2.3 Advantages and Limitations

The 4400 Series Displacement Transducers are fabricated entirely from stainless steel and are waterproof to 1.75 MPa, which, coupled with their excellent long-term stability, guarantees reliability and performance in even the harshest environments.

An advantage of vibrating wire displacement transducers over more conventional linear devices lies mainly in the use of a frequency, rather than a voltage, as the output signal. Frequencies may be transmitted over long lengths of electrical cable without appreciable degradation caused by variations in cable resistance or leakage to ground. This allows for a readout location that may be over a thousand meters from the transducer.

3.2.2.4 Model 4430 Deformation Meter

The model 4430 Deformation Meter shown in Figure 3.15 is designed to measure axial strains or deformations in boreholes in rock, concrete or soil. It can be also embedded in soils in embankments such as earth dams and high way fills. The Model 4430 can be installed in series to give a total deformation profile along a particular axis. Base lengths of the gage can vary from a minimum of one meter to over 25 meters. When used in rock in horizontal or inclined downward boreholes a special grouting apparatus and hydraulic or snap-ring anchors are required. Direct placement for pre-wiring to a rubber cage allows use in concrete.

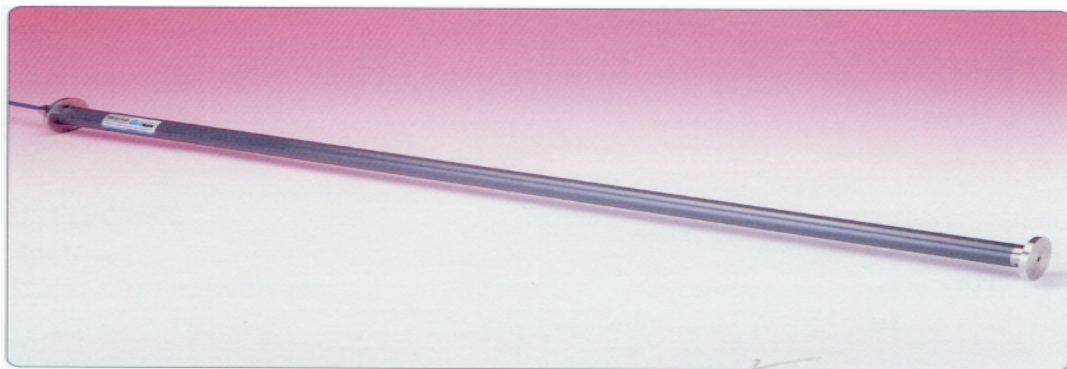


Figure 3.15 - Model 4430 Deformation Meter

3.2.2.5 Technical Specifications

Table 3-5 shows the technical specifications of different types of eformation Meters

Table 3-5, Technical Specifications of Vibrating Wire Deformation Meter

Model	Standard Ranges	Temperature Ranges	Dimensions
4400 Embedment Jointmeter	12, 25, 50 mm	-20°C to +80°C	Length: 406 mm Flange Diameter: 51 mm
4410 Strandmeter	20,000 ge	-20°C to +80°C	Length: 203 mm Clamp Width: 45 mm
4420 Crackmeter	12, 25, 50, 100 mm	-20°C to +80°C	Lengths: 318, 362, 527 mm Coil Diameter: 25 mm
4425 Convergence Meter	25, 50, 100 mm	-20°C to +80°C	Transducer Lengths: 356, 508, 838 mm Transducer Diameter: 25 mm
4427 Long-Range Displacement Meter	0.5, 1, 2 m (without resetting)	-30°C to +60°C	Enclosure (L x W x H): 610 x 152 x 152mm
4430 Deformation Meter	25, 50, 100 mm	-20°C to +80°C	Length: varies Flange Diameter: 50 mm
4450 Displacement Transducer	12, 25, 50, 100 mm	-20°C to +80°C	Lengths: 210, 212, 270, 410 mm Coil Diameter: 19 mm

3.2.2.6 Theory of Operation

The basic sensing element is a vibrating wire strain gage in series with a precision music wire spring which is coupled to a movable shaft. As the shaft moves in or out of the sensor body, the tension in the spring, and also in the vibrating wire element, change. This change in tension is directly proportional to the amount of extension and, through calibration, a calibration factor that relates the frequency of vibration to the amount of extension is determined. The unit is stress relieved after manufacture providing for excellent stability over long periods of time.

The gage sensor is attached to a flange at one end and by a connecting rod of some length to a flange at the other end. The sensor and the rod are covered by a plastic (PVC) tube which holds the end flanges apart at a predetermined distance (gage length), and insures that the rod is free to move. As the flanges move apart the movement is conveyed by the connecting rod to the sensor and measured by the readout system. Different combinations of gage length and sensor range provide for optimum sensitivity.

For maximum strain resolution, a long base gage with a short range transducer will give best results. For maximum deformation: short base length, longer transducer range. The flexibility of the system allows the user to choose the most useful combination of range and sensitivity according to predicted movements.

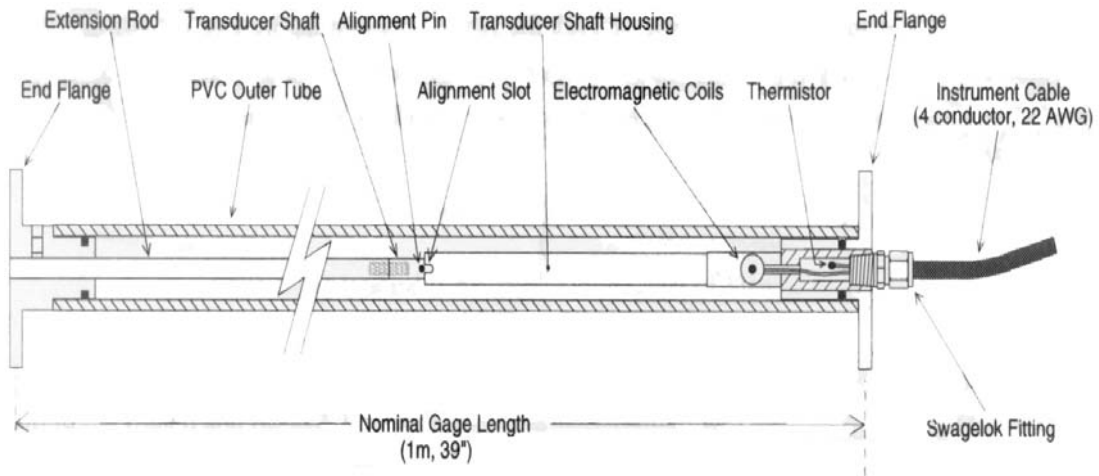


Figure 3.16 - Model 4430 Deformation Meter, detailed view

Readouts available from Geokon, used in conjunction with the Vibrating Wire Deformation Meter, will provide the necessary voltage pulses to pull out the wire and convert the measured frequencies so as to display the reading.

3.2.2.7 Preliminary Tests

Upon receipt of the instrument, the gage should be checked for proper operation (including the thermistor) as described in Section 3.2.2.12 for readout instructions. In position "B" the gage will read between 2000 and 8000 digits. Pull slightly on the end flanges as shown in Figure 3.16, the reading should increase.

Checks of electrical continuity can also be made using an ohmmeter. Resistance between the gage leads should be approximately 180Ω , $\pm 10\Omega$. Remember to add cable resistance when checking (22 AWG stranded copper leads are approximately $14.7\Omega / 1000'$ or $48.5\Omega / \text{km}$, multiply by 2 for both directions). Between the green and white should be approximately 3000 ohms at 25° , and between any conductor and the shield should exceed 2 megohms.

3.2.2.8 Deformation Meter Installation in Fills & Embankments

The model 4430 can be used as a soil deformation meter in fills and embankments (as used in our case study) by placing the unit in shallow, horizontal trenches in the fill.

If the sensor is used this way, special couplings are added to insure a free "slip" at the flange connections. Multiple sensors can be installed in series to give a total deformation profile along a particular axis as in a dam or highway embankment. Figure 3.17 shows installation along crest of Dam.

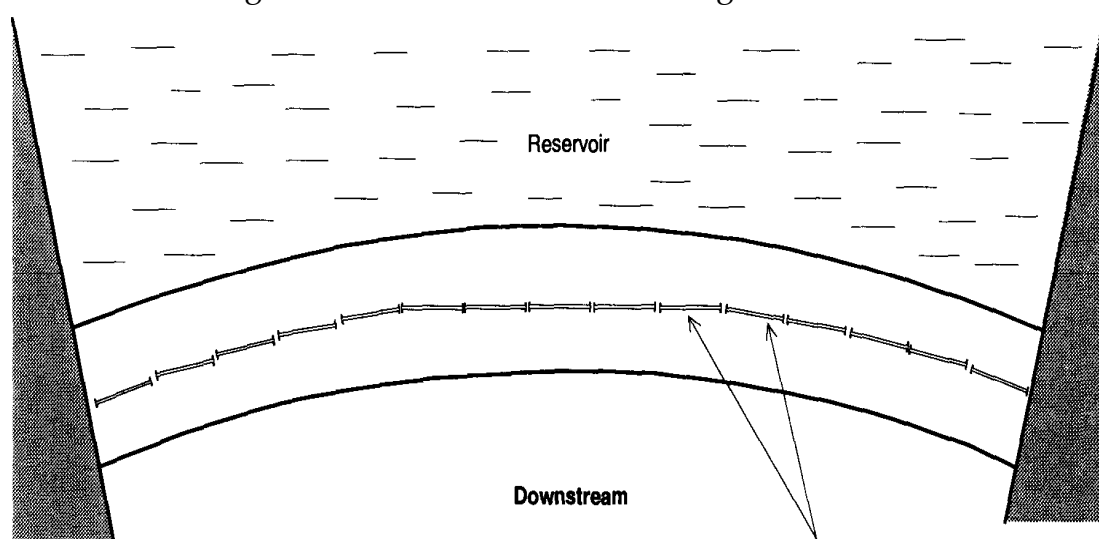


Figure 3-17 - Installation Along; Crest of Dam

A narrow flat bottom trench should be excavated in previously compacted fill. The sensor is laid in the trench and backfilled with material which has had any large (>10 mm, 0.5") aggregate removed. Small indentations should be made in the bottom of the trench for the flanges in order that the sensor is kept relatively straight. Backfill and hand tamp the first 15 cm (≈6") and then proceed with the compaction of the fill in the normal way. Cables should also be run in trenches and backfilled in the same manner as above. Figure 3.18 shows installation in borehole in embankment.

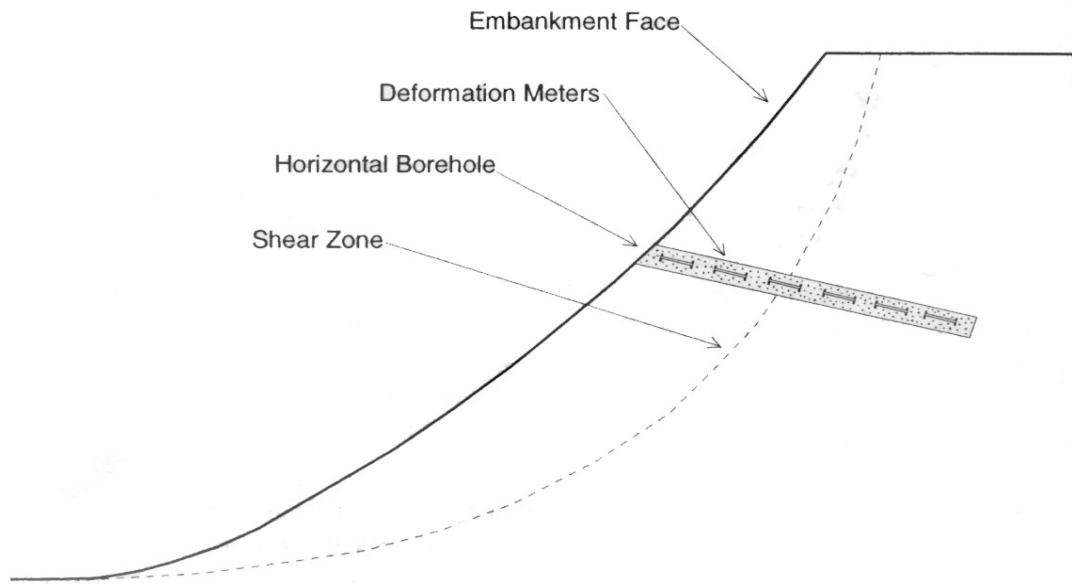


Figure 3-18 - Borehole Installation in Embankment

3.2.2.9 Cable Protection and Termination

As noted above, the cable from the gages can be protected by the use of flexible conduit. Terminal boxes with sealed cable entries and covers are also available, allowing many gages to be terminated at one location with complete protection of the lead wires.

The panel can have built-in jacks or a single connection with a rotary position selector switch. Lightning protection components can also be installed in the terminal boxes.

Cables may be spliced to lengthen them, without affecting gage readings. Always waterproof the splice completely.

3.2.2.10 Initial Readings

All readings are referred to an initial reading so it is important that this initial reading be carefully taken. Conditions should be noted at the time of all readings, especially during curing, i.e., temperature, time after placement, local conditions, etc.

3.2.2.11 Electrical Noise

Care should be exercised when installing instrument cables to keep them as far away as possible from sources of electrical interference such as power lines, generators, motors, transformers, arc welders, etc. **Cables should never be buried or run with AC power lines!**

The instrument cables will pick up the 50 or 60 Hz (or other frequency) noise from the power cable and this will likely cause a problem obtaining a stable reading.

3.1.3.12 Taking Readings, Operation of the GK-401 Readout Box

The GK-401 is a basic readout for all Vibrating Wire Deformation Meters.

Connect the Readout using the flying leads or in the case of a terminal station, with a connector. The red and black clips are for the vibrating wire gage, the green or blue clip for the shield drain wire.

1. Turn on the Readout. Turn the display selector to position "B" as shown in Table 3-3. Readout is in "digits" as described in section 3.2.2.13, Equation 3-6.
2. Turn the unit on and a reading will appear in the front display window. The last digit may change one or two digits while reading. Record the value displayed. The unit will automatically turn itself off after approximately 4 minutes to conserve power.

3.2.3.13 Deformation Calculation

The basic units utilized by Geokon for measurement and reduction of data from Vibrating Wire Deformation Meters are "digits". The units displayed by the GK-401 in position "B" as shown in Table 3-3 are digits.

To convert digits to deformation the following Equation applies;

Deformation = (Current Reading - Initial Reading) x Calibration Factor x Conversion Factor or

$$D = (R_1 - R_0) \times C \times F \dots \dots \dots (3-6)$$

Where; R_1 is the Current Reading.
 R_0 is the Initial Reading usually obtained at installation as described in section 3.2.2.10).

C is the Calibration Factor, usually in terms of millimeters or inches per digit.
 F is an engineering units conversion factor (optional) as shown in Table 3-6.

Table 3-6, Engineering Units Conversion Multipliers

From → To ↓	Inches	Feet	Millimeters	Centimeters	Meters
Inches	1	12	0.03937	0.3937	39.37
Feet	0.0833	1	0.003281	0.03281	3.281
Millimeter	25.4	304.8	1	10	1000
Centimeter	2.54	30.48	0.10	1	100
Meters	0.0254	0.3048	0.001	0.01	1

For example, the Initial Reading (R_0) at installation of a deformation meter with a 25 mm transducer range is 4250 digits. The Current Reading (R_1) is 6785. The Calibration Factor is 0.00619 mm/digit. The deformation change is;

$$D = (6785 - 4250) \times 0.00619 = +15.692 \text{ mm}$$

Note that increasing readings (digits) indicate increasing extension.

3.2.2.14 Temperature Correction

The Model 4430 Deformation Meter has a very small coefficient of thermal expansion so in most cases correction is not necessary. However, if maximum accuracy is desired or the temperature changes are extreme ($>10^\circ \text{C}$) corrections may be applied. The following Equation applies;

$$D_{\text{corrected}} = ((R_1 - R_0) \times C) + ((T_1 - T_0) \times K) + L_c \dots \dots \dots (3-7)$$

- Where;
- R_1 is the Current Reading.
 - R_0 is the Initial Reading.
 - C is the Calibration Factor.
 - T_1 is the Current Temperature.
 - T_0 is the Initial Temperature.
 - K is the Thermal Coefficient.
 - L_c is the correction for the gage length.

Tests have determined that the Thermal Coefficient, K, changes with the position of the transducer shaft. Hence, the first step in the temperature correction process is determination of the proper Thermal Coefficient based on the following Equation;

Thermal Coefficient = ((Reading in Digits x Multiplier) + Constant) x Calibration Factor or

$$K = ((R_I \times M) + B) \times C \dots\dots\dots(3-8)$$

Table 3-7 shows the Multiplier and Constant values used in Equation 3-8. The Multiplier (M) and Constant (B) values vary for the stroke of the transducer used in the Deformation Meter.

Table 3-7, Thermal Coefficient Calculation Constants

Model:	4430-12 mm	4430-25 mm	4430-50 mm
Multiplier (M):	0.000295	0.000301	0.000330
Constant (B):	1.724	0.911	0.415
Transducer Length (L):	267 mm	267 mm	292 mm

The gage length correction (L_c) is calculated using Equation 3-9.

$$L_c = 17.3 \times 10^{-6} \times L \times (T_I - T_o) \dots\dots\dots(3-9)$$

Where L is the length of deformation meter in millimeters or inches, minus the transducer length as shown in Table 3-7 in millimeters or inches, respectively.

Consider the following example using a Model 4430 Deformation Meter with a 1 meter gage length and 25 mm transducer.

$$R_o = 4250 \text{ digits } R_I = 6785 \text{ digits } T_o = 10^\circ \text{C}$$

$$T_I = 20^\circ \text{C}$$

$$C = 0.00619 \text{ mm/digit}$$

$$K = ((6785 \times 0.0003) + 0.911) \times 0.00619 = 0.01824$$

$$L = 1000 - 267 = 733$$

$$L_c = 17.3 \times 10^{-6} \times 733 \times (20 - 10) = 0.1268$$

$$D_{\text{corrected}} = ((R_I - R_o) \times C) + ((T_I - T_o) \times K) + L_c$$

$$D_{\text{corrected}} = ((6785 - 4250) \times 0.00619) + ((20 - 10) \times 0.01824) + 0.1268$$

$$D_{\text{corrected}} = (2535 \times 0.00619) + (10 \times 0.01824) + 0.1268$$

$$D_{\text{corrected}} = 15.692 + 0.1824 + 0.1268 \quad D_{\text{corrected}} = 16.001 \text{ mm}$$

As can be seen from the above example, the corrections for temperature change are small and can often be ignored.

3.2.2.15 Environmental Factors

Since the purpose of the Deformation Meter installation is to monitor site conditions, factors which may affect these conditions should always be observed and recorded.

Seemingly minor effects may have a real influence on the behavior of the structure being monitored and may give an early indication of potential problems. Some of these factors include, but are not limited to: blasting, rainfall, tidal levels, excavation and fill levels and sequences, traffic, temperature and barometric changes, changes in personnel, nearby construction activities, seasonal changes, etc.

3.2.2.16 Specifications

Table 3-8 shows general specifications of Deformation Meter model 4430.

Table 3-8, Model 4430 Specifications

Gage Length:	1 meter
Ranges Available:	12, 25, 50 mm
Overran e:	115%
Accuracy:	0.1 % (with polynomial expression)
Stability:	< 0.2%/ (under static conditions)
Temperature Range:	-40 to +60°C
Frequency Range:	1200 - 2800 Hz
Coil Resistance:	180 Ω , $\pm 10 \Omega$
Cable Type:	2 twisted pair (4 conductor) 22 AWG Foil shield, PVC jacket, nominal OD=6.3 mm
Length: (end to end)	1 meter
Diameter:	26.7 mm (body) 51 mm (flange)
Weight:	1 kg

3.2.3 Vibrating Wire Readout (Model GK-401)

Figure 3-19 shows a photo of Vibrating Wire Readout Box, model GK-401.

3.2.3.1 Applications

The model GK-401 Vibrating Wire Readout Box can be used with all of Geokon's vibrating wire gages and transducers in all kinds of weather conditions. The rugged and reliable, user friendly GK-401 provides the following...

- Portability;
- Easy operation;
- Control via microprocessor;
- High accuracy and resolution;
- Waterproofed enclosure and
- Rechargeable batteries Cold weather operation.



Figure 3-19 - Model GK-401 Vibrating Wire Readout Box

3.2.3.2 Operating Principle

The Model GK-401 Vibrating Wire Readout Box is a portable, waterproofed, battery-operated instrument for the readout of all Geokon vibrating wire gages and transducers.

Gages are read out by connecting them to the readout box using the input plug or patch cord provided. The box is switched on and set to the appropriate display setting, whereupon the gage reading is displayed on a 5-digit liquid crystal display (LCD).

It also manipulates the data to provide a readout directly in engineering units (strain gages) or in units proportional to pressure, load, etc. (piezometers, total pressure cells, etc.).

3.2.3.3 Advantages and Limitations

The microprocessor utilizes an ultra-stable 6 MHz quartz oscillator for control and timing functions.

The gage is plucked or excited by a swept square wave frequency pulse and senses the period of vibration of the return signal to a resolution of 0.1 microseconds. A program function for reading weak gages is provided automatically. There are five separate switch positions for different readout functions as shown in Table 3-3.

3.2.3.4 Technical Specifications

Table 3-9 shows technical specifications of the Readout Box.

Table 3-9, Technical Specifications of Vibrating Wire Readout Box

Excitation Range	400 Hz to 6000 Hz, 5 Volt Square Wave
Measurement Resolution	0.1 μ s
Timebase Accuracy	0.01%
Temperature Range	-10°C to +50°C
Battery (Rechargeable)	(<i>type</i>) Nickel Hydride 7.2 V, 3 Ah (life) 10 hours (<i>charger</i>) 115 V \pm 10% 50-60 Hz
Weight	2.25 kg
LxWxH	165 x100 x215 mm

3.2.3.5 Theory of Operation

The GK-401 Vibrating Wire Readout is used to excite and read out vibrating wire gages which include: strain gages, crackmeters, piezometers, total pressure cells, etc. The basic principle is that a wire that is held under tension has a specific natural or resonant frequency of vibration which is dependent on the strain and the length of the wire. If the wire is plucked, as in a stringed instrument, the frequency will always be the same provided that the strain and length do not change. Vibrating wire gages have specific fixed lengths of wire, and the change in strain is measured by measuring the change in vibration frequency. The readout box provides the means of exciting the wire and reading the resultant frequency.

In use, a pulse of varying frequency is generated by the Readout Box and is applied to an electromagnetic coil assembly which is located close to the sensing wire. When a frequency corresponding to that of the wire is generated, the wire is "plucked" and vibrates at that frequency. The wire continues to vibrate after the "pluck" ends and a signal, primarily the resonant frequency, is induced in the coil assembly and transmitted to the readout where it is conditioned and displayed.

The GK-401 amplifies the return signal, converts it to a square wave and counts 255 cycles of vibration. This is then manipulated by the processor to display the required units: period, frequency squared or microstrain. For weaker gage signals the processor counts fewer cycles to try to obtain consistent readings during the signal period.

3.2.3.6 Taking Readings

Different gages have different frequency characteristics and the GK-401 has a 6-position selector: five positions with specific functions and one general position for period readout.

Generally, positions B, C, D and E are used for all Geokon gages as shown in Table 3-3. Position A is used to obtain period of vibration readings for gages in the range of approximately 500 to 5000 Hz. Table 3-3 shows the model numbers, readout positions and pertinent information.

To take readings the gage is connected via the patch cord to the readout, the readout display is set to the proper position and the box is turned on. A reading will appear in the display and should remain constant, plus or minus one digit. The readout will turn itself off after approximately 4 minutes. The reading is updated once a second and the display is updated only when the reading changes. Readings should be checked against previously recorded data and any unusual data should be retaken and noted.

3.2.3.7 Data Reduction

Individual gage instruction manuals discuss how data is taken, recorded and reduced, but a few important procedures for taking data are noted here:

- 1) Always take zero or no load readings and record pertinent data which may include but not be limited to: temperature, barometric pressure, weather conditions, water levels, fill levels, nearby construction activity, etc. Initial readings properly obtained are the baseline for all further measurements.
- 2) Always obtain stable readings; if a reading fluctuates be sure to note it.

- 3) Compare current readings with previous readings while at the site; numbers sometimes get transposed in notebooks.
- 4) Use permanent notebooks or field data sheets whenever possible.

3.2.3.8 Maintenance and Trouble Shooting

- **Battery**

The GK-401 uses one 12-volt rechargeable, lead acid type battery to run the Readout. This battery has an extremely long shelf life and will lose approximately 2% of it's charge per month sitting on the shelf. At 60°F (15°C) the box will operate continuously for a minimum of 20 hours; at -20°F (-30°C) this period is cut to less than 10 hours. At higher temperatures the capacity goes up however, the useful service life decreases.

This battery can be expected to last 3 to 5 years, or between 250 and 500 discharge and recharge cycles.

Recharging is accomplished by a charger, which is included with each readout. Overnight (10 to 12 hours) is usually long enough to bring the battery to full charge. The charger can be left plugged in whenever the Readout is not in use (recommended) to ensure full charge on the battery at all times. As the battery ages, the on-time will be reduced, and at some point, will be very short and recharging will not help. At this point the battery will need to be replaced. Battery packs are available from Geokon, or a battery can be purchased locally as described in Section 3.2.3.10 for battery specifications.

3.2.3.9 Readout System

If the readout system fails to operate properly, and the cause is not the battery, Geokon should be contacted. The unit should not be opened in the field. A few checks can be made, however:

- If zeros appear in the display with gages connected, patch cords should be checked for continuity between contacts and clip leads.
- The gage itself should be checked.
- The processor may need to be reset, which can be accomplished by turning the unit off and on.
- The selector position may be incorrect. Positions are described in Table 3-3.

- Noise levels may be excessive; try reading a gage in a different area; try connecting the ground lead (white or green clip) to the shield drain wire.

3.2.3.10 Specifications

Table 3-10 shows general specifications of Readout Box GK-401.

Table 3-10, GK-401 Readout Box Specifications

Excitation Range:	450 to 6000 Hz, 170 to 2250 μ seconds
Measurement Range:	400 to 9500 Hz, 105 to 2500 μ secods
Measurement Resolution:	Period: 0.1 μ second
	Strain: 1 μ strain
Accuracy:	0.1 % of reading
Excitation:	5 volt square wave
Temperature Range:	-20° to +120°F, -30° to +50°C
Oscillator Frequency:	6.144 MHz
Display:	5-digit LCD, .7" high
Battery:	(1) 12 volt Panasonic lead acid
Battery Capacity:	2.0 Amp Hour
Operating Current:	110 mA
Operating Time:	minimum 20 hours @ 60°F
Dimensions:	165x 102x216mm
Weight:	2.3 kg.

3.2.3.11 Reading Other Manufactures Instruments

Most vibrating wire gages available today have frequency characteristics that are within the range of operation of the GK-401 Readout Box, and if they have the type of electromagnetic coil that is used in the pluck and read system of the GK-401, it can be used to read them.

Gage factors need to be known in order to convert readings to engineering units. The reading can be taken in the period mode, Position A and, conversions to strain, pressure, etc. can be made using the manufactures' factors supplied with the gages.

Table 3-11 lists approximate operating frequency ranges for different wire lengths for reference.

Table 3-11 Vibrating Wire Length vs. Frequency Range

Wire Length	Frequency Range
1"	2500-5000Hz
2"	1200-3000Hz
3"	825-2000Hz
4"	600-1600Hz
6"	450-1000Hz
10"	250-650Hz

3.3 Field Testing Programme

3.3.1 Method of Project Construction

Alignment of the gabion wall was determined on the ground by surveyors using surveying equipment, thediolite. Excavation for the apron of the wall was carried out for each two or three stations (100m to 150m). Two meters depth of sand of toe was excavated with slope 1:2 to form a trapezoidal section until the design level reached where a layer of geotextile was laid to avoid the rocks eroding into the sub-layers. The excavated area was filled by rocks with 80-230 kg in weight. A filter media of crushed stone, layer of standard base course of 40 cm thickness, was placed before laying the coarse rock. The purpose of laying this layer was to protect the geotextile from apron rocks and to work as a filter for the apron. The main objective of using geotextile was to prevent sand entering gabions.

Therefore, the permeability of geotextile has to be high to prevent collection of water behind gabions which causes hydrostatic pressure. A woven geotextile material was used for this purpose. The rocks were filled and on the top of the apron rocks a layer of crushed stone, base course, of 40 cm thickness was laid, levelled by a grader and compacted very well using a heavy compactor, 15 ton capacity.

Galvanized steel gabion boxes of 2*1*1m size were used. Gabions were constructed manually using intensive labour force. Gabion steel boxes were installed in the place first after preparing and compacting the land under it. The volume of rocks filled in the galvanized steel gabion boxes varies from 110mm to 230mm The rocks were filled one by one where the largest has to be in front to avoid rocks getting out from the steel mesh. The geotextile has to be located between the steel mesh and backfill material to prevent sand from entering the gabion.

The new slope of the cliff was constructed at 1:2.5 which will be safe against sliding or over turning. The sand was used as fill material behind the gabion

wall. This type of backfill is matching the project specifications and available at the local market.

Figure 3-20 shows a general view of gabion retaining wall constructed at different levels including the apron as foundation of the wall.

3.3.2 Site Preparation for Tests

The site prepared for conducting earth pressure tests is located at a place about 720m north of the starting point of the project, UNRWA's Sanitation Office at Beach camp. The location is about 20m north of a stormwater culvert No.64 next to Blakhya area adjacent to the coastal road. According to the project drawings the location lies at 20m north of station No. 14. At this location, these gabions form a retaining wall consists of 2 rows, 2.0m height, 1.0m for each. The thickness of the gabion wall is 2.0m at the first row and 1.0m at the second row.

The internal face of the gabion retaining wall, next to backfilling, was covered with geotextile material to prevent sand entering gabions.

The site was excavated manually to a depth of 1.5m until reaching the lower level of the gabion wall, top level of the apron and the width of excavation was about 2.0m, the length of excavation was about 4.0m.

3.3.3 Test Procedures:

3.3.3.1 For Loose Case:

The site at the selected location of experiments was excavated up to 1.5m below the surface level of the gabion retaining wall. The soil was levelled carefully without any type of compaction.

One of the vibrating wire earth pressure cell was placed horizontally on the soil to measure the vertical earth pressure. The cable connecting the cell with the readout box was embedded in the sand and this cable was marked by using coloured labels. (black colour) at the part of the cable laid on the top of the ground near the readout box location. This mark was a temporary classification to avoid confusion during taking the readings.

The other one of vibrating wire earth pressure was placed vertically adjacent to the gabion retaining wall to measure the horizontal earth pressure. The cable connecting the device with the readout box was embedded in the sand and this cable was marked of (red colour) at the part of the cable laid on the top of the ground near the readout box location as temporary classification in order to avoid confusion when taking the readings of horizontal earth pressure.

The third device, vibrating wire deformation meter, was placed adjacent to the location of the two pressure cells in a position perpendicular to the gabion retaining wall to measure the deformation. The cable connecting the deformation meter with the readout box was embedded in the sand. This cable was marked by using coloured labels (green colour) at the part of the cable laid on the top of the ground near the readout box location as temporary classification when taking the reading of deformation. Figure 3.21 shows positions of each of the three devices installed behind the gabion retaining wall.

The three cables were covered by PVC flexible conduits as sleeves to protect these cables from damage and to ensure that each cable is free to move. Initial readings (R0) were taken separately for each of the three devices since each device was connected separately with the Readout Box. The Readout Box can read from one device only at one time.

The vertical earth pressure reading was taken after connecting the cable marked with the black colour lable with the readout box, the horizontal earth pressure reading was taken after connecting the cable marked with the red colour lable with the readout box and the deformation reading was taken by of the cable connecting the deformation meter device which marked with the green colour lable with the readout box. All three readings taken were digit numbers and they were considered as initial readings before laying the sand on the top of the devices behind the gabion retaining wall.

The backfill soil (sand) was placed carefully on the top of the devices on layers. To ensure reaching the Loose Case, the soil was laid using PVC buckets where the soil was distributed and scattered horizontally on layers until reaching the top level of the gabion wall.

Final readings as second readings (R1) were taken separately for each of the three devices using the same practice used in the initial readings. The different colours given to each of the cables were taken into consideration when specifying the type of pressure (horizontal, vertical or deformation). These readings were digit numbers.

The difference between each two readings was converted to pressure or deformation values using formulas given by the manufacturer of the devices (Geokon Company) as shown in the description of the devices in sections 3.1.2.13 and 3.1.3.14 respectively.

After completion of above stage of 1.5m below the surface, the sand was excavated and removed carefully from the top of the devices. The three devices were removed and put aside. The sand was backfilled and levelled using the same procedures mentioned above until reached a depth of 1.0m below the surface of the gabion wall.

The devices were placed at this level and the same steps used in the case of 1.5m above were repeated for this case where initial and final readings were taken.

After completion of above stage of 1.0m below the surface, the sand was excavated and removed carefully from the top of the devices. The three devices were removed and put aside. The sand was backfilled and levelled until reaching a depth of 0.50m below the surface of the gabion wall using the same procedures mentioned above.

The devices were placed at this level and the same steps used in the above two cases (1.5 & 2.0m) were repeated where initial and final readings were taken.

After completion of this stage of 0.5m below the surface the sand was excavated and removed carefully from the top of the devices. The devices were removed and prepared for the next test.

3.3.3.2 For Medium Case

The same procedures and steps used in the Loose Case were repeated except for the state of the backfill soil where the sand was compacted using a steel hand tamper to reach the medium case.

3.3.3.3 For Dense Case

The same procedures and steps used in the above two cases were repeated except for the state of the backfill soil where the sand was wetted and compacted using a steel tamper and vibrating steel plate to reach the dense case. A laboratory compaction test was conducted in this case to ensure reaching the dense state. The results showed 100% compaction as described in the Test Results (Chapter 4).

3.3.3.4 Other Tests

The rest of position of the devices for other different tests are listed in Table 3.12 Figure 3.21 shows the position of the devices installed adjacent to the gabion retaining wall and , detailed of placing one of earth pressure calls inside the soil.

Table 3.12: Placement of Devices at different levels behind the gabion wall.

<i>Test No.</i>	<i>Compaction Status</i>	<i>Deformation meter, Vertical and Horizontal Earth Pressure Cells Level (m)*</i>	<i>Remarks</i>
1	Loose Case	0.5	Horizontal, vertical and deformation, loose case where sand dropped from fixed distance (about 10cm) using PVC buckets.
		1.0	
		1.5	
2	Medium Case	0.5	Horizontal, vertical and deformation, medium case, where sand was compacted manually by steel hand tamper only.
		1.0	
		1.5	
3	Dense Case	0.5	Horizontal, vertical and deformation, dense case, the sand was wetted and compacted by steel tamper and steel vibrating plate.
		1.0	
		1.5	
4	Dense Case	0.5	Horizontal earth pressure.
		1.0	
5	Dense Case	0.5	Horizontal earth pressure with loading case at 50cm from edge of the wall.
		1.0	
6	Dense Case	0.5	Horizontal earth pressure with loading case at 100cm from edge of the wall.
		1.0	
7	Dense Case	0.5	The same as above with loading case at 150cm from edge of the wall.
		1.0	
8	Dense Case	0.5	The same as above with loading case at 25cm from edge of the wall.
		1.0	
9	Dense Case	0.5	Horizontal earth pressure with inclination of surface of sand at different angles.
		1.0	
10	Loose Case	0.5	Horizontal earth pressure, loose case as described in test No.1 above.
		1.0	
11	Loose Case	0.5	Horizontal earth pressure only with loading case at 25cm from edge of the wall.
		1.0	
12	Loose Case	0.5	The same as above with loading case at 50cm from edge of the wall.
		1.0	
13	Loose Case	0.5	The same as above with loading case at 100cm from edge of the wall.
		1.0	

* The level mentioned in the table is the level measured from the surface of the gabion wall up to the level of placing the devices.

Table 3.12: (continued)

Test No.	Compaction Status	Deformation meter, Vertical and Horizontal Earth Pressure Cells Level (m)*	Remarks
14	Loose Case	0.5	The same as above with loading case at 150cm from edge of the wall.
		1.0	
15	Loose Case	0.5	Horizontal earth pressure with inclination case at different angles.
		1.0	
16	Medium Case	0.5	Horizontal earth pressure only.
		1.0	
17	Medium Case	0.5	Horizontal earth pressure with loading case at 25cm from edge of the wall.
		1.0	
18	Medium Case	0.5	The same as above with loading case at 50cm from edge of the wall
		1.0	
19	Medium Case	0.5	The same as above with loading case at 100cm from edge of the wall
		1.0	
20	Medium Case	0.5	The same as above with loading case at 150cm from edge of the wall
		1.0	
21	Medium Case	0.5	Horizontal earth pressure with inclination of surface of sand at different angles
		1.0	
22	Medium Case	1.0	Horizontal earth pressure.
		1.5	
23	Medium Case	1.0	Horizontal earth pressure, second loading case at 25cm from edge of the wall.
		1.5	
24	Medium Case	1.0	The same as above with loading case at 50cm from edge of the wall.
		1.5	
25	Medium Case	1.0	The same as above with loading case at 100cm from edge of the wall.
		1.5	
26	Medium Case	1.0	The same as above with loading case at 150cm from edge of the wall.
		1.5	
27	Medium Case	1.0	Horizontal earth pressure with indication at different angles.
		1.5	
28	Medium Case	1.0	Horizontal earth pressure, deformation and internal movement at loading case at 25cm from edge of the wall.
		1.5	

* The level mentioned in the table is the level measured from the surface of the gabion wall up to the level of placing the devices.

Fig 3.20

Fig 3.21

Chapter 4

Test Results

4.1 Introduction

This Chapter presents the result of tests conducted during the design stage, implementation of the project as well as the tests carried out for the purpose of this study. The soil of the cliff was tested during the design works and other construction materials such as backfill sand, base course, rocks and geotextile were tested during construction of the gabion retaining wall.

The results of these tests are important to show the behavior of the gabion retaining wall under lateral earth pressure. Special experimental tests were carried out during the course of this study on the backfill sand, in order to determine the compaction and to measure lateral earth pressure forces and deformation affecting the gabion wall. The value of coefficient of earth pressure (k) was calculated by knowing vertical and horizontal pressure.

The results of these tests are described in this chapter. The analysis of results and comparison among them are discussed in the following chapter No. 5.

4.2 Soil Investigation Results during Design Stage

In order to collect the necessary data for the geotechnical design an extensive soil investigation programme was carried out through the Arab Center Laboratory.

The field investigation consisted of 6 boreholes, carried out using the rotary air flush and the water circulation drilling methods. Three deep boreholes were carried out on top of the cliff (to a depth of 20 m) and three shallow ones down at the beach (to a depth equal to 5 m). At regular intervals split spoon samples were taken. Furthermore, standard penetration tests were carried out in order to assess the formation strength. The laboratory tests were focusing mainly on soil classification and determination of strength properties of the soils encountered.

For a detailed description of the soil investigation programme, test results and resulting foundation recommendations reference was made in the final report from the Arab Center on site investigation for Beach Camp Coastal Defence Project, Beach Camp Gaza, Palestine GS 98001, dated February 1998. From this report the following conclusions are drawn:

- According to the particle size distributions the soil in the project area consists mainly of medium to fine sand with gravels of sandstone and occasionally with a relatively small silt and clay fraction as well.

- The phreatic water level was encountered at an elevation varying between almost zero and 0.3 m above mean sea level (MSL) in the shallow boreholes and between 0.2 m and 1.6 m + MSL in the deep boreholes.
- Dry densities (volumetric weights) were reported to vary between 13.9 kN/m³ (1420 kg/m³) and 17.1 kN/m³ (1745 kg/m³) for the minimum and maximum dry density (volumetric weight) respectively.
- From the standard penetration test results, it was concluded that the soil material encountered can be classified as medium dense with respect to its relative compaction.
- From the direct shear box tests and the unconsolidated (undrained) triaxial tests, carried out on samples prepared in different dry densities, the correlation between the effective peak friction angle and the dry density was established.
- From the points above the formation peak friction angle was estimated at 31 to 33 degrees.

4.3 Backfill Sand Test Results During Construction Stage

Field density tests were carried out on the soil used for backfilling behind the gabion wall. About 20 tests were conducted at several points along the gabion wall. The results of these tests showed that the maximum dry density varied between 16.87 kN/m³ (1.72 g/cm³) and 17.17 kN/m³ (1.75 g/cm³) while the compaction ratio varied between 95 and 103%.

4.4 Rocks Test Results during Construction Stage

Tests to specify gabion stone grading, impact value, specific gravity, absorption and soundness were conducted during construction of the gabion retaining wall, which extended from January 2002 until December 2003. The majority of tests were carried out through the Islamic University Laboratory and part of these tests were conducted through the Arab Centre Laboratory for the purpose of cross checking of results.

Stone Fill Material in the Apron as well as Stone Fill Material in the Gabion Boxes were tested and the results of these tests are summarized in the following sections within this chapter.

4.4.1 Stone Fill Material in Apron

- *Description of Rocks:*

The rocks used in the stone fill material in the apron were described as dark brown dolomatic limestone ($\text{CaCO}_3 + \text{MgCO}_3$).

- *Grading:*

Gabion stone grading was determined for 9 samples which were taken randomly during supplying of rock materials.

The size of rocks was determined by measuring three dimensions X, Y and Z and the weight of each piece were recorded.

The size of about 80% of the samples was found to be between 125mm and 510mm matching the project specifications. About 10% of the rocks were found to be less than 125mm and about 10% of the rocks their size was larger than 510mm which is allowed according to the project specifications.

- *Impact Value:*

The Impact Value was determined for 9 samples according to B.S.812 specifications as required by the project specifications. The max Impact Value according to these specifications is 30%.

The result of Impact Value varied between 16.6% and 30.3% which is acceptable.

- *Specific Gravity:*

The results of 9 samples tested at the laboratory showed that the specific gravity varied between 24.62 kN/m³ (2.51 g/cm³) and 27.66 kN/m³ (2.82 g/cm³). The specified limit is 2.6 g/cm³ according to B.S.812. The results are acceptable.

- *Absorption:*

The absorption ratio found by testing of 9 samples varied between 0.11% and 3.00% which lies within the specified range, max. 3.0% according to B.S.812.

- *Soundness:*

The soundness test results for 9 samples found to be between 0.14% and 0.90%. The project specification is 18% max. according to ASTM C88-90.

4.4.2 Stone Fill Material in Gabion Boxes

- **Description of Rocks:**

The rocks used in the fill of gabion boxes were limestone boulders.

- **Grading:**

The grading of rocks of gabion boxes was determined to several samples taken randomly during supplying of rock materials.

The size of majority of rocks was found to be between 110mm and 230mm according to the project specifications.

About 10% of the rocks size was less than 110mm and about 10% of the rocks size was larger than 230mm which is allowed according to the specifications.

The size of rocks was determined by measuring three dimensions X, Y and Z and the weight of each piece was recorded.

- **Impact Value:**

The Impact Value was determined for 6 samples according to B.S.812 specifications. The values varied between 9.88% and 24.2% within the allowable value, 30% max. according to the above specifications.

- **Specific Gravity:**

The results of 6 samples tested showed that the specific gravity was between 2.59 g/cm³ and 2.81 g/cm³. The specified limit is 2.6 g/cm³ according to B.S.812.

- **Absorption:**

The absorption ratio found by testing of 6 samples varied between 0.7% and 3.05% which lies within the specified range, max. 3.0% according to B.S.812.

- **Soundness:**

The soundness test results conducted for 6 samples found to be between 0.098% and 0.899%. The project specification is 18% max. according to ASTM C88-90.

4.5 Test Results of Base Course Filter for Apron

This type of base course of 40cm thickness was laid directly on the surface of geotextile underneath the big size rocks. The gradation test results showed that the base course size varied between 3 and 10cm as per the project specifications. About 10% of the amount was smaller than 3cm and 10% larger than 10cm and this is allowed according to the specifications.

4.6 Test Results of Base Course Surface Apron

A base course layer of 40cm was laid on top surface of the apron. This layer was leveled and compacted by 15 ton, capacity heavy roller. The Plasticity Index of the base course was determined for several samples and found between 1.31% and 6%, the specific gravity between 2.6 g/cm³ and 2.75 g/cm³ and Loss Angeles was between 25% and 40%. The results are acceptable according to the project specifications.

4.7 Test Results of Geotextile Material during Construction Stage

The geotextile material was tested in the Netherlands due to unavailability of equipment and experience to test such type of materials in the local laboratories.

Static Puncture Test was carried out according to ISO 12236(1996). The results for 5 samples were between 4.96 kN and 5.51 kN and the average was 5.342kN, within the acceptable range.

The result of average tensile strength for 5 samples tested was 40.82 kN/m, the strain at max tensile strength was 15.53% as average, the breaking strength was 8.53 kN/m and the strain at failure was 19.61%.

All results were acceptable and within the specifications of the project. Photos of the test preparation and the equipment used in carrying out these tests of geotextile material are shown in Appendix B.

4.8 Test Results of Experimental Case Study

4.8.1 Backfill Sand Results

The sand used in the backfill behind the gabion retaining wall was tested. Three samples were taken and the results of the test are summarized in Table 4-1. The result of degree of Compaction in the dense case was 100% according to the Field test carried out during the course of experiments.

Table 4-1 Test Results of Backfill Sand During Experiments.

Sample No.	Dry Density kN/m ³	Water Content %	Void Ratio %	Internal Friction Angle (degree)	Description
1	17.5	4	48.6	42.2	Dense, 100% Compaction
2	16.3	4	59.5	32.2	Medium
3	15.0	4	73.3	25.3	Loose

4.8.2 Lateral Earth Pressure Results

Horizontal and vertical earth pressures as well as the deformation were measured using vibrating wire devices, two load cells and a deformation meter. About 28 tests were conducted and each test was carried out at different depths measured from the surface of the gabion wall. Loads were placed at different distances from the internal edge of the gabion retaining wall. These loads were increased gradually from 600kg up to 1800kg and readings were taken during each change in depth, loading and distance. Details about one of these tests is shown in section 4.8.2.1 and summary of the whole results is described in section 4.8.2.2.

Table 4-2, presents the lateral earth pressure, K value and deformation for loose case as an example. The readings were taken in digits then vertical, horizontal earth pressures, value of coefficient of earth pressure (k) and the deformation were calculated using relevant formulas described in chapter 3.

The Figures 4.1, 4.2 and 4.3 show samples of these results together with the plotted curves. Table 4-3 summarizes the test results of all 28 tests carried out during the course of study including the relevant curves. Full details about these tests together with the curves are shown in Appendix A.

4.8.2.1 Results of Loose case experiment, Tests No.1

- **Information about the test:**

Location: station No. 14+20m, 20m north of culvert No.64

Date: 21/06/03

Temp. : 28 C

Calibration factor for horizontal pressure cell (Ch)=0.1196 (kPa/digit)

Calibration factor for vertical pressure cell (Cv)=0.1299 (kPa/digit)

Calibration factor for deformation meter (Cd)=0.01828 (mm/digit)

Type of soil: sand

Compaction status: loose case by using screen 5x5 cm size

Table 4-2 Lateral Earth Pressure, K value and Deformation for Loose Case

Depth (m)	Roh (digit)	R1h (digit)	Rov (digit)	R1v (digit)	Ph (kPa)	Pv (kPa)	K	Rod (digit)	R1d (digit)	Deformation (mm)
0					0	0	0			
0.50	8764	8752	8978	8906	1.4352	9.3528	0.15345	5034	5226	3.50976
1.00	8746	8726	8966	8837	2.392	16.7571	0.14275	5156	5150	-0.10968
1.5	8728	8711	8934	8807	2.0332	16.4973	0.12324	5109	5125	0.29248

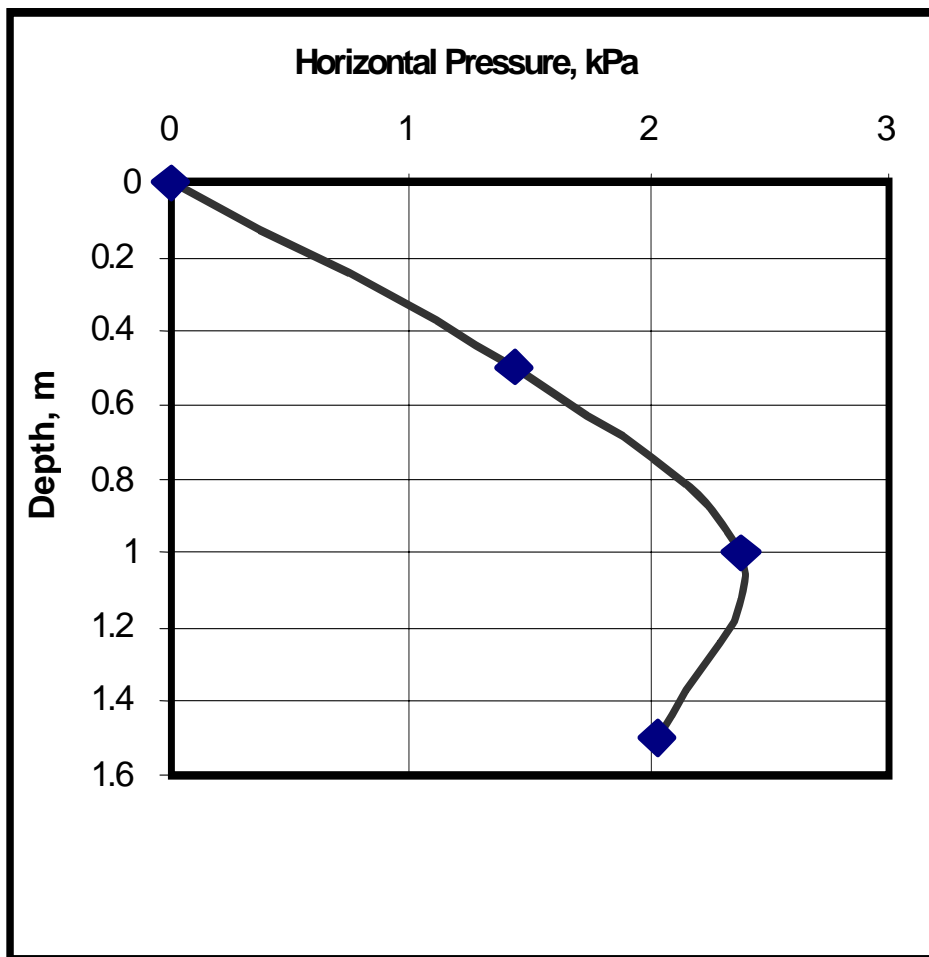


Figure 4.1 Horizontal Earth Pressure versus Depth

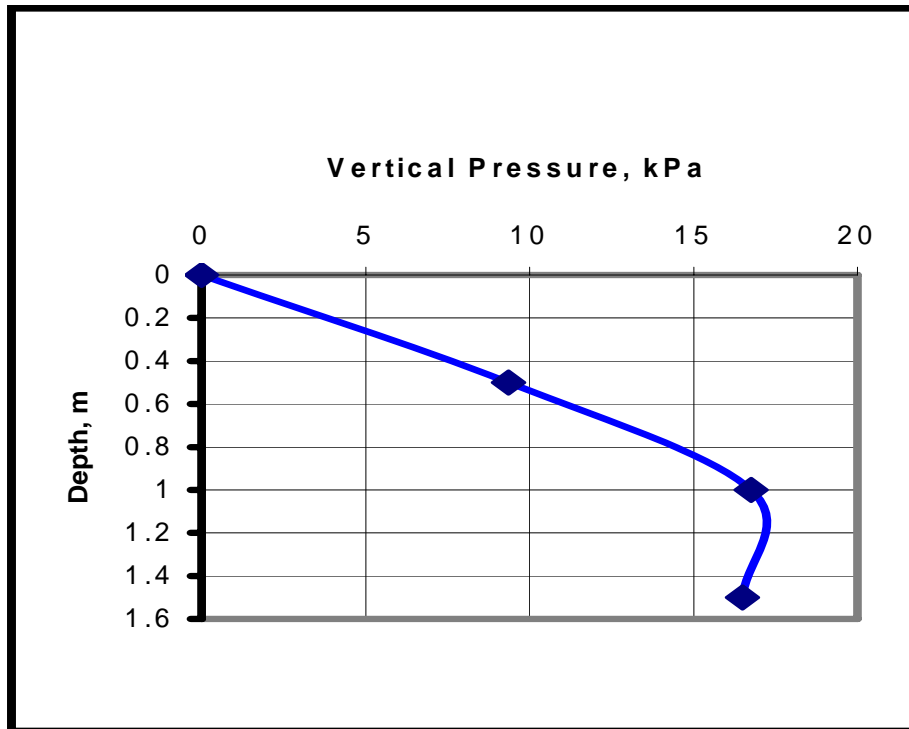


Figure 4.2 Vertical Earth Pressure versus Depth

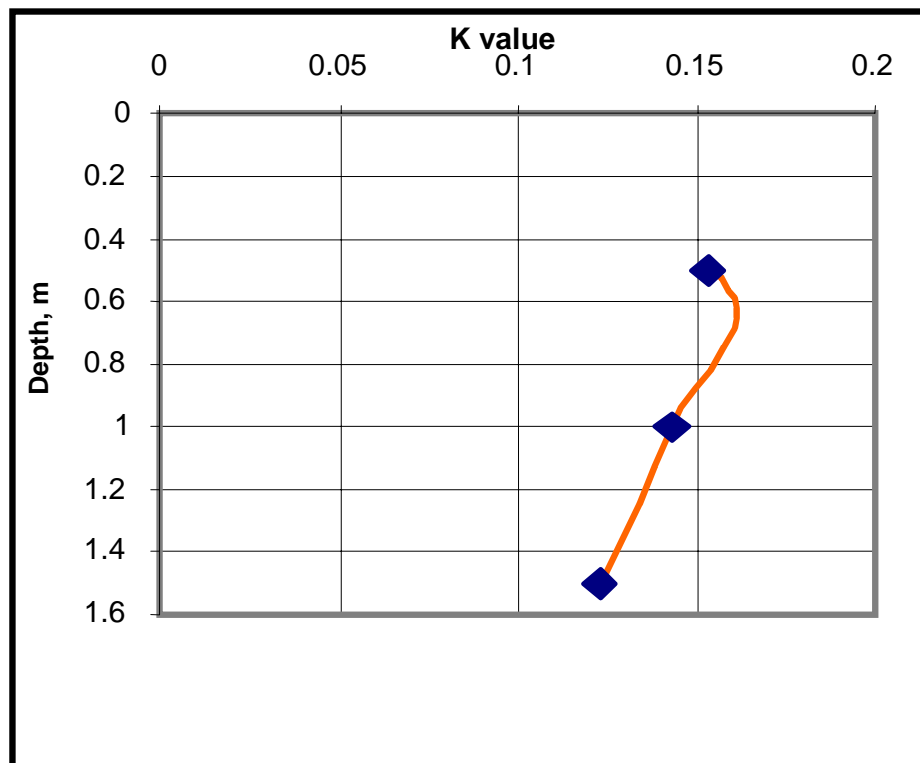


Figure 4.3 Earth Pressure Coefficient (k) versus Depth

4.8.2.2 Results of all Tests

The results of all tests carried out during the course of the study are summarized in Table 4-3. Full details about these tests including the relevant curves are shown in Appendix A.

Table 4-3: lateral Earth Pressure, k value and Deformation Test Results, All Cases

Test No.	Depth ⁽¹⁾ (m)	Horizontal Pressure (kPa)	Vertical Pressure (kPa)	K	Deformation (mm)	Case Description
1.	0.5	1.4352	9.3528	0.15345	3.80	Loose Case without Loading
	1.0	2.3920	16.7571	0.14275	0.50	
	1.5	2.0332	16.4973	0.12324	0.30	
2.	0.5	4.0664	11.1714	0.3640	0.53	Medium Case without Loading
	1.0	4.5448	17.2767	0.26306	0.24	
	1.50	4.9368	17.2767	0.40151	0.10	
3.	0.5	4.7840	12.8601	0.3720	0.30	Dense Case without Loading
	1.0	7.1760	22.9923	0.3121	0.22	
	1.50	6.9368	21.5634	0.32169	0.07	
4.	0.5	5.1960				Dense Case without Loading
	1.0	9.5680				
5.	0.5	0.5196				Dense Case with 1800 kg Loading at 50cm ⁽²⁾
	1.0	-2.990				
6.	0.5	-0.3897				Dense Case with 1800 kg Loading at 100cm
	1.0	-0.25116				
7.	0.5	-0.9093				Dense Case with 1800 kg Loading at 150cm
	1.0	-3.4684				
8.	0.5	0.9093				Dense Case with Loading 600, 1200 and 1800kg respectively at 25cm
		1.4289				
		1.6887				
	1.0	0.9568				
		1.4352				
2.0332						
9.	0.5	2.9877				Dense Case with inclination 10°, 15° and 20°, without Loading
		3.1176				
		2.4681				
	1.0	2.0332				
		2.0332				
1.7940						
10.	0.5	3.7671				Loose Case without Loading (Repeated Test)
	1.0	5.1428				

(1) Measured from the top surface of the gabion wall.

(2) Measured from the back face of the gabion wall in contact with the soil.

Table 4-3: lateral Earth Pressure and Deformation Test Results (Continued)

Test No.	Depth ⁽¹⁾ (m)	Horizontal Pressure (kPa)	Vertical Pressure (kPa)	K	Deformation (mm)	Case Description
11.	0.5	1.8186 3.7671 5.1960				Loose Case with Loading 600, 1200 and 1800kg respectively at 25cm
	1.0	0.7176 1.3156 2.6312				
12.	0.5	0.2598 0.9093 1.5588				Loose Case with Loading 600, 1200 and 1800kg respectively at 50cm
	1.0	0.1196 0.3588 1.0764				
13.	0.5	0.1299 0.2598 0.5196				Loose Case with Loading 600, 1200 and 1800kg respectively at 100cm
	1.0	0.1196 0.1196 0.3588				
14.	0.5	0.2598 0.2598 0.0000				Loose Case with Loading 600, 1200 and 1800kg respectively at 150cm
	1.0	0.1196 0.1196 0.2392				
15.	0.5	0.0000 0.2598 0.3897				Loose Case with inclination 10°, 15° and 20°, without Loading
	1.0	-0.2392 0.0000 0.2392				
16.	0.5	6.7548				Medium Case without Loading or inclination (Repeated Test)
	1.0	7.0564				
17.	0.5	1.4289 3.6372 5.5857				Medium Case with Loading 600, 1200 and 1800kg respectively at 25cm
	1.0	0.9568 1.4352 2.1528				
18.	0.5	0.7794 2.2083 3.7671				Medium Case with Loading 600, 1200 and 1800kg respectively at 50cm
	1.0	0.3588 0.9568 1.5548				

(1) Measured from the top surface of the gabion wall.

Table 4-3: lateral Earth Pressure and Deformation Test Results (Continued)

Test No.	Depth ⁽¹⁾ (m)	Horizontal Pressure (kPa)	Vertical Pressure (kPa)	K	Deformation (mm)	Case Description
19.	0.5	0.5196 1.0392 1.6887				Medium Case with Loading 600, 1200 and 1800kg respectively at 100cm
	1.0	0.2392 0.4784 0.8372				
20.	0.5	-0.1299 0.0000 0.3897				Medium Case with Loading 600, 1200 and 1800kg respectively at 150cm
	1.0	0.5000 0.1196 0.2392				
21.	0.5	0.5196 0.5196 -0.2598				Medium Case with inclination 10°, 15° and 20°, without Loading
	1.0	-0.1196 -0.1200 0.0000				
22.	1.0	4.3056				Medium Case without Loading or inclination (Repeated Test)
	1.5	8.5734				
23.	1.0	1.0764 1.9140 1.4352				Medium Case with Loading 600, 1200 and 1800kg respectively at 25cm (Repeated Test)
	1.5	0.6495 0.9090 1.2990				
24.	1.0	1.0764 2.7510 3.1096				Medium Case with Loading 600, 1200 and 1800kg respectively at 50cm (Repeated Test)
	1.5	0.1299 0.6500 1.1691				
25	1.0	0.7176 1.1960 1.6744				Medium Case with Loading 600, 1200 and 1800kg respectively at 100cm
	1.5	0.2598 0.5200 1.0392				
26.	1.0	0.0000 0.1200 0.2392				Medium Case with Loading 600, 1200 and 1800kg respectively at 150cm
	1.5	-0.1300 0.0000 0.2598				

(1) Measured from the top surface of the gabion wall.

Table 4-3: lateral Earth Pressure and Deformation Test Results (Continued)

Test No.	Depth ⁽¹⁾ (m)	Horizontal Pressure (kPa)	Vertical Pressure (kPa)	K	Deformation (mm)	Case Description
27.	1.0	0.5980				Medium Case with inclination 10°, 15° and 20° respectively (Repeated Test)
		0.7180				
	1.5	0.3588				
		0.1299				
		0.3900				
28.	1.0	29.0630			23.6726	Medium Case with Internal Movement and Loading at 25cm.
	1.5	1.4289				

(1) Measured from the top surface of the gabion wall.

Chapter 5

Data Analysis and Discussion

5.1 Introduction

Lateral earth pressure magnitude and distribution problems are encountered in retaining walls. In general, it is not a well-defined and fixed quantity, depending upon the soil nature, interaction between the structure and the soil and is a function of the deflections and deformations of the structure (Prakash, 1981). The classical earth pressure theories were presented by Coulomb (1776) and Rankine (1857). Other theories are adding improvements over the earlier theories. However, if a retaining wall does not undergo any movement, as an abutment of a basement, none of these theories is applicable. The stability of a gravity retaining wall (e.g. gabion) is due to the self-weight of the wall. Cantilever walls of reinforced concrete are more economic because the backfill itself is used to provide most of the required dead weight (Craig, 1992). For general case, Rankine or Coulomb theories are used for the calculation of lateral pressures. The question of lateral earth pressures on gabion retaining wall will be studied in detail.

For the medium case about 5 tests were repeated for several amounts of loading and inclination angles with respect to horizontal. The purpose of this repetition was for double checking of the results. The difference between the results found to be negligible, therefore, the mean values of these results were used in the analysis.

5.2 Measured Vertical and Horizontal Pressures

In Figures 5.1 and 5.2 the measured vertical and lateral earth pressures have been plotted as a function of depth. The pressure gradually increases up to some depth (about 0.6m) and then starts to decrease for the case under study. It should be noted that once the lateral earth pressure is achieved to the maximum value at a certain depth, further reduction in the horizontal pressure occurs with depth increasing, as shown in Figure 5.2. The coefficient of lateral earth pressure (k) for the three conditions of sand (i.e loose, medium, and dense cases) is calculated.

For the case of an inclination ground soil surface, values of inclination angle with horizontal 10, 15, and 20 degrees are prepared. The increment in lateral pressure was recorded in two levels (0.5 and 1 m). For the dense sand case the measured increment pressure values are plotted versus depth as shown in Figure 5.3.

5.3 Additional Lateral Earth Pressures

Loads due to roadways machinery, and other influences resting on the soil surface in the vicinity of the gabion wall cause an increment in the lateral pressures on the wall.

In this case study, it is found necessary to investigate the effect of additional loads (surcharge), acting on the soil surface behind the wall, on lateral earth pressures. However, in order to estimate the lateral increment of loaded gabions, dead weights 1x1 square meter footing were prepared to be placed in a distance of 25, 50, 100 and 150cm behind the gabion internal face. In the model field tests reported in the previous section, increment in lateral pressure was measured in two levels (0.5 and 1.0). Maximum increment in lateral pressure occurs at 0.5 m depth as shown in Figures 5.4, 5.5 and 5.6, due to the loads (6, 12, and 18 kPa) that have been applied on 25cm away from the gabion face.

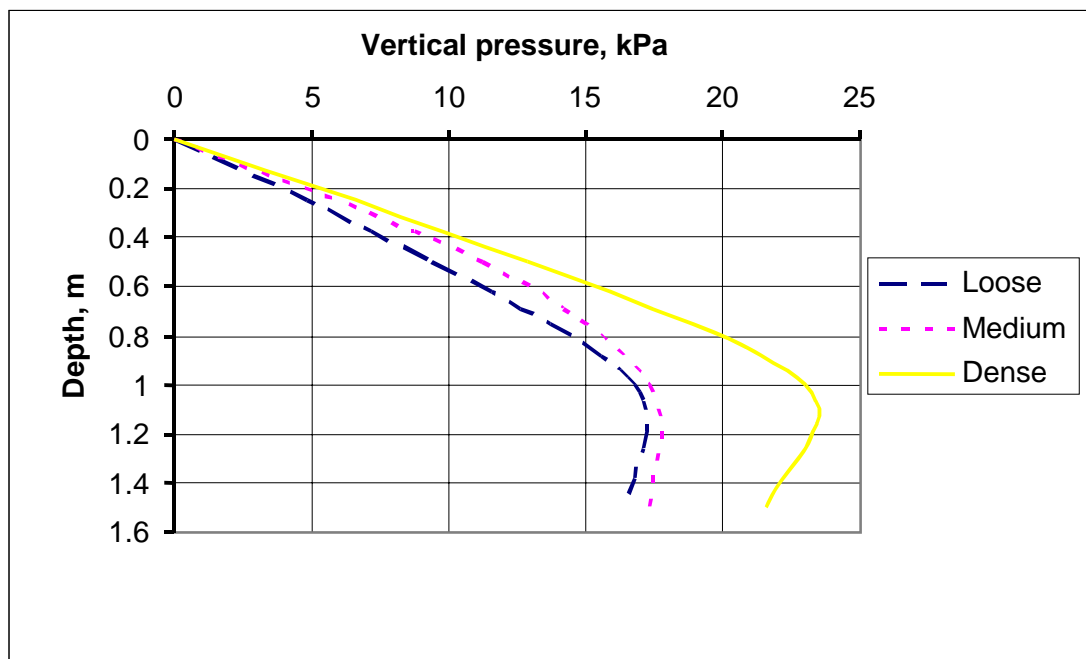


Figure 5.1 Depth versus Vertical Pressure for Horizontal Soil Surface.

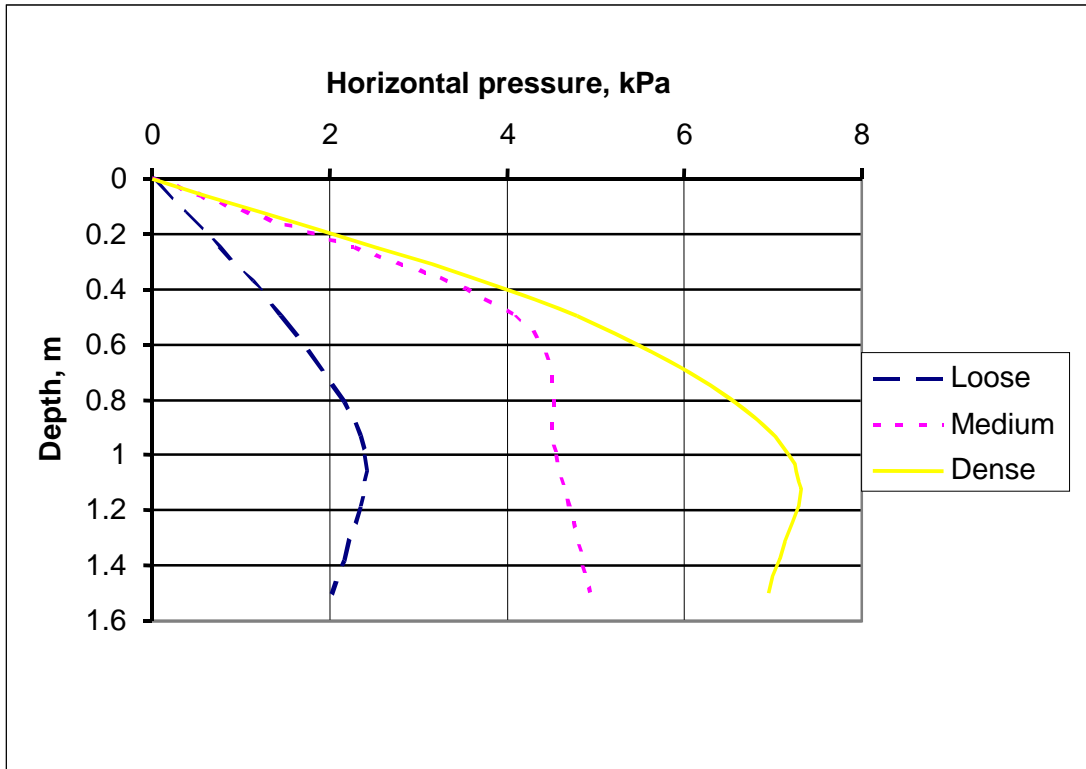


Figure 5.2 Depth versus Horizontal Pressure for Horizontal Soil Surface.

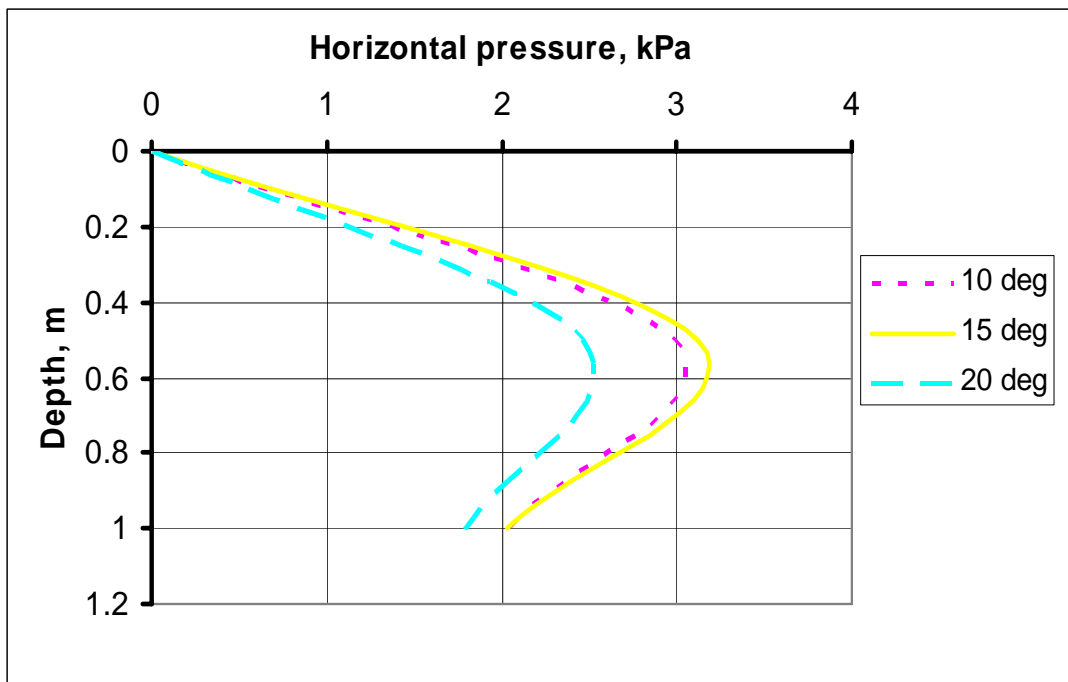


Figure 5.3 Depth versus Increment of Horizontal Pressure due to Soil Surface Inclinations (Dense Case).

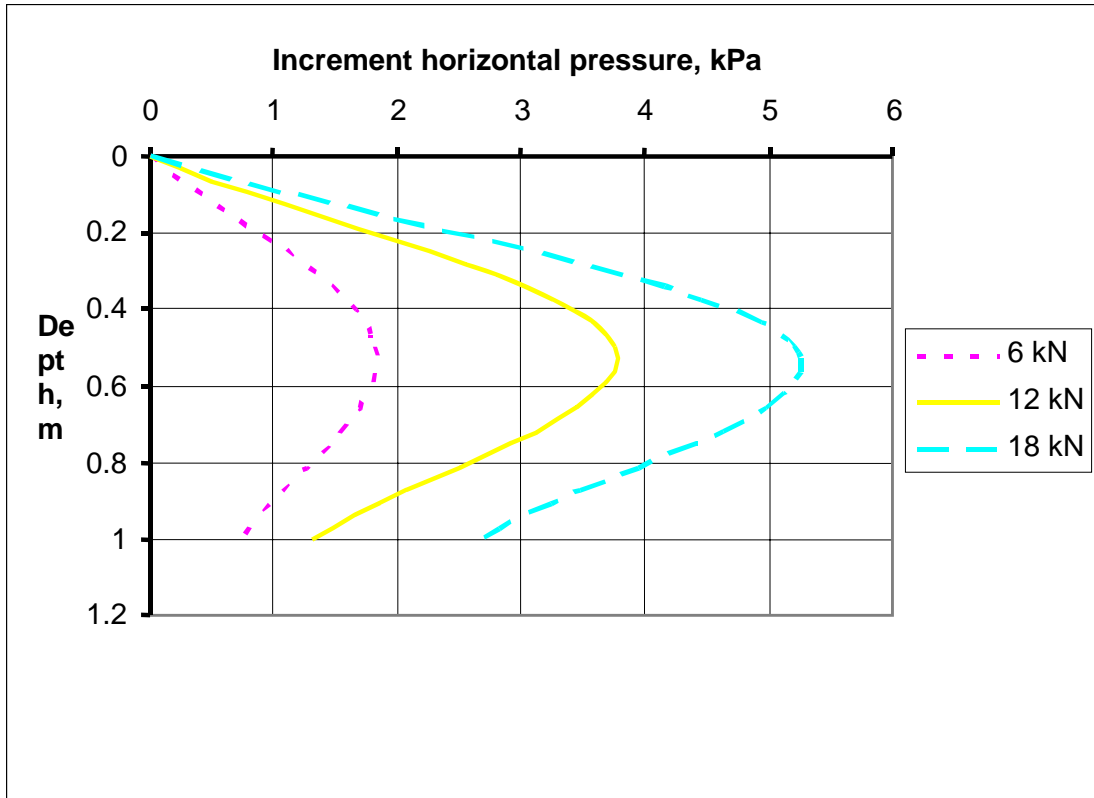


Figure 5.4 Depth versus Loading Increment at 25 cm from the Gabion Face (Loose Case)

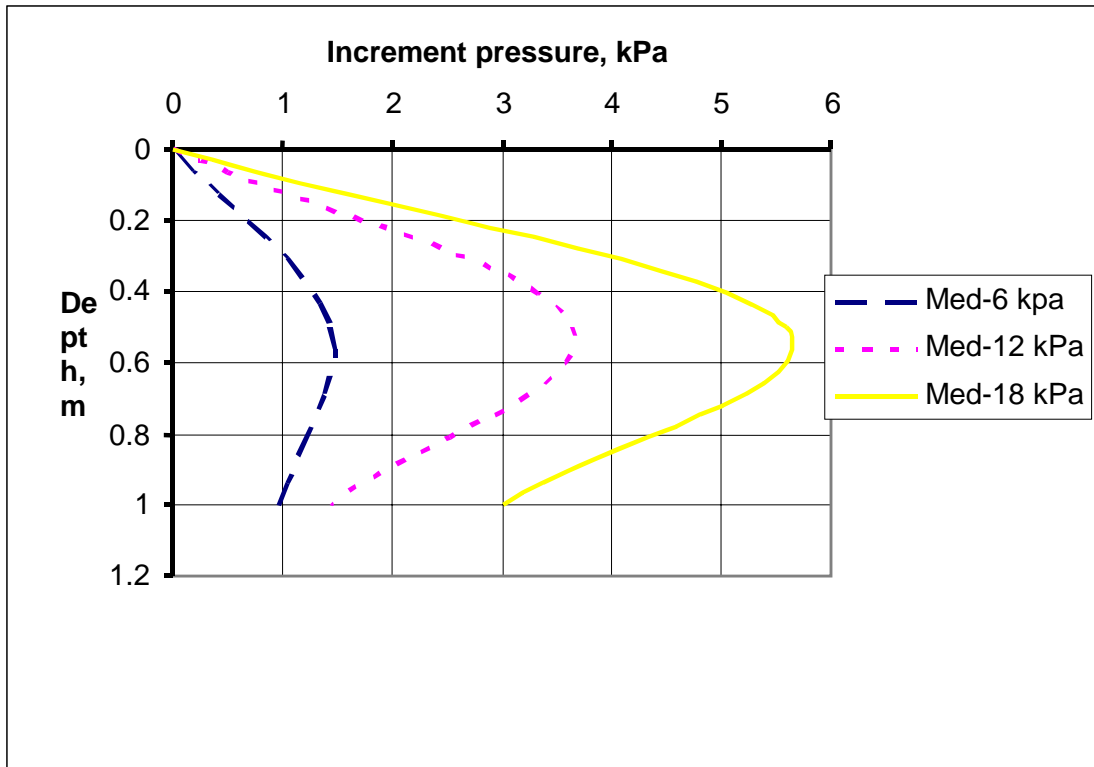


Figure 5.5 Depth versus Increment Load due to Square Footing at 25 cm (Medium Sand Filling)

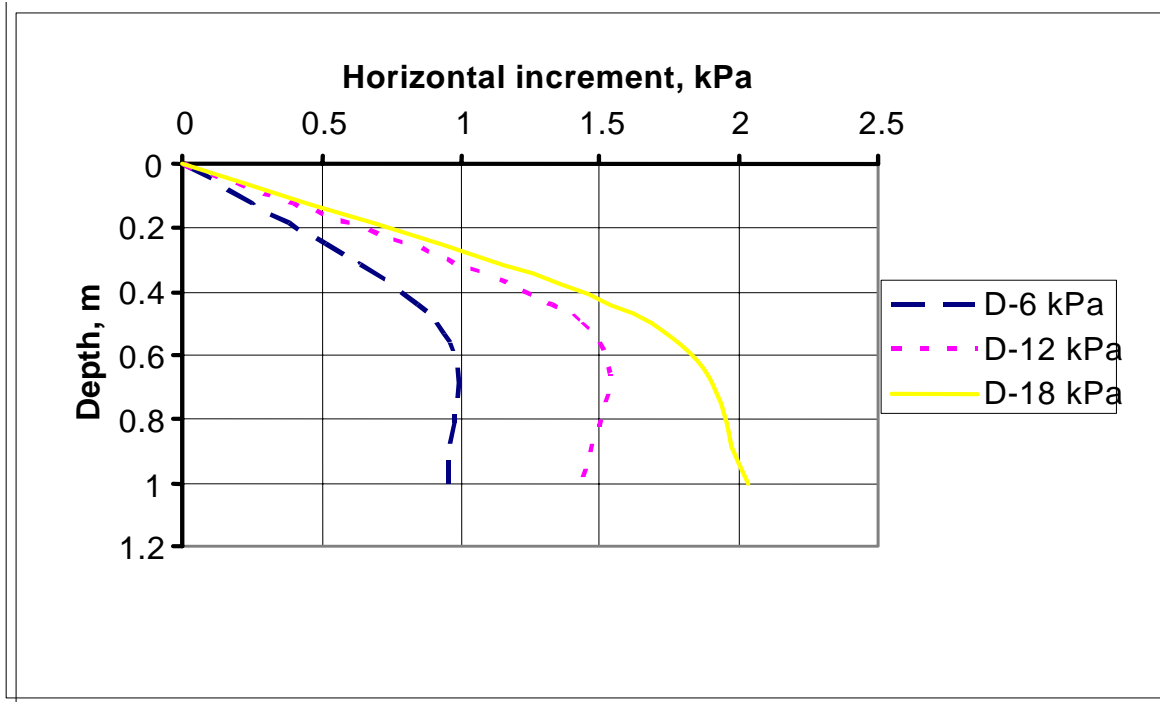


Figure 5.6 Depth versus Increment Loading (25 cm, Dense Case)

To obtain a particular effect of distance between the applied load and the gabion wall (d), it is found necessary to plot the relationship between depth and applied load with respect to their distances. In Figures 5.7, 5.8, and 5.9 increments in horizontal pressure due to 6 kPa loading is plotted for values of horizontal distances 25, 50, 100, and 150 cm. It can be seen that as the applied load distance from the internal face increases the corresponding increment pressure decreases. It is found that as the distance increases more than 150cm, the effect of the surcharge becomes minimum and can be neglected. Further, from the same figures it is obvious that the transferred increment pressure through the loose sand is more than that of medium and dense cases. Loose, Medium and dense cases have been used to evaluate the effect of the horizontal distance from the head of the wall to the edge of the applied load on the increment in the lateral earth pressure. The distance at which the increment in the lateral earth pressure is small almost zero, is called safe distance. It is found that the safe distance in loose sand is more than dense and medium ones. In general, it can be taken as 1.5m in loose sand and 0.5 for dense sand as listed in Table 5-1. There is a good agreement between the calculated safe distance and measured one. It can be concluded that, the increment in lateral earth pressures due to area loads varies with depth below the ground surface and with horizontal distance perpendicular to the wall.

Table 5-1: Summary of Safe Horizontal Distance (d) in (m)

q (kPa)	Loose		Medium		Dense	
	Measured	Calculated	Measured	Calculated	Measured	Calculated
6	>1.5	1-1.5	1-1.5	1-1.5	0.50	0.5- 1
12	-	1.5-2	-	1-1.5	-	0.5-1
18	-	1.5-2	-	1-1.5	-	1-1.5

5.4 Coefficient of Earth Pressure (K)

The values of lateral earth pressure coefficient (K) for the case of a vertical wall and horizontal soil surface are given in some engineering codes. In general, the coefficient K depends on the values of soil shear parameters. The selection of an appropriate value of the angle of internal friction (Φ) is of most importance in finding K value. The difficulty is clear in strains variety throughout soil mass and in particular along the failure surface. In the earth pressure theories, the strain effect is neglected and a constant value of Φ is assumed throughout the soil above the failure surface.

The average values of the measured K along the investigated depth are 0.14, 0.30 and 0.33 corresponds to loose, medium, and dense sands respectively as shown in Figure 5.12. It should be noted; however, that the calculated values of K obtained from Rankine's theory are normally differs from corresponding measured values. This trend is obvious in Figures 5.13 and 5.14.

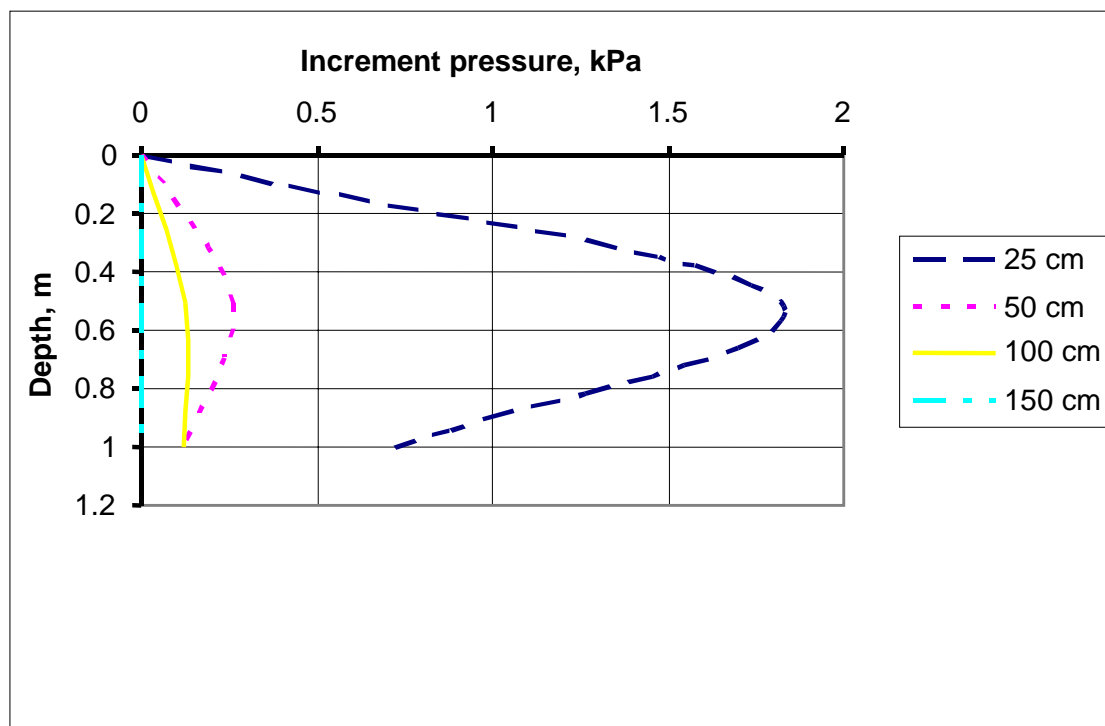


Figure 5.7 Depth versus Pressure Increment due to 6 kPa Loading at Different Surface Distances (Loose Case)

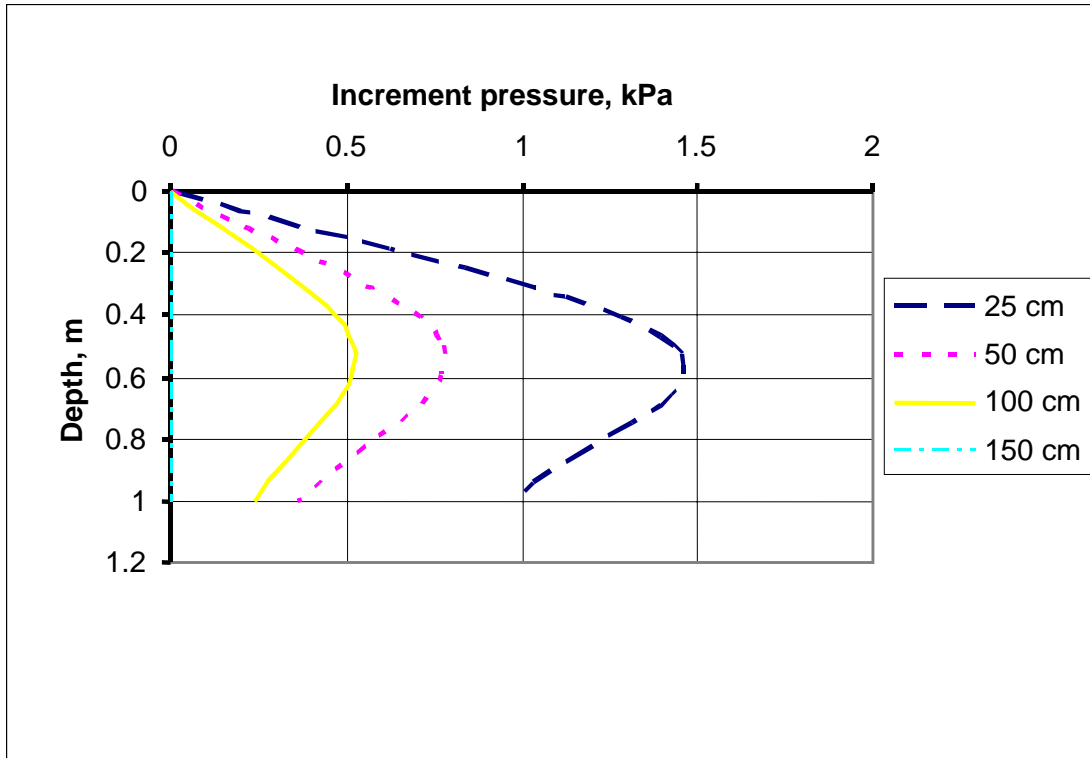


Figure 5.8 Depth versus Increment Load due to 6 kPa with Different Surface Distances (Medium Case).

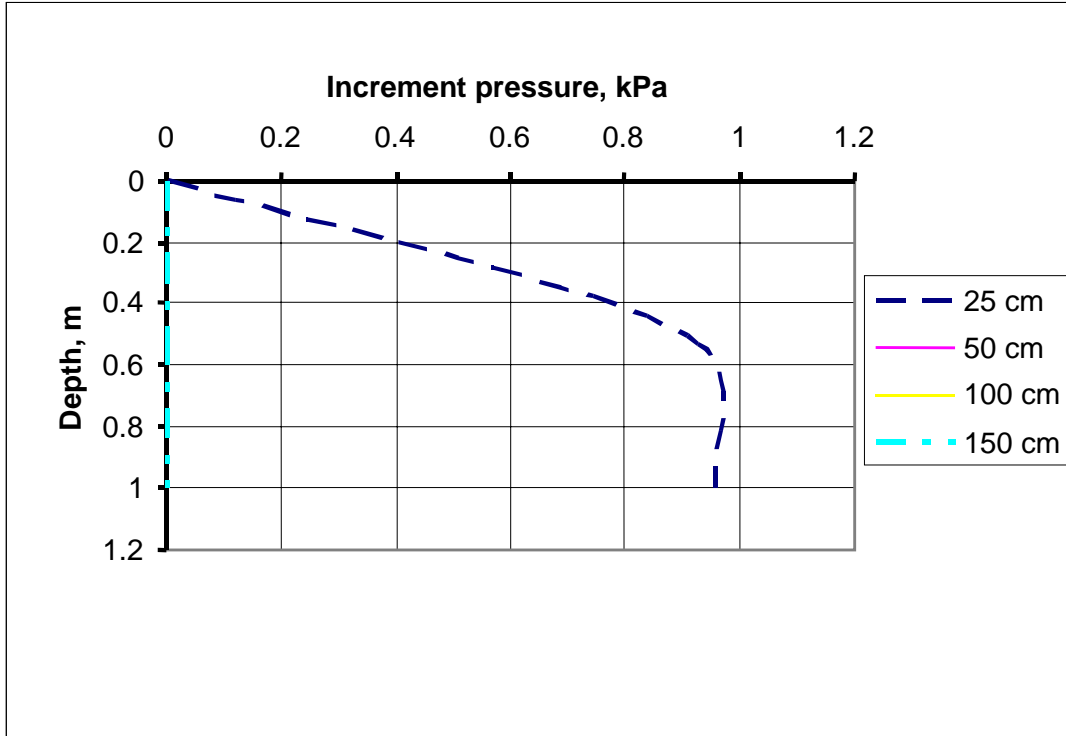


Figure 5.9 Depth versus Increment Load due to 6 kPa with Different Surface Distances (Dense Case).

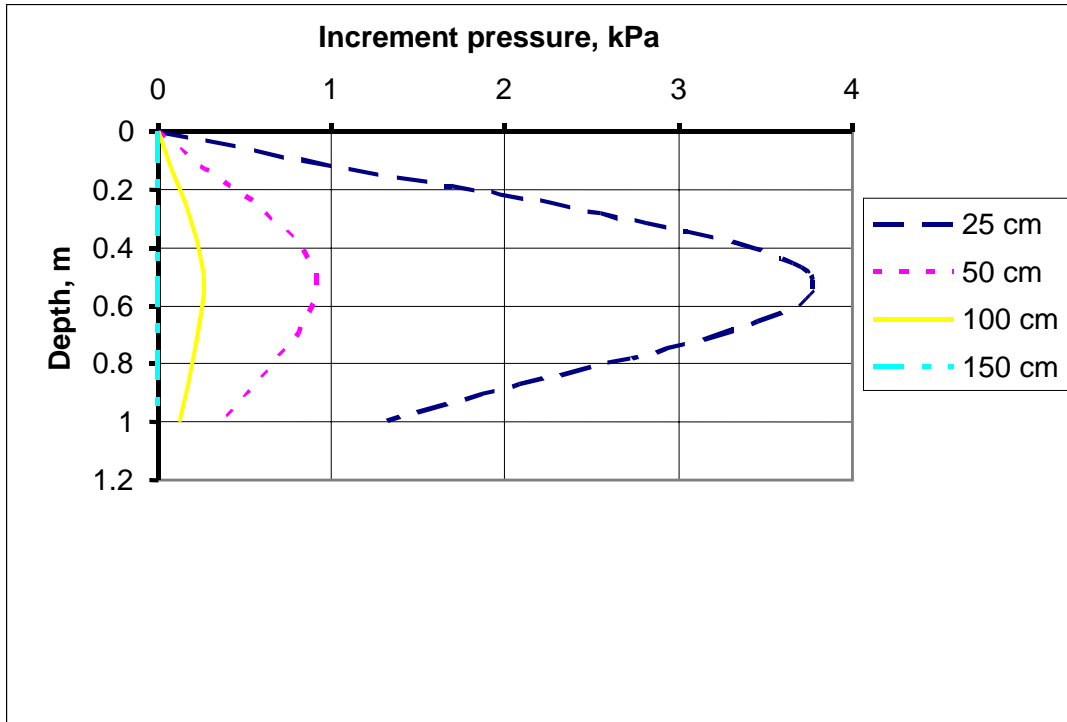


Figure 5.10 Depth versus Pressure Increment due to 12 kPa Loading at Different Surface Distances (Loose Case)

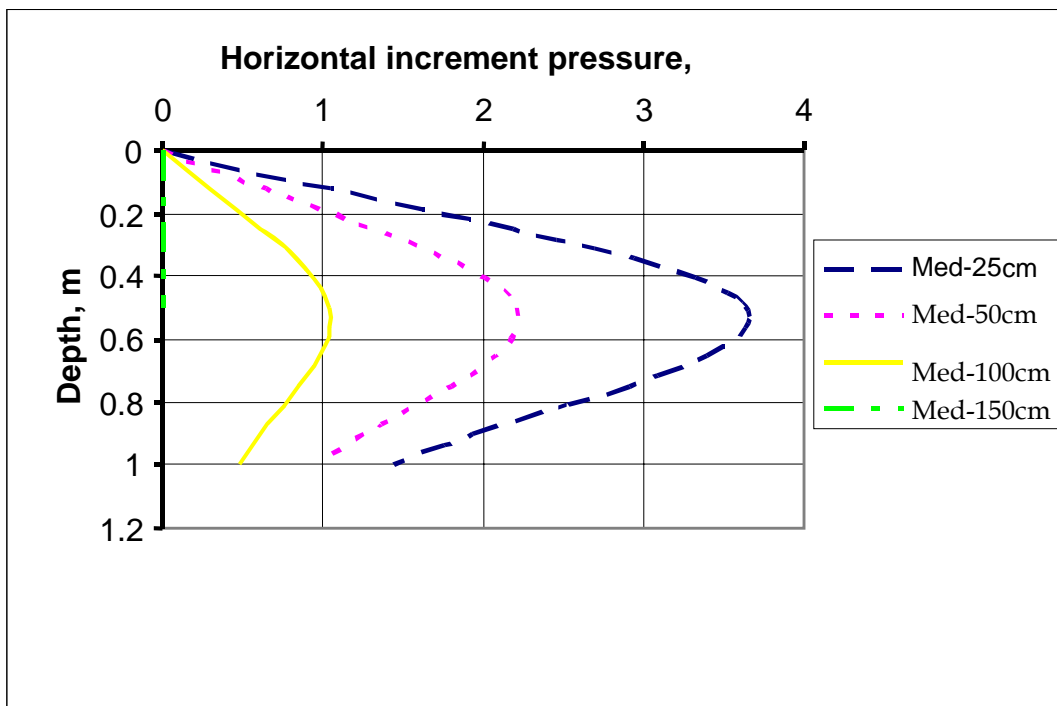


Figure 5.11 Depth versus Horizontal Increment due to 12 kPa (Medium Sand).

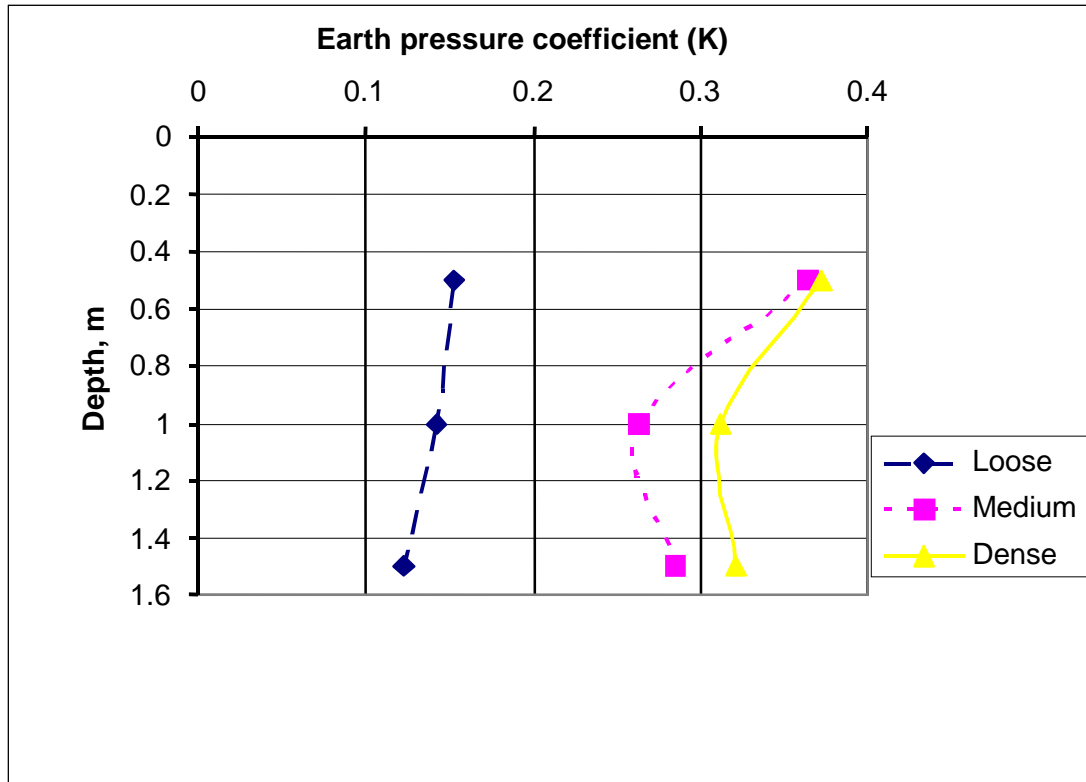


Figure 5.12 Earth Pressure Coefficients versus Depth for Three Sand Cases.

5.5 Displacement Analysis

It was mentioned in the above section that the displacement of retaining walls is important to apply the Rankine and other theories. It is worth mentioning that the displacement, the vertical and horizontal earth pressures were measured simultaneously during measuring lateral earth pressure due to the soil weight. Figure 5.15, shows the measured soil displacement at three different levels from the surface of the wall. It is obvious that the displacement decreases as the depth from the surface increases. According to U.S. Army Corps of Engineers material, (ASCE, 1996), they indicate that in a loose case, a movement of the wall away from the fill by 0.3 percent of the wall height is adequate to develop active earth pressure condition.

The measured value of movement at a depth of 50cm below the wall surface in loose case, is found to be about 4mm which is within the limit specified above, 4.5mm. These results prove that we have reached the active condition in the loose case. However, the occurred displacements in both medium and dense cases were not adequate to reach the limit specified by ASCE and hence creation of an active case was not achieved as in the loose case. This could justify the considerable difference found between values of estimated K, from the measured horizontal and vertical pressures, and the calculated ones. The above conclusion for medium and dense cases is in agreement with Goh, 1993, as mentioned in Chapter 2.

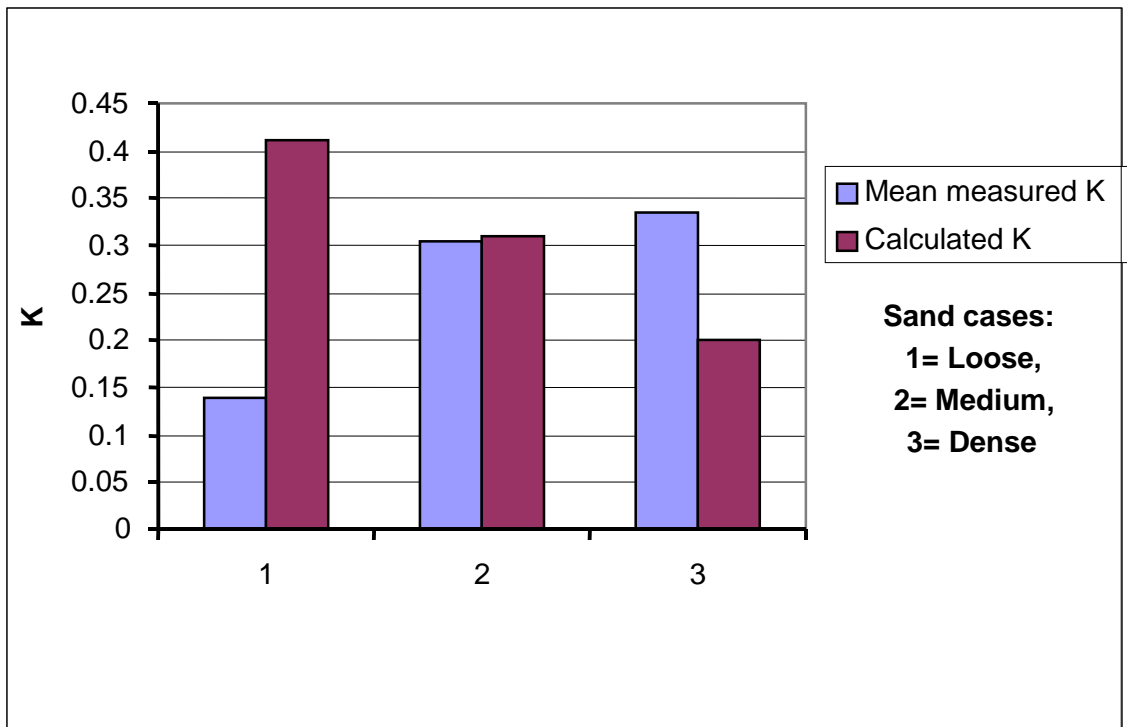


Figure 5.13 Comparison between the Measured and Calculated K Values.

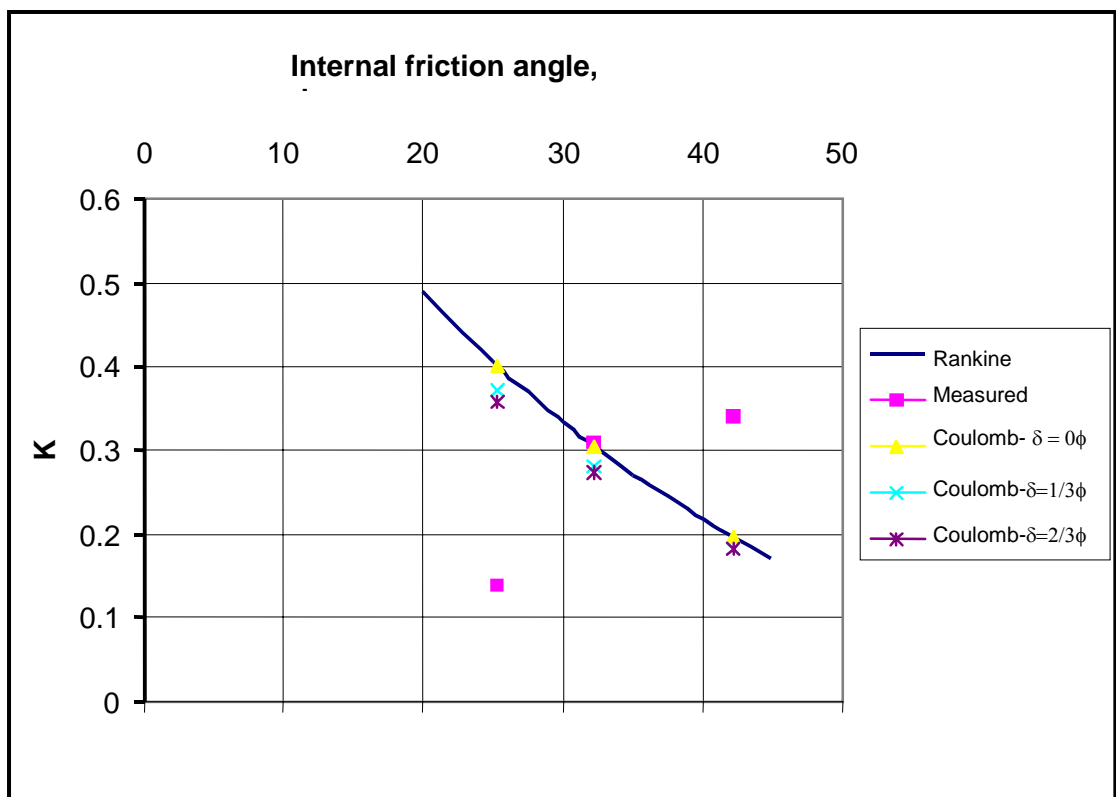


Figure 5.14 K versus Internal Friction Angle.

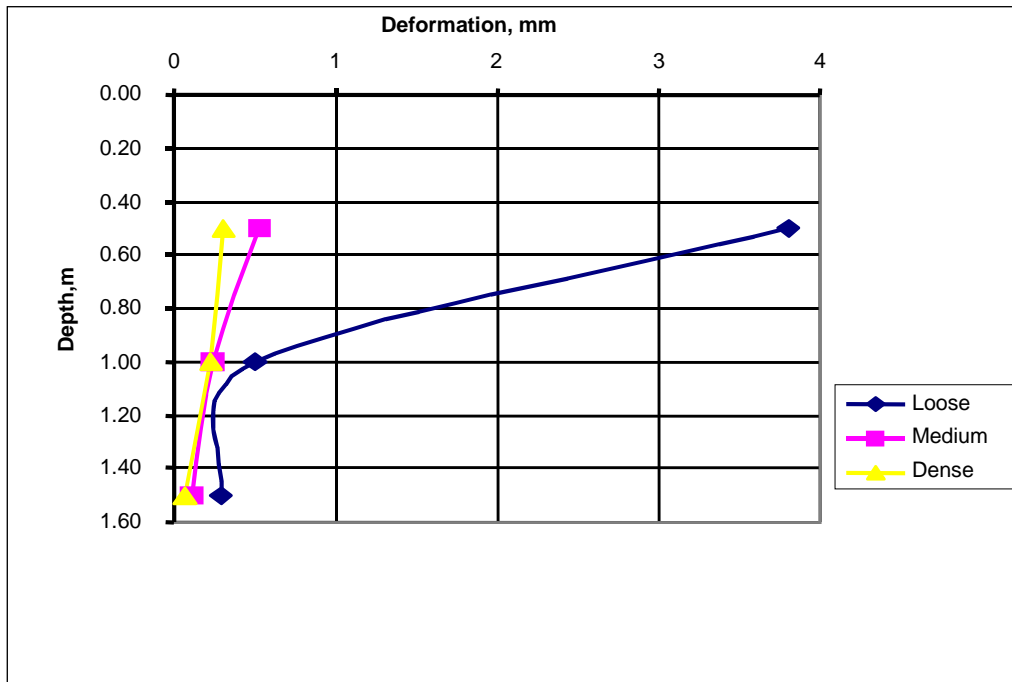


Figure 5.15 Measured Deformation versus Depth (Loose Case).

5.6 Comparison between Coulomb and Measured Value of k

Values in Table 5-2 of Motta, 1994, were verified by the Author using Motta closed form solution for critical failure angle and its related parameters of K_a , S_a and W_t . The following Table shows this comparison.

Table 5-2: Motta quantities and the Author Verification for:
($\Phi = 30$ degree, $\beta = I = 0.0$, $\gamma = 20\text{kN/m}^3$, $q = 40$ kPa, $H = 4\text{m}$.)

α (Degree)	Total Weight of the Failure Wedge (W_t) based on Coulomb Method (kN)		Active Earth Pressure (S_a) based on Coulomb Method (kN)	
	(a)	(b)	(a)	(b)
40	341.1	341.36	60.2	60.19
50	228.5	228.51	83.2	83.17
55	184.1	184.07	85.8	85.83
60	144.7	144.75	83.5	83.57
70	76.5	76.47	64.2	64.17

(a) values calculated by Motta,

(b) values calculated by the Author using Motta Procedures in solving Coulomb Equation

The previous mentioned procedures in chapter 2 were used to evaluate K_a values, for three sand cases: loose, medium and dense, to be compared with the estimated K_a values as shown in Tables 5.3, 5.4 and 5.5. For the loose case, it was found that, using Motta closed form solution, the critical angle of failure (α_c) is equal to 57.65 degree and the related K_a value is 0.402 for $\delta = 0.0$. However, for $\delta = 1/3 \Phi = 8.433$ degree, K_a was found to be 0.372 and for $\delta = 2/3 \Phi = 16.867$ degree, K_a was found to be 0.357.

Table 5-3: Calculated Coulomb K_a values using Motta procedures for sand loose case: ($\Phi = 25.3$ degree, $\beta = I = 0.0$, $\gamma = 15\text{kN/m}^3$, $q = 0.0$, $H = 2\text{m}$.)

α (Degree)	Wt (kN)	Sa (kN)	K_a
40	35.75	9.39	0.313
45	30	10.74	0.358
50	25.17	11.58	0.386
55	21.01	11.98	0.399
60	17.32	11.99	0.399
65	13.99	11.61	0.387

For the medium case, it was found that, using Motta closed form solution, the critical angle of failure (α_c) is equal to 61.1 degree and the related K_a value is 0.305 for $\delta = 0.0$. However, for $\delta = 1/3 \Phi = 10.733$ degree, K_a was found to be 0.282 and for $\delta = 2/3 \Phi = 21.47$ degree, K_a was found to be 0.273.

Table 5-4: Calculated Coulomb K_a values using Motta procedures for sand medium case: ($\Phi = 32.2$ degree, $\beta = I = 0.0$, $\gamma = 16.2\text{kN/m}^3$, $q = 0.0$, $H = 2\text{m}$.)

α (Degree)	Wt (kN)	Sa (kN)	K_a
40	38.61	5.29	0.16
45	32.4	7.36	0.227
50	27.19	8.73	0.269
55	22.69	9.54	0.294
60	18.71	9.86	0.304
65	15.11	9.74	0.301
70	11.79	9.15	0.282

Finally, for the dense case, it was found that, using Motta closed form solution, the critical angle of failure (α_c) is equal to 66.1 degree and the related K_a value is 0.196 for $\delta = 0.0$. However, for $\delta = 1/3 \Phi = 14.07$ degree, K_a was found to be 0.183 and for $\delta = 2/3 \Phi = 28.14$ degree, K_a was found to be 0.182

Table 5-5: Calculated Coulomb K_a values using Motta procedures for sand dense case: ($\Phi = 42.2$ degree, $\beta = I = 0.0$, $\gamma = 17.5\text{kN/m}^3$, $q = 0.0$, $H = 2\text{m}$.)

α (Degree)	Wt (kN)	Sa (kN)	K_a
45	35	1.71	0.049
50	29.37	4.02	0.115
55	24.51	5.57	0.159
60	20.21	6.49	0.185
65	16.32	6.86	0.196
70	12.74	6.72	0.192
75	9.38	6.04	0.173

It should be noted that the calculated critical angle of failure (α_c) increases as the compaction degree increases; K_a decreases as δ increases.

Chapter 6

Conclusions and Recommendations

6.1 General Conclusions

Comparison is made between observed behavior and assumptions and calculations. Based on this comparison, the following statements can be made:

1. The distribution of vertical stress measured in the adjacent soil mass is non-linear with the lowest value at the end of wall facing and this is contrary to the linear distribution assumed in the design calculations.
2. The experimental study showed that the distribution of static active pressure behind a gabion wall is also nonlinear (parabolic).
3. Experimental data indicate that the increment in lateral pressure due to the applied loads is much greater near the surface of the ground than at lower depths.
4. It was seen that lateral earth pressure increases with the compaction degree.
5. The calculated coefficient of earth pressure (K) using the measured earth pressure decreases with depth increasing; in general, it can be assumed constant as the variation with depth can be neglected.
6. Computation of coefficient of earth pressure (K) using Rankine's and coulomb procedure are in general not satisfactory to gabion wall design.
7. It can be concluded that the active condition can not be achieved for medium and dense cases but it can be achieved successfully for the loose case.

6.2 Conclusions Related to Beach Camp Shore Protection Project

It is found that at the horizontal distance of the applied surcharge of more than 1.5 m from the internal edge of the wall, facing the sand, the increment in the lateral earth pressures is limited. This means that the minimum existing distance between the edge of the road and the wall, about 6.0m, is sufficient to eliminate the effect of the road and the weight due to traffic movement on the gabion retaining wall.

Therefore, shifting the location of the wall from the sea side (west) towards the coastal road (east) has a slight effect on the performance and function of the wall.

6.3 Recommendations

It is recommended for future work that:

1. The experiments to be repeated using other types of sand such as coarse sand (kurkar) since the kurkar is used widely in Gaza Strip as a backfill material.
2. Further field studies may be conducted to determine displacement of gabion walls. These tests could satisfy both active and passive cases.
3. A model test could be prepared to simulate the gabion behavior.

LIST OF REFERENCES

1. ASTM C88-90, Annual Book of ASTM STANDARDS, Section 4, construction, volume 0.4.02 Concrete and Aggregates, 1996.
2. Bowles, J.E. (1988). Foundation Analysis and Design, 4th Edition, McGRAW-HILL. PP. 476-484
3. BS 812, British Standards, BS812, Part 2, 1995 Method of determination of Density.
4. Burroughs, M.A. (1979). Gabions: economical, environmentally compatible bank control, Journal of American Society for civil Engineers, January, PP.58-61.
5. C.E. Shepherd Company LP., Modular Gabion Systems, available: <http://www.gabions.net>
6. Concrete network, (2003), available: <http://www.concretenetwork.com>
7. Craig, R.F. (1992). Soil Mechanics, 5th Edition , EHPMAN & HALL. PP. 183-188
8. Georgiadis, M. and Anagnostopoulos, C. (1998). Lateral Pressure on Sheet Pile Walls due to Strip Load, Journal of Geotechnical and Geoenvironmental Engineering, Vol. 124, No. 1, PP. 95-98.
9. Goh A.T.C. (1993). Behavior of Cantilever Retaining Walls, Journal of Geotechnical Engineering, Vol. 119, No. 11, PP. 1751-1770
10. Haskoning Consulting Engineers, (1998). Final Design Report of Beach Camp Shore Protection Project, UNRWA's SEHP, Gaza, No. F080.21/02/RGS/MaVe.
11. Hausmann, R.M. (1990). Engineering Principles of Ground Modification, McGraw- Hill.
12. Instruction Manuals by GEOKON Incorporated for Geotechnical Instrumentation, (1984, 1996). Lebanon, NH 03766, USA.
13. International Erosion Control Association, (2004), available: <http://www.ieca.org/public/articles>
14. ISO 12236 (1996).

15. Maccaferri Company, available: <http://www.maccaferri.co.uk>
16. Motta, E. (1994). Generalized Coulomb Active Earth Pressure for Distanced Surcharge, Journal of Geotechnical Engineering, Vol.120, No.6, PP. 1072-1079.
17. Prakashs, Soil Dynamics. (1981). McGraw-Hill Book Comp.
18. Seok, J.W; kim, O.Y; Chung, C.K; and Kim, M.M. (2001). Evaluation of Ground and Building Settlement near Braced Excavation Sites by Model Testing. Canadian Geotechnical Journal, No. 38, PP.112 7-1133.
19. Shields, D. H. & Tolunay, A. Z. (1974). Passive Pressure Coefficients By Method of Slices, Journal of the Soil Mechanics and Foundation, (ASCE), Vol. 99,
20. Site investigation report for Beach Camp Coastal Defense Project, Gaza UNRWA's SEHP, February 1998.
21. US Army Corps of Engineers, ASCE. (1996). Design of Sheet Pile Walls, Technical Engineering and Design Code No. 15, pp. 21-25
22. Zaker Zadeh, N.; Fredlund, D.G; and Pufahl, D.E. (1999) Interstice force functions for computing active and passive earth force, Canadian Geotechnical Journal, No. 36, pp. 1015 - 1029.

APPENDICES

APPENDIX (A)

LATERAL EARTH PRESSURE RESULTS

Measurements of Horizontal, Vertical Pressures and Deformation, Loose Case Field Tests

Test No.1

location: station No. 14+20m,

20m north of culvert No.64

Date:21/06/03

Temp.: 28 C

Calibration factor for horizontal pressure cell (Ch)=0.1196 (kPa/digit)

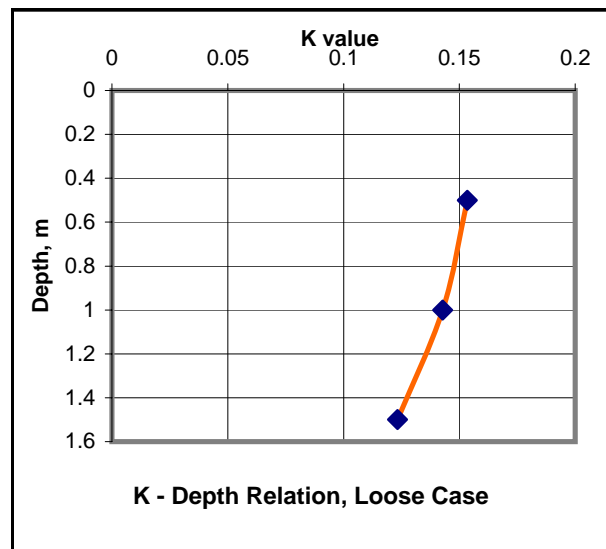
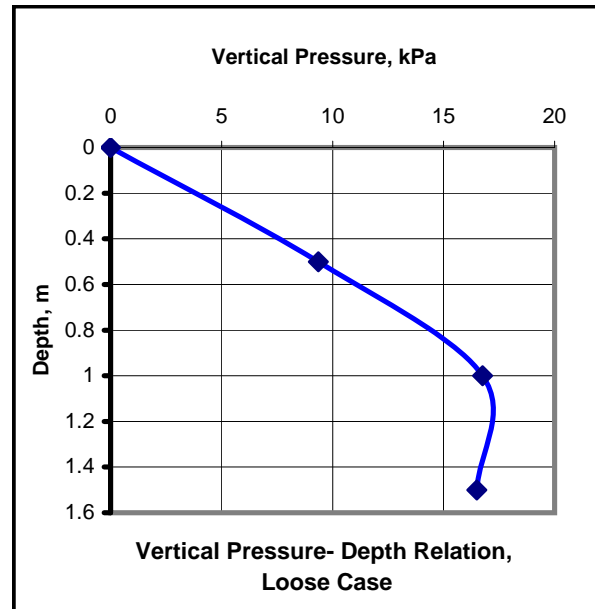
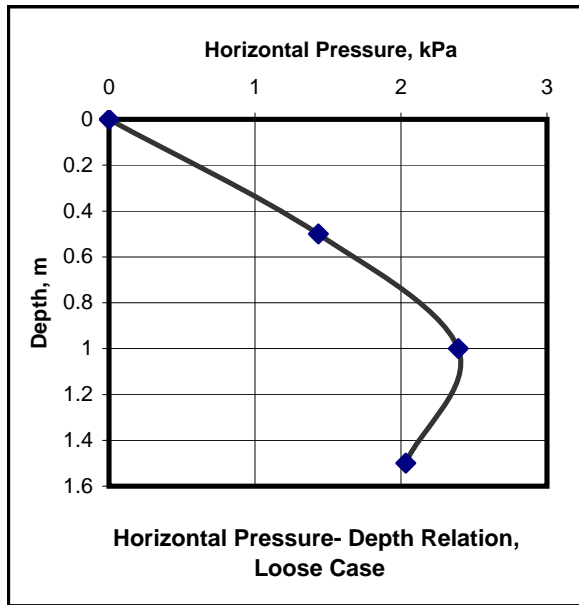
Calibration factor for vertical pressure cell (Cv)=0.1299 (kPa/digit)

Calibration factor for deformation meter (Cd)=0.01828 (mm/digit)

Type of soil: sand

Compaction status: loose case by using screen 5x5 cm size

Depth (m)	Roh (digit)	R1h (digit)	Rov (digit)	R1v (digit)	Ph (kPa)	Pv (kPa)	K	Rod (digit)	R1d (digit)	Deformation (mm)
0					0	0				
0.50	8764	8752	8978	8906	1.4352	9.3528	0.15345	5034	5226	3.8
1.00	8746	8726	8966	8837	2.392	16.7571	0.14275	5156	5150	0.5
1.5	8728	8711	8934	8807	2.0332	16.4973	0.12324	5109	5125	0.3



Measurements of Horizontal, Vertical Pressures and Deformation, Medium Case Field Tests

Test No.2

location: station No. 14+20m,
20m north of culvert No.64

Date:22/06/03

Temp.: 32 C

Calibration factor for horizontal pressure cell (Ch)=0.1196 (kPa/digit)

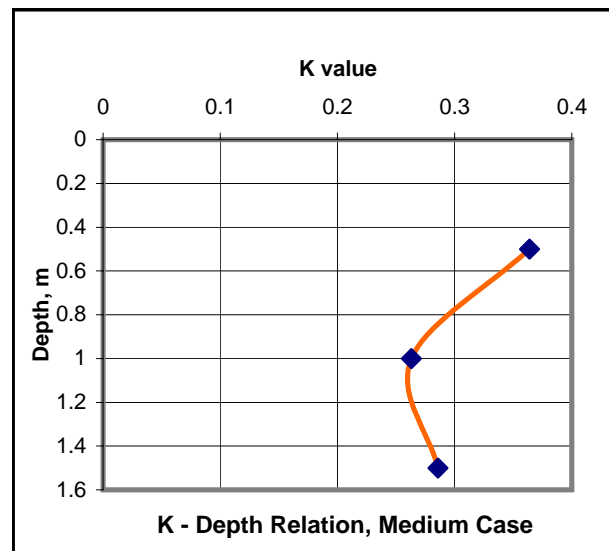
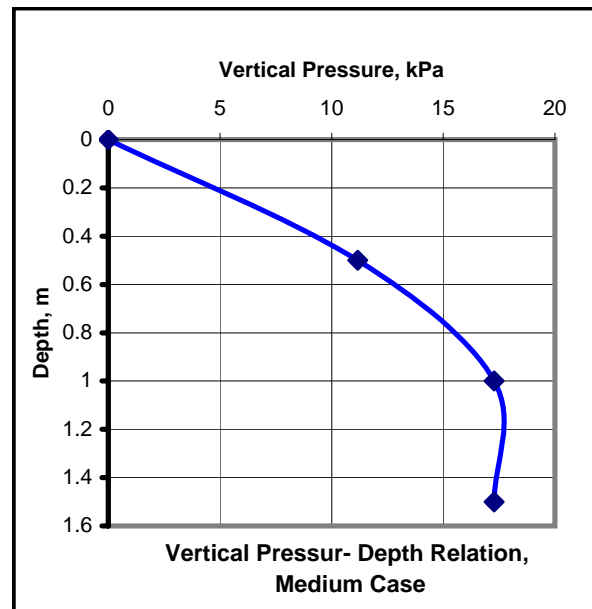
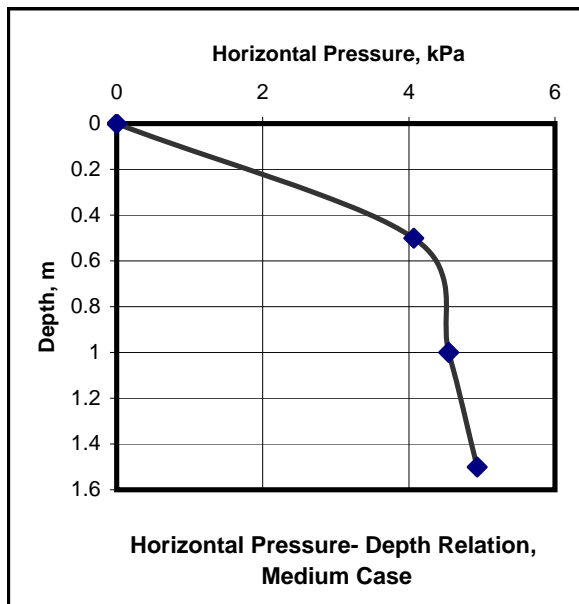
Calibration factor for vertical pressure cell (Cv)=0.1299 (kPa/digit)

Calibration factor for deformation meter (Cd)=0.01828 (mm/digit)

Type of soil: sand

Compaction status:medium case by using steel hand tamper

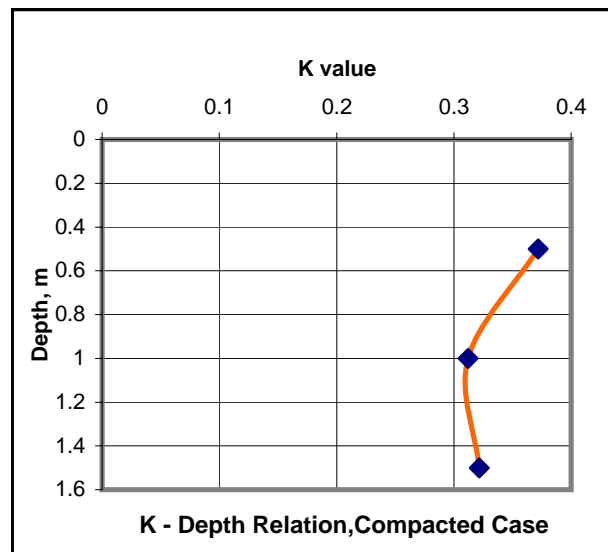
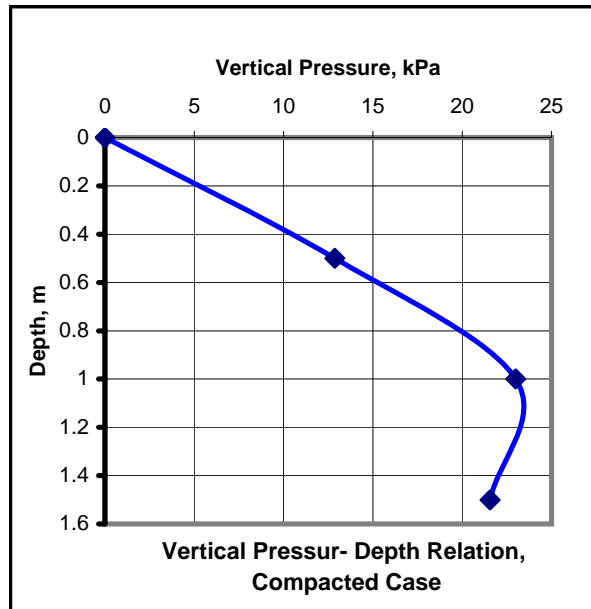
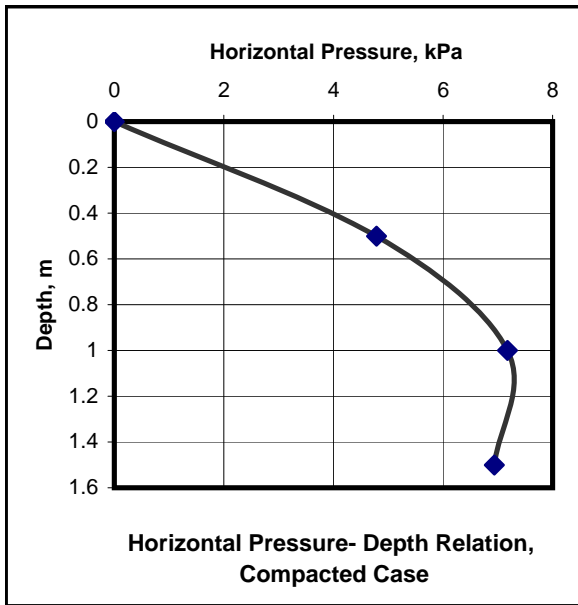
Depth (m)	Roh (digit)	R1h (digit)	Rov (digit)	R1v (digit)	Ph (kPa)	Pv (kPa)	K	Rod (digit)	R1d (digit)	Deformation (mm)
0					0	0				
0.50	8741	8707	8972	8886	4.0664	11.1714	0.364	3684	3689	0.53
1.00	8752	8714	8972	8839	4.5448	17.2767	0.26306	3669	3682	0.24
1.5	8761	8703	8948	8815	4.9368	17.2767	0.28575	3647	3676	0.1



Measurements of Horizontal, Vertical Pressures and Deformation, Dense Case Field Tests

Test No.3
 location: station No. 14+20m,
 20m north of culvert No.64
 Date:25/06/03
 Temp.: 31 C
 Calibration factor for horizontal pressure cell (Ch)=0.1196 (kPa/digit)
 Calibration factor for vertical pressure cell (Cv)=0.1299 (kPa/digit)
 Calibration factor for deformation meter (Cd)=0.01828 (mm/digit)
 Type of soil: sand
 Compaction status:Dense case by using water, steel hand tamper and steel vibrating plate

Depth (m)	Roh (digit)	R1h (digit)	Rov (digit)	R1v (digit)	Ph (kPa)	Pv (kPa)	K	Rod (digit)	R1d (digit)	Deformation (mm)
0					0	0				
0.50	8753	8713	8984	8885	4.784	12.8601	0.372	5114	5126	0.3
1.00	8759	8699	8992	8815	7.176	22.9923	0.3121	5139	5143	0.22
1.5	8748	8690	8967	8801	6.9368	21.5634	0.32169	5135	5149	0.07



Measurements of Horizontal Pressure, Dense Case

Field Tests

Test No.4

location: station No. 14+20m,

20m north of culvert No.64

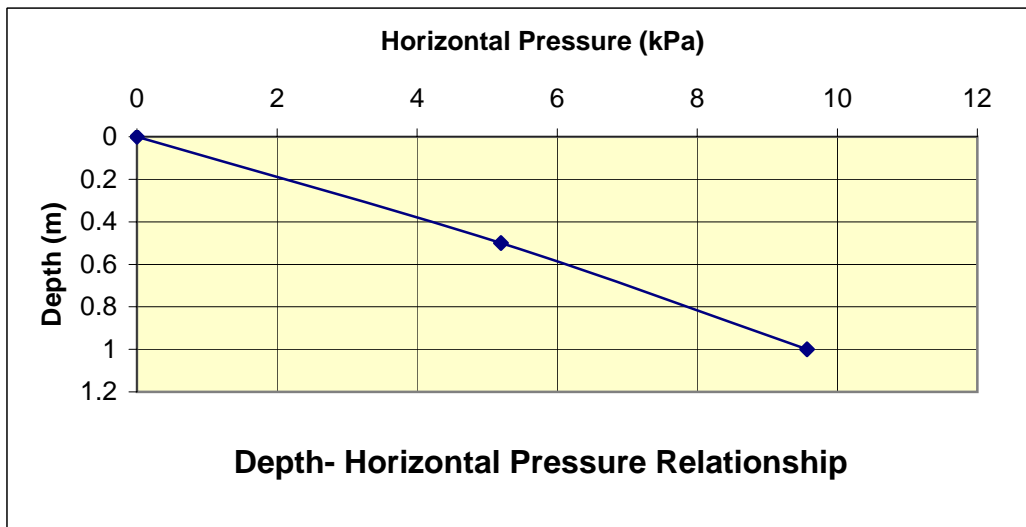
Date:26/06/03

Temp.: 32 C

Type of soil: sand

Compaction status: Dense case by watering
and using hand steel tamper

Depth (m)	Roh (digit)	R1h (digit)	Calibration Factor (C)	Ph (kPa)
0				0
0.50	8980	8940	0.1299	5.196
1.00	8785	8705	0.1196	9.568



Measurements of Horizontal Pressure, Loading Case at 50 cm, Dense sand

Field Tests

Test No. 5

location: station No. 14+20m,

20m north of culvert No.64

Date:26/06/03

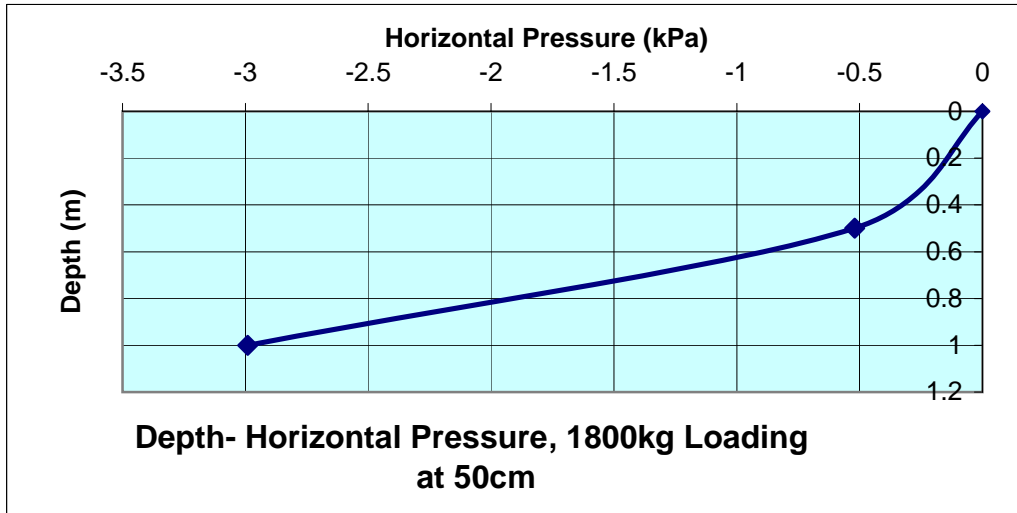
Temp.: 34 C

Type of soil: sand

Compaction status: Dense case by watering

and using steel hand tamper

Depth (m)	Roh (digit)	Calibration Factor (C)	R1h 1800kg (digit)	P1h (kPa)	R2h 0.0kg (digit)
0				0	
0.50	8940	0.1299	8944	-0.5196	8946
1.00	8705	0.1196	8730	-2.99	8734



Measurements of Horizontal Pressure, Loading Case at 100 cm, Dense sand Field Tests

Test No. 6

location: station No. 14+20m,
20m north of culvert No.64

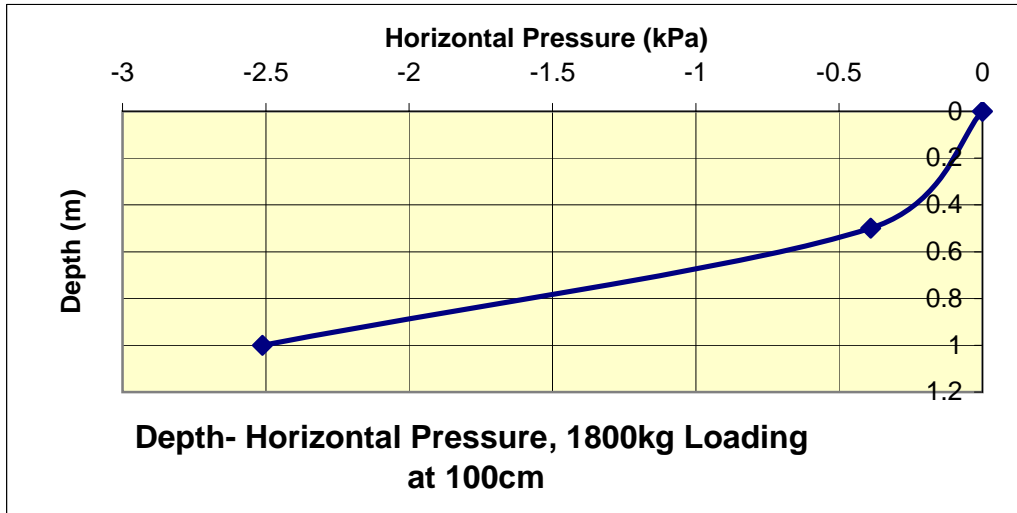
Date:26/06/03

Temp.: 34 C

Type of soil: sand

Compaction status: Dense case by watering
and using steel hand tamper

Depth (m)	Roh (digit)	Calibration Factor (C)	R1h 1800kg (digit)	P1h (kPa)	R2h 0.0kg (digit)
0				0	
0.50	8940	0.1299	8943	-0.3897	8946
1.00	8705	0.1196	8726	-2.5116	8734



Measurements of Horizontal Pressure, Loading Case at 150 cm, Dense sand Field Tests

Test No. 7

location: station No. 14+20m,
20m north of culvert No.64

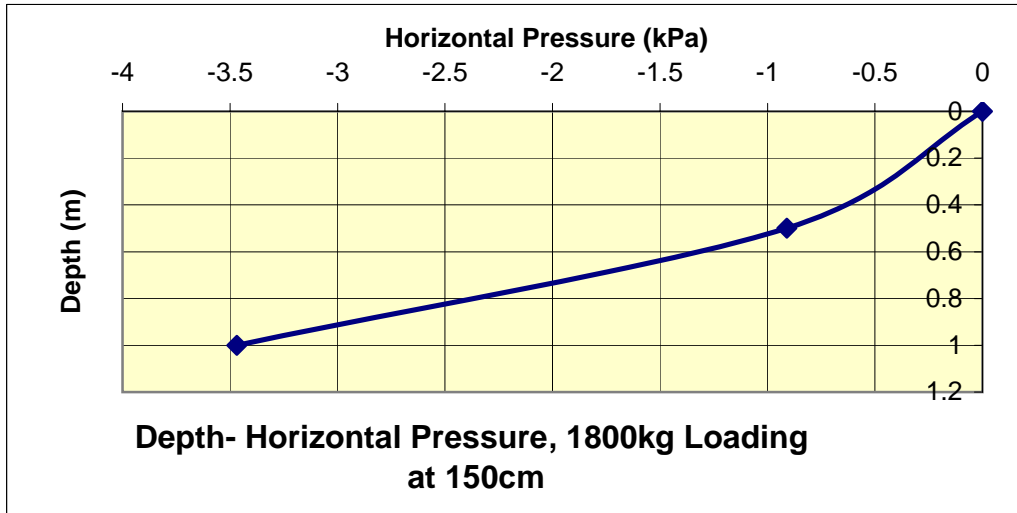
Date:26/06/03

Temp.: 34 C

Type of soil: sand

Compaction status: Dense case by watering
and using steel hand tamper

Depth (m)	Roh (digit)	Calibration Factor (C)	R1h 1800kg (digit)	P1h (kPa)	R2h 0.0kg (digit)
0				0	
0.50	8940	0.1299	8947	-0.9093	8946
1.00	8705	0.1196	8734	-3.4684	8734



Measurements of Horizontal Pressure, Loading Case at 25 cm, Dense sand Field Tests

Test No. 8

location: station No. 14+20m,
20m north of culvert No.64

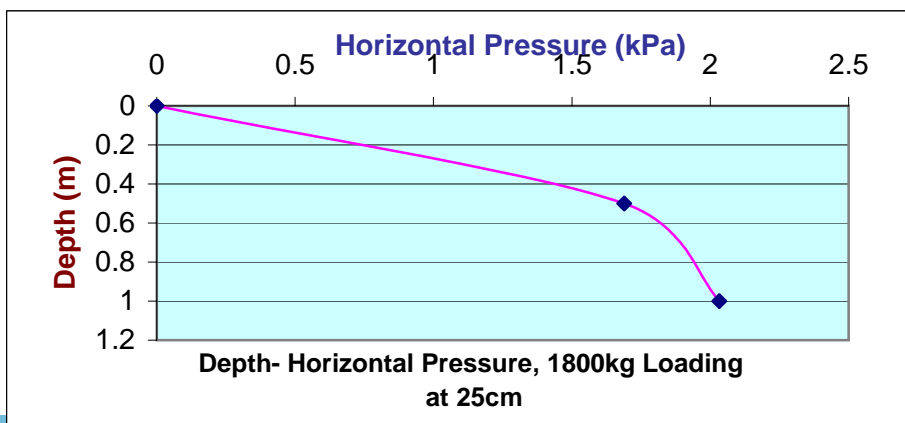
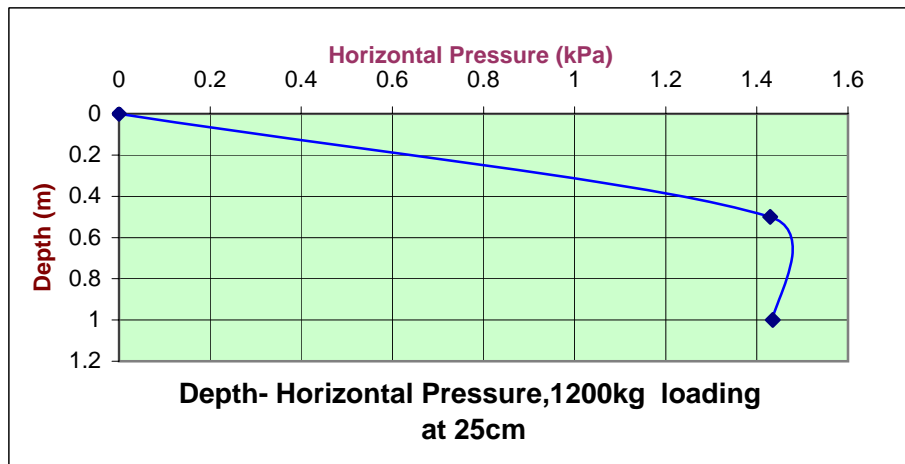
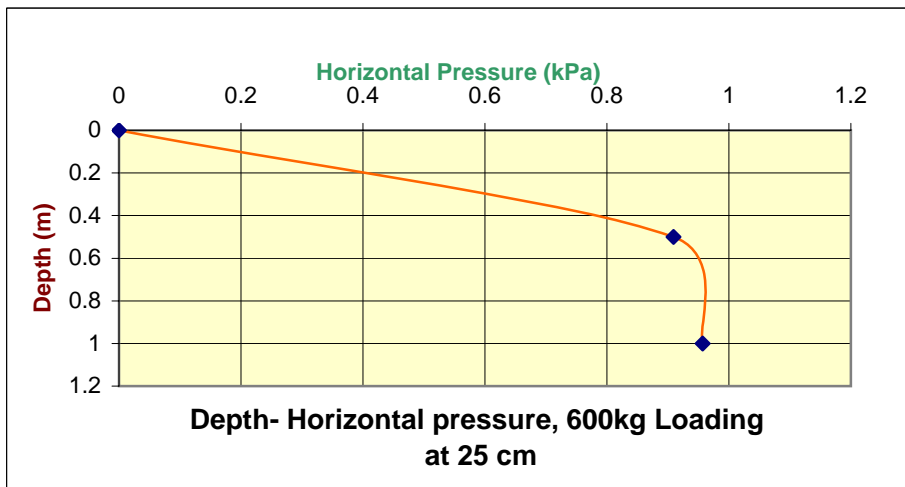
Date:26/06/03

Temp.: 34 C

Type of soil: sand

Compaction status: Dense case by watering
and using steel hand tamper

Depth (m)	Roh (digit)	Calibration Factor (C)	R1h 600kg (digit)	P1h (kPa)	R2h 1200kg (digit)	P2h (kPa)	R3h 1800kg (digit)	P3h (kPa)	R4h 0.0kg (digit)
0				0		0		0	
0.50	8946	0.1299	8939	0.9093	8935	1.4289	8933	1.6887	8962
1.00	8734	0.1196	8726	0.9568	8722	1.4352	8717	2.0332	8751



Measurements of Horizontal Pressure, Inclined Case, Dense sand

Field Tests

Test No. 9

location: station No. 14+20m,
20m north of culvert No.64

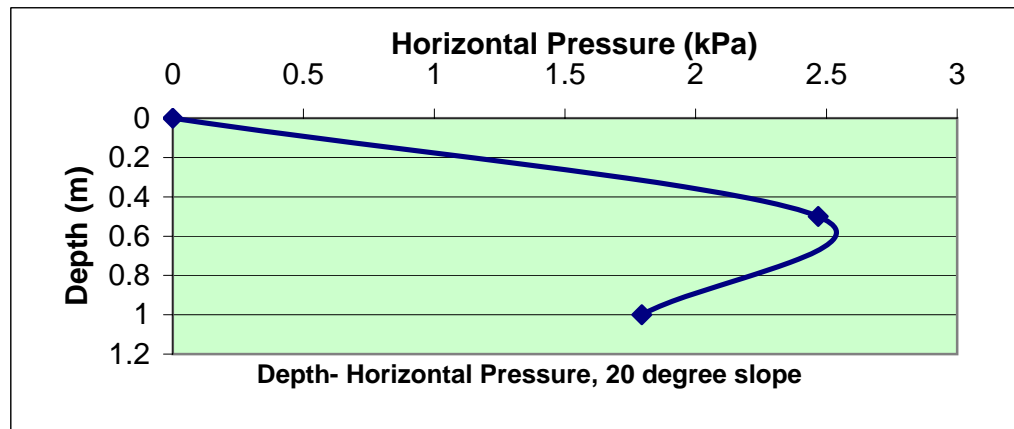
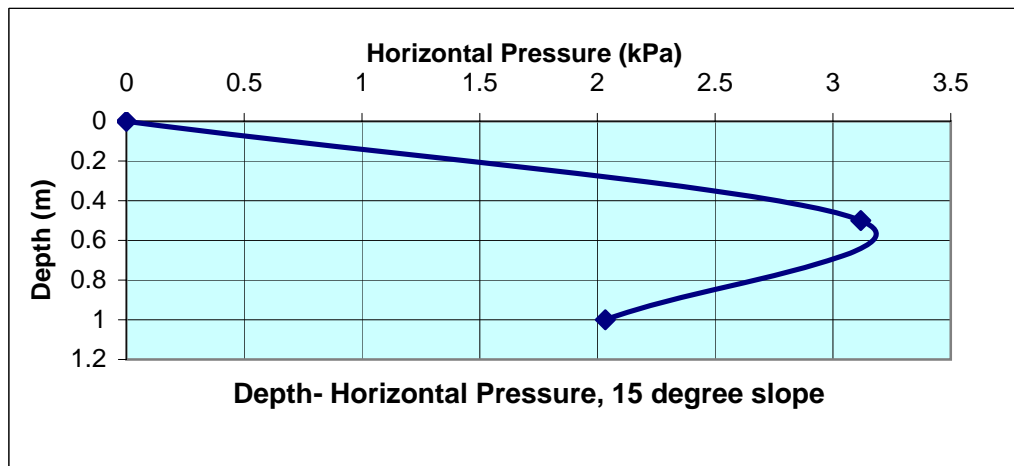
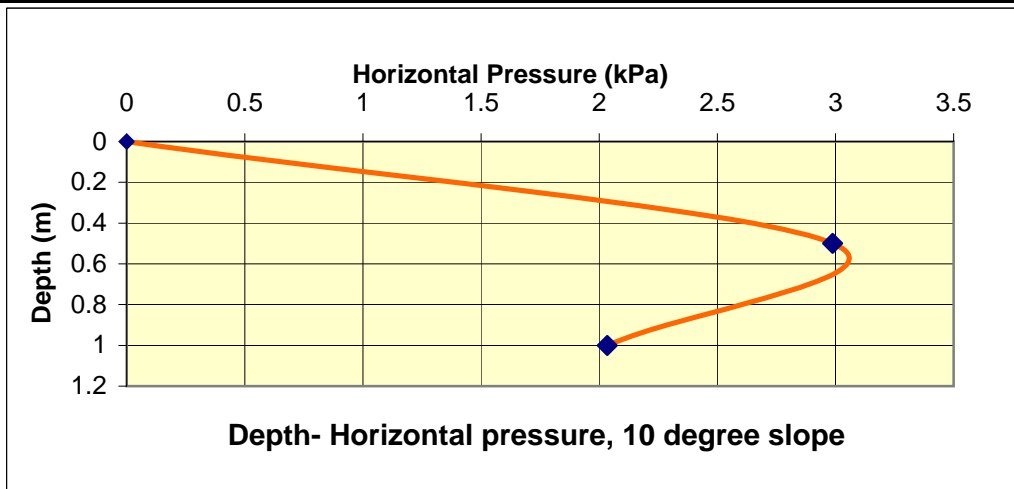
Date:26/06/03

Temp.: 34 C

Type of soil: sand

Compaction status: Dense case by watering
and using steel hand tamper

Depth (m)	Roh (digit)	Calibration Factor (C)	R1h 10 degree (digit)	P1h (kPa)	R2h 15 degree (digit)	P2h (kPa)	R3h 20degree (digit)	P3h (kPa)
0				0		0		0
0.50	8962	0.1299	8939	2.9877	8938	3.1176	8943	2.4681
1.00	8751	0.1196	8734	2.0332	8734	2.0332	8736	1.794



Measurements of Horizontal Pressure, Loose Case, Repeated Test

Field Tests

Test No. 10

Type of soil: sand

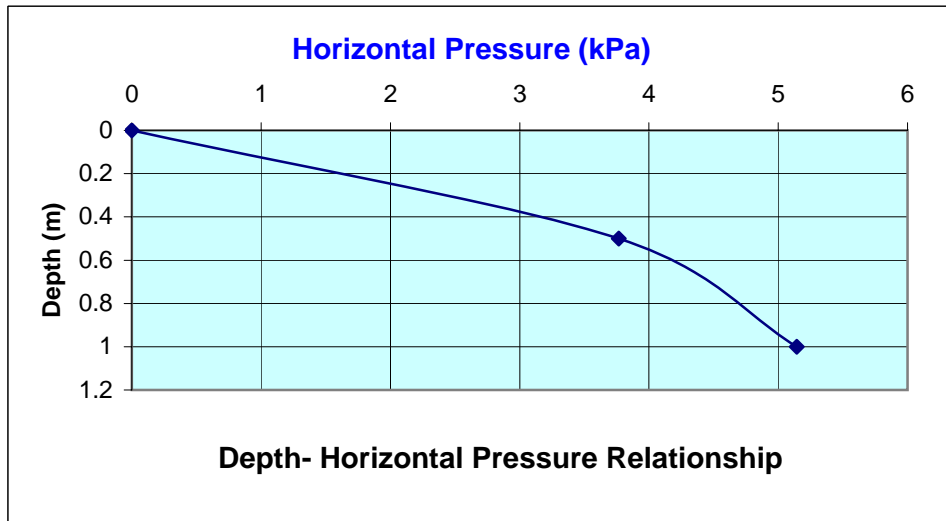
location: station No. 14+20m,
20m north of culvert No.64

Compaction status: loose case by using PVC buckets dropped from fixed distance

Date:28/06/03

Temp.: 34 C

Depth (m)	Roh (digit)	R1h (digit)	Calibration Factor (C)	Ph (kPa)
0				0
0.50	8982	8953	0.1299	3.7671
1.00	8785	8742	0.1196	5.1428



Measurements of Horizontal Pressure, Loading Case at 25 cm, loose case

Field Tests

Test No. 11

location: station No. 14+20m,
20m north of culvert No.64

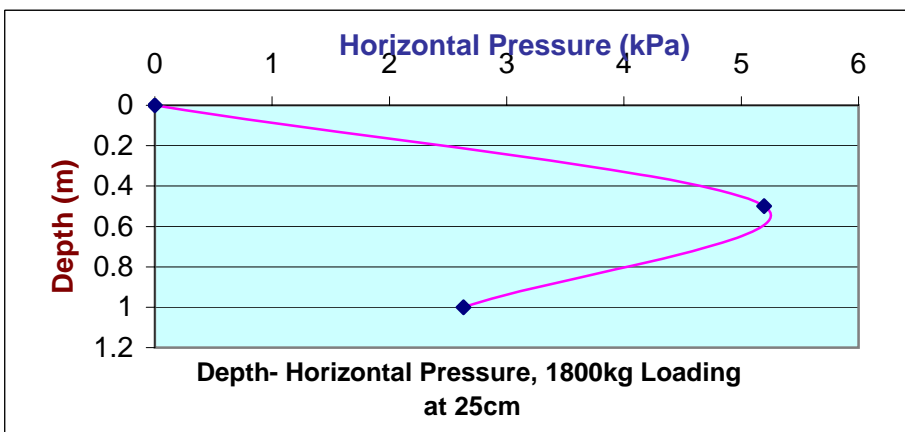
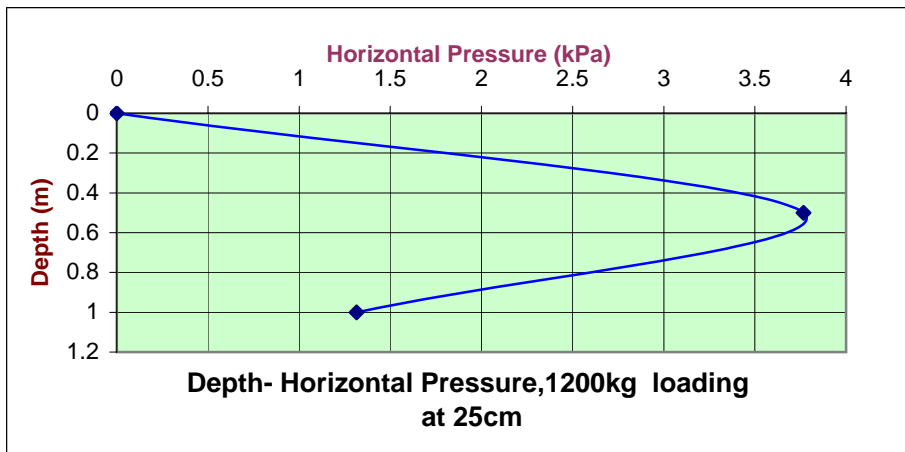
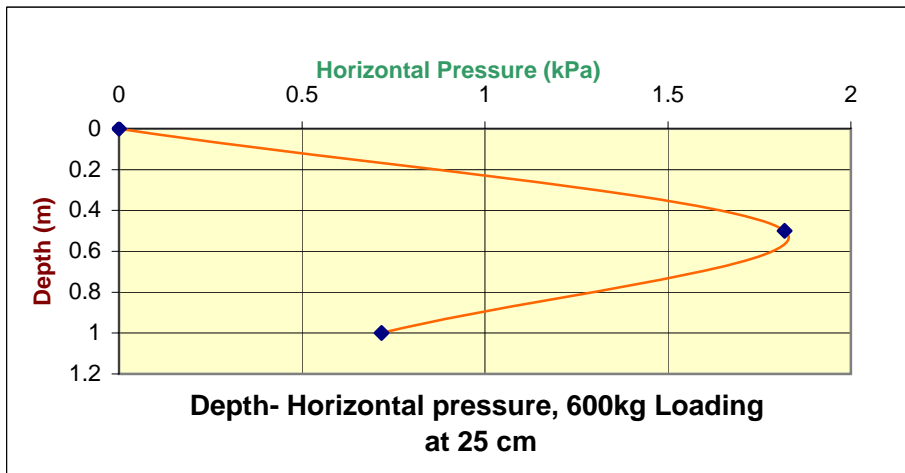
Date:28/06/03

Temp.: 34 C

Type of soil: sand

Compaction status: loose case by using PVC buckets
dropped from fixed distance

Depth (m)	Roh (digit)	Calibration Factor (C)	R1h 600kg (digit)	P1h (kPa)	R2h 1200kg (digit)	P2h (kPa)	R3h 1800kg (digit)	P3h (kPa)	R4h 0.0kg (digit)
0				0		0		0	
0.50	8953	0.1299	8939	1.8186	8924	3.7671	8913	5.196	8923
1.00	8742	0.1196	8736	0.7176	8731	1.3156	8720	2.6312	8728



Measurements of Horizontal Pressure, Loading Case at 50 cm, loose case

Field Tests

Test No. 12

location: station No. 14+20m,
20m north of culvert No.64

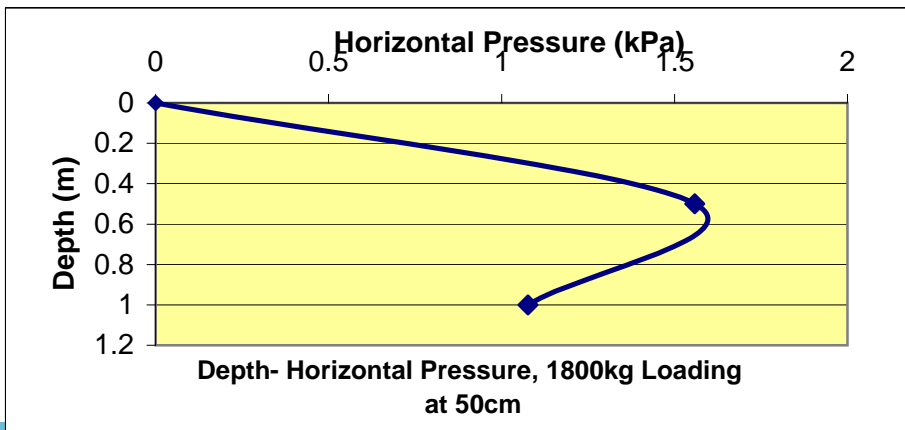
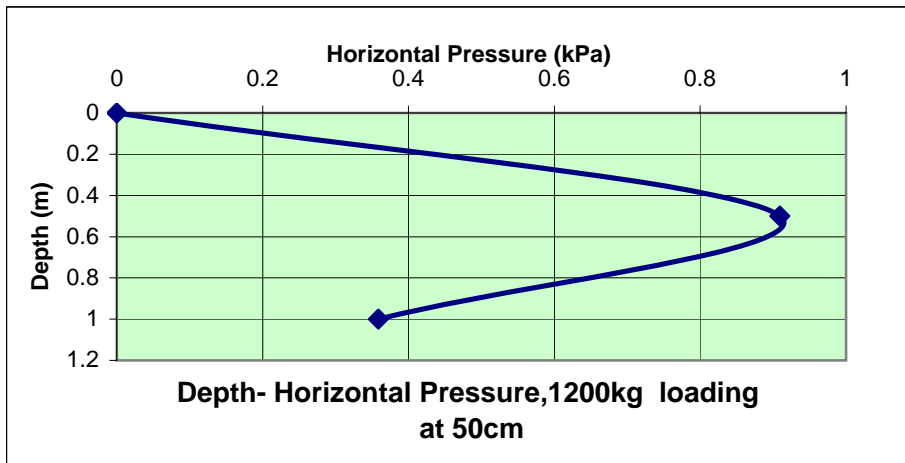
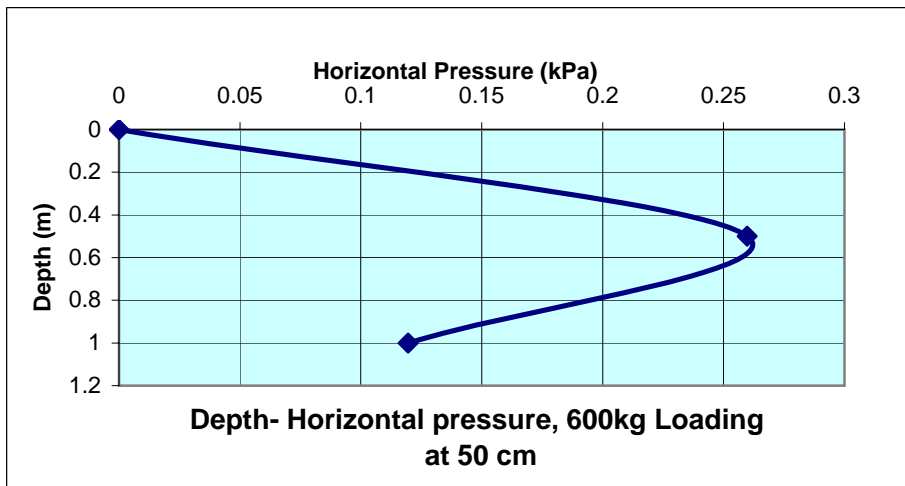
Date:28/06/03

Temp.: 34 C

Type of soil: sand

Compaction status: loose case by using PVC buckets
dropped from fixed distance

Depth (m)	Roh (digit)	Calibration Factor (C)	R1h 600kg (digit)	P1h (kPa)	R2h 1200kg (digit)	P2h (kPa)	R3h 1800kg (digit)	P3h (kPa)	R4h 0.0kg (digit)
0				0		0		0	
0.50	8923	0.1299	8921	0.2598	8916	0.9093	8911	1.5588	8919
1.00	8728	0.1196	8727	0.1196	8725	0.3588	8719	1.0764	8726



Measurements of Horizontal Pressure, Loading Case at 100 cm, loose Case Field Tests

Test No. 13

location: station No. 14+20m,
20m north of culvert No.64

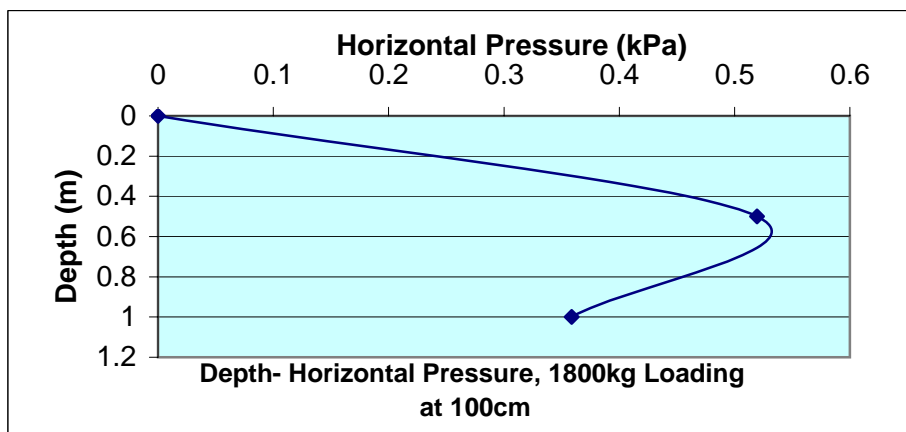
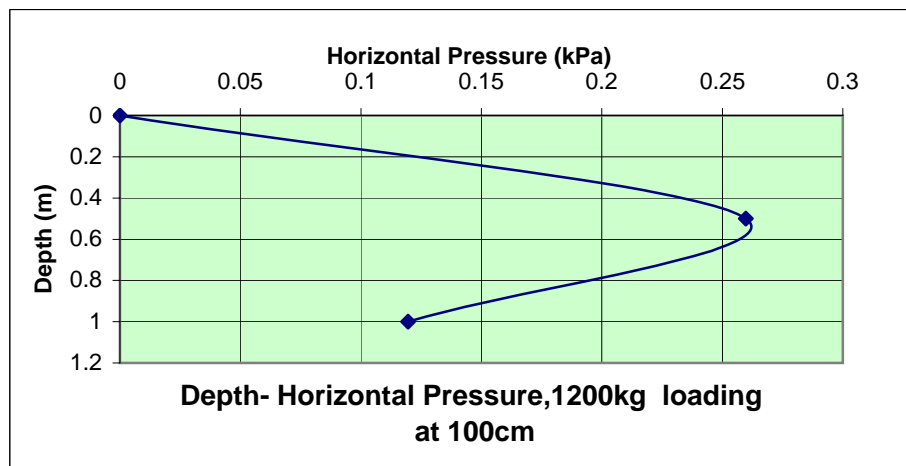
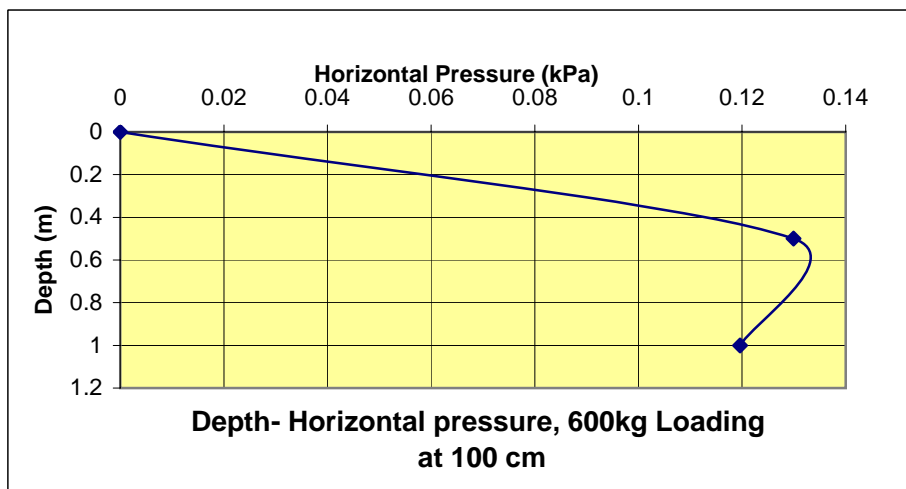
Date:28/06/03

Temp.: 34 C

Type of soil: sand

Compaction status: loose case by using PVC buckets
dropped from fixed distance

Depth (m)	Roh (digit)	Calibration Factor (C)	R1h 600kg (digit)	P1h (kPa)	R2h 1200kg (digit)	P2h (kPa)	R3h 1800kg (digit)	P3h (kPa)	R4h 0.0kg (digit)
0				0		0		0	
0.50	8919	0.1299	8918	0.1299	8917	0.2598	8915	0.5196	8918
1.00	8726	0.1196	8725	0.1196	8725	0.1196	8723	0.3588	8726



Measurements of Horizontal Pressure, Loading Case at 150 cm, loose Case Field Tests

Test No. 14

Type of soil: sand

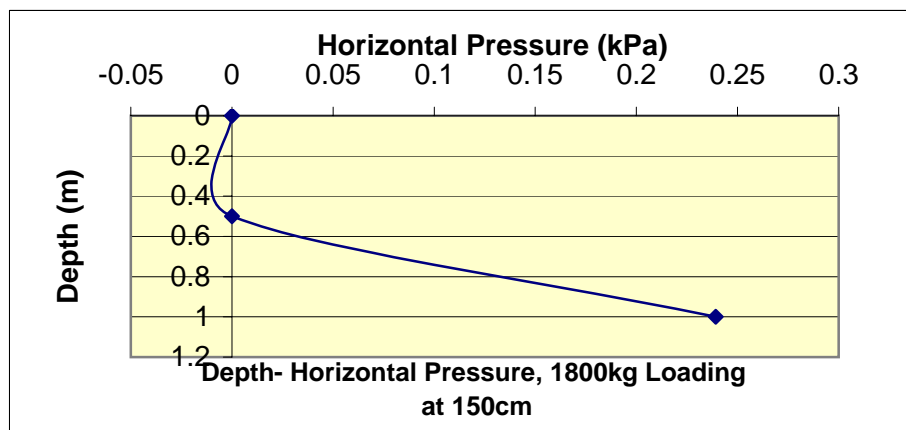
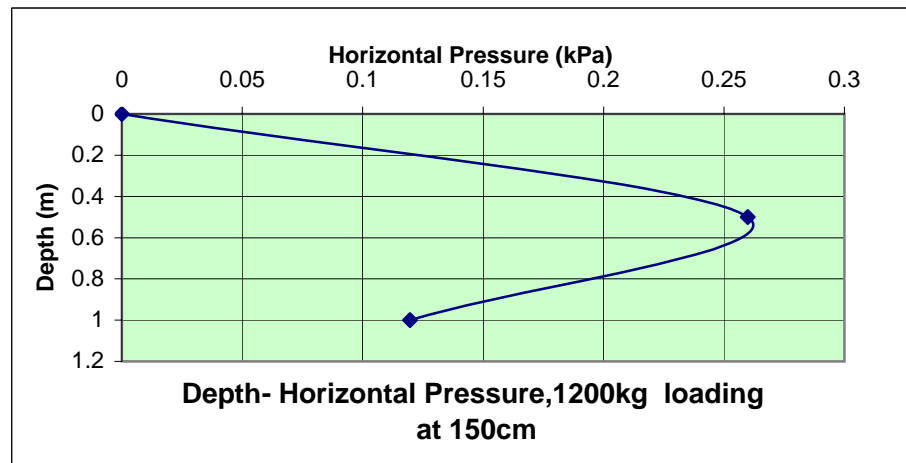
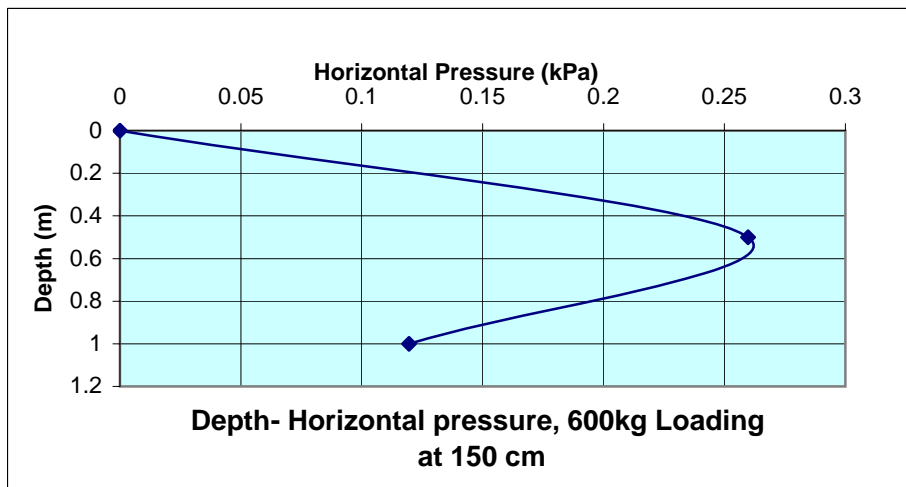
location: station No. 14+20m,
20m north of culvert No.64

Compaction status: loose case by using PVC buckets
dropped from fixed distance

Date:28/06/03

Temp.: 34 C

Depth (m)	Roh (digit)	Calibration Factor (C)	R1h 600kg (digit)	P1h (kPa)	R2h 1200kg (digit)	P2h (kPa)	R3h 1800kg (digit)	P3h (kPa)	R4h 0.0kg (digit)
0				0		0		0	
0.50	8918	0.1299	8916	0.2598	8916	0.2598	8918	0	8919
1.00	8726	0.1196	8725	0.1196	8725	0.1196	8724	0.2392	8725



Measurements of Horizontal Pressure, Inclined Case, loose case

Field Tests

Test No. 15

location: station No. 14+20m,
20m north of culvert No.64

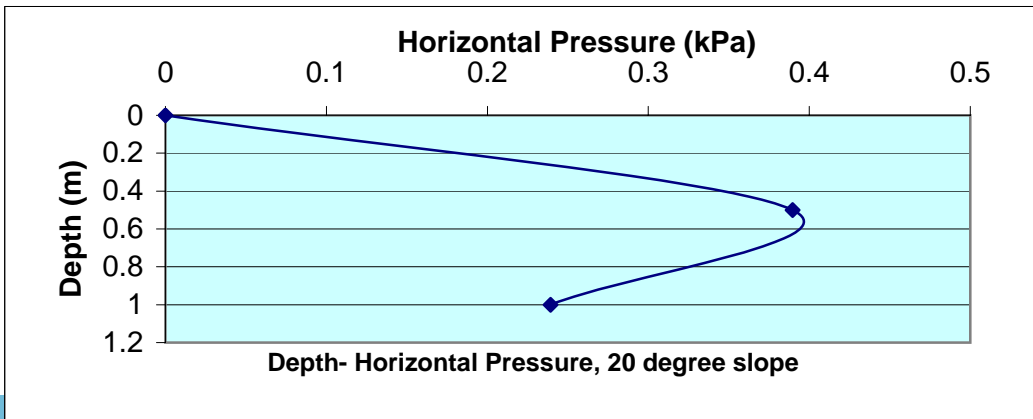
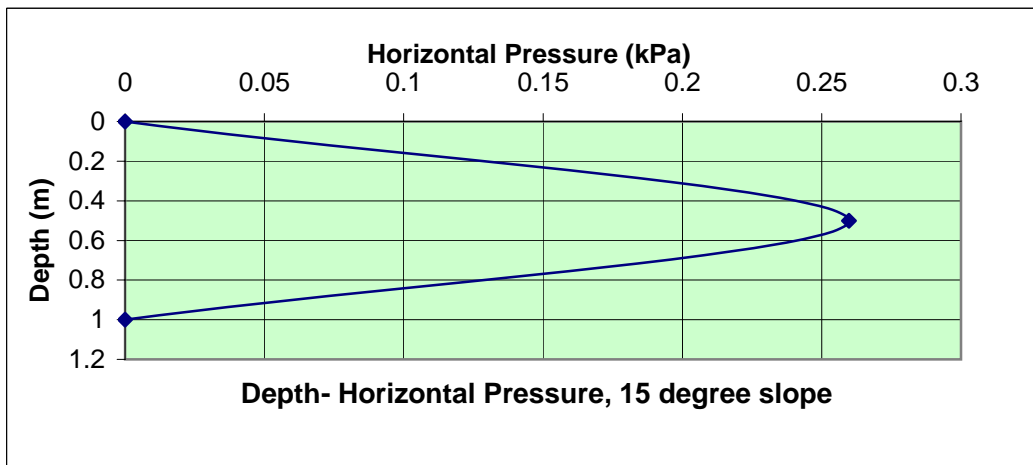
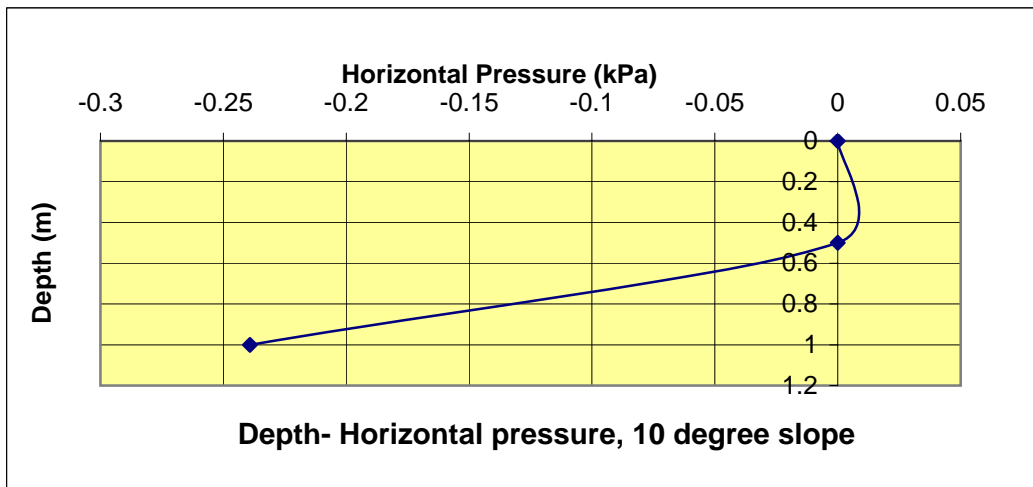
Date:28/06/03

Temp.: 34 C

Type of soil: sand

Compaction status: Loose case by using
PVC buckets from fixed distance

Depth (m)	Roh (digit)	Calibration Factor (C)	R1h 10 degree (digit)	P1h (kPa)	R2h 15 degree (digit)	P2h (kPa)	R3h 20degree (digit)	P3h (kPa)
0				0		0		0
0.50	8919	0.1299	8919	0	8917	0.2598	8916	0.3897
1.00	8725	0.1196	8727	-0.2392	8725	0	8723	0.2392



Measurements of Horizontal Pressure, Medium Case, Repeated Test

Field Tests

Test No.16

location: station No. 14+20m,

20m north of culvert No.64

Date:29/06/03

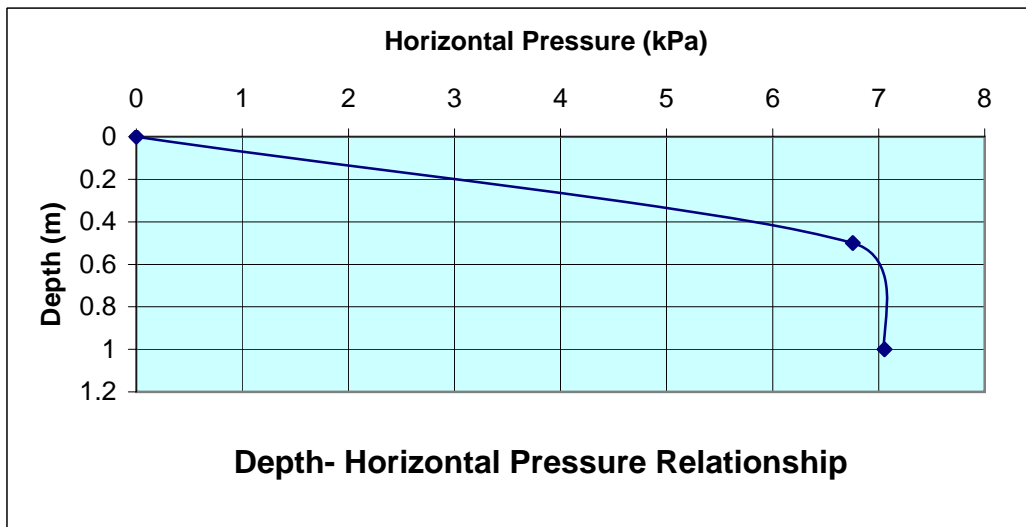
Temp.: 28 C

Type of soil: sand

Compaction status: Medium compaction by

using steel hand tamper

Depth (m)	Roh (digit)	R1h (digit)	Calibration Factor (C)	Ph (kPa)
0				0
0.50	8972	8920	0.1299	6.7548
1.00	8774	8715	0.1196	7.0564



Measurements of Horizontal Pressure, Loading at 25 cm, Medium Case sand Field Tests

Test No.17

location: station No. 14+20m,
20m north of culvert No.64

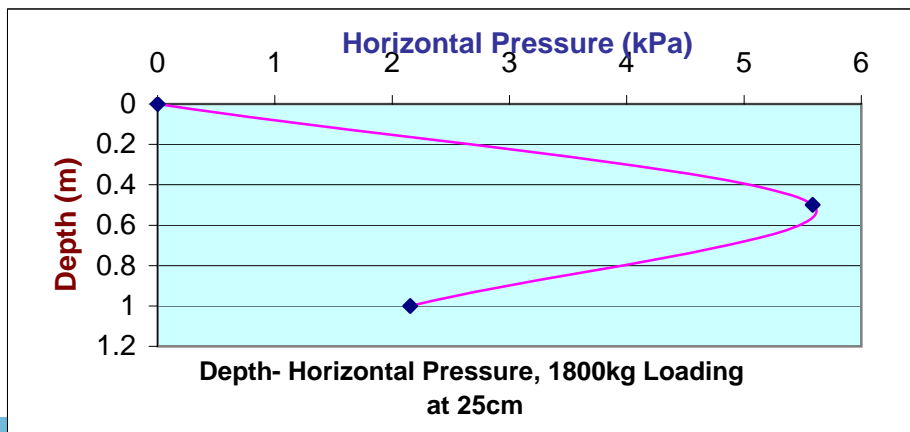
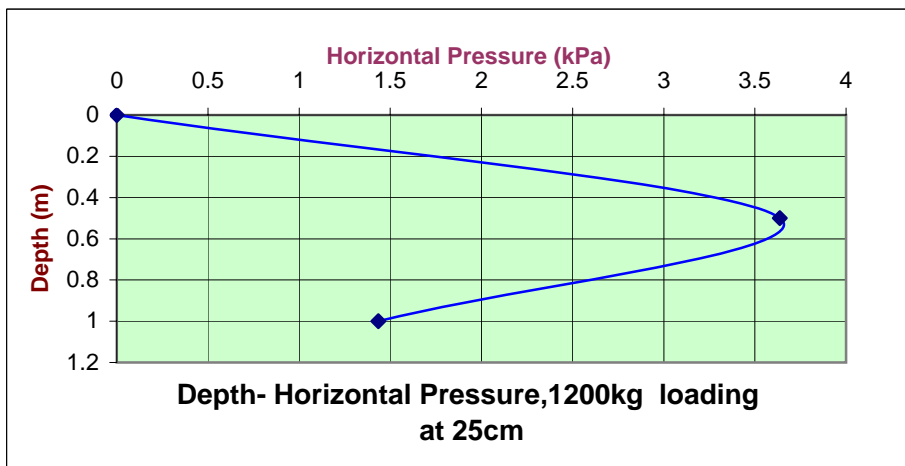
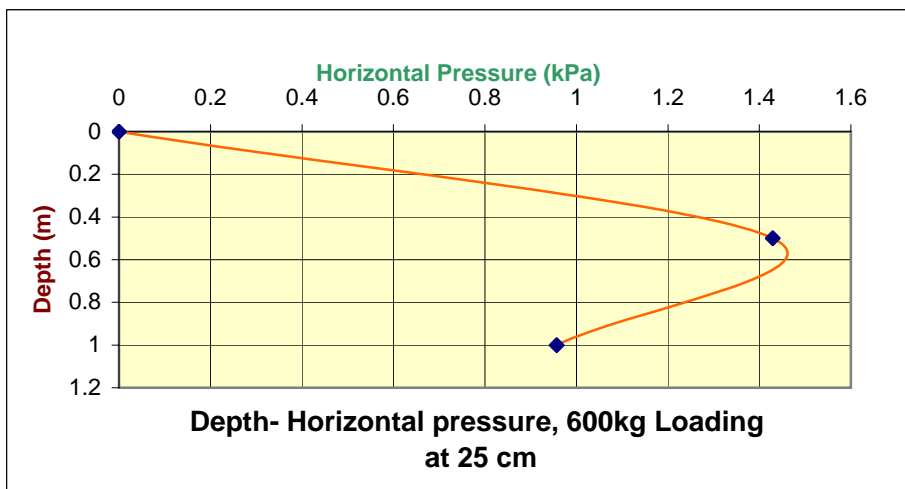
Date:29/06/03

Temp.: 28 C

Type of soil: sand

Compaction status: Medium Compaction case
by using steel hand tamper

Depth (m)	Roh (digit)	Calibration Factor (C)	R1h 600kg (digit)	P1h (kPa)	R2h 1200kg (digit)	P2h (kPa)	R3h 1800kg (digit)	P3h (kPa)	R4h 0.0kg (digit)
0				0		0		0	
0.50	8920	0.1299	8909	1.4289	8892	3.6372	8877	5.5857	8913
1.00	8715	0.1196	8707	0.9568	8703	1.4352	8697	2.1528	8708



Measurements of Horizontal Pressure, Loading at 50 cm, Medium Case sand Field Tests

Test No.18

location: station No. 14+20m,
20m north of culvert No.64

Date:29/06/03

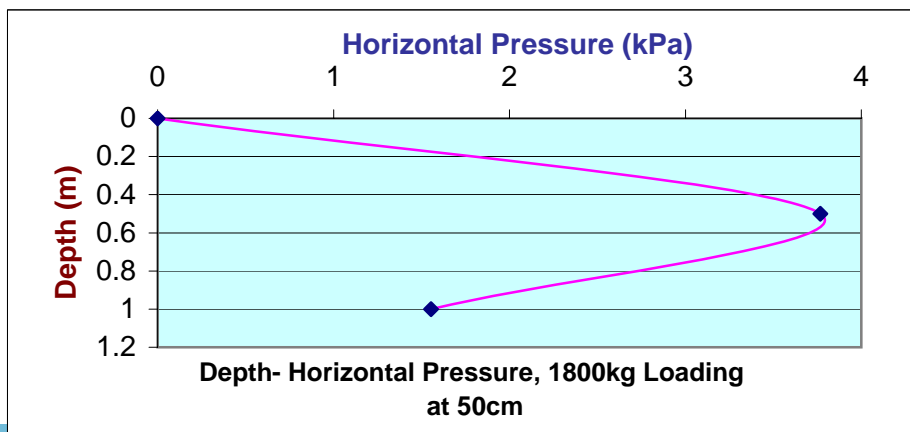
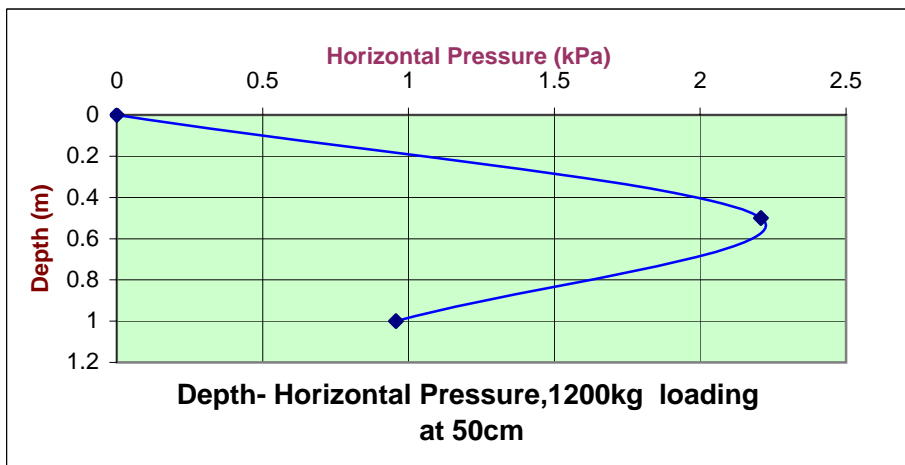
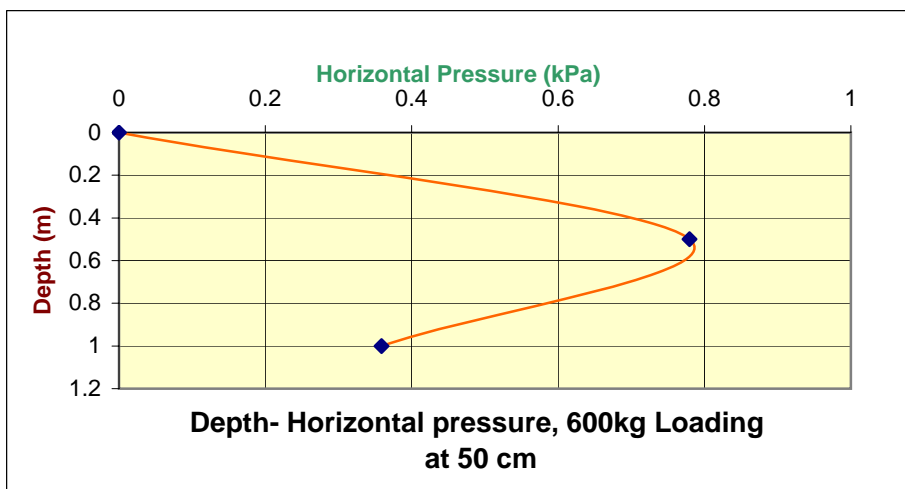
Temp.: 28 C

Type of soil: sand

Compaction status: Medium Compaction case

by using steel hand tamper

Depth (m)	Roh (digit)	Calibration Factor (C)	R1h 600kg (digit)	P1h (kPa)	R2h 1200kg (digit)	P2h (kPa)	R3h 1800kg (digit)	P3h (kPa)	R4h 0.0kg (digit)
0				0		0		0	
0.50	8913	0.1299	8907	0.7794	8896	2.2083	8884	3.7671	8907
1.00	8708	0.1196	8705	0.3588	8700	0.9568	8695	1.5548	8704



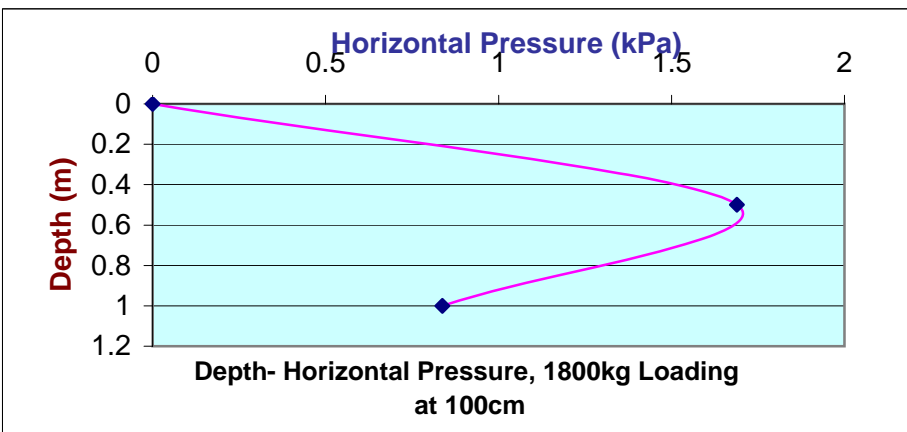
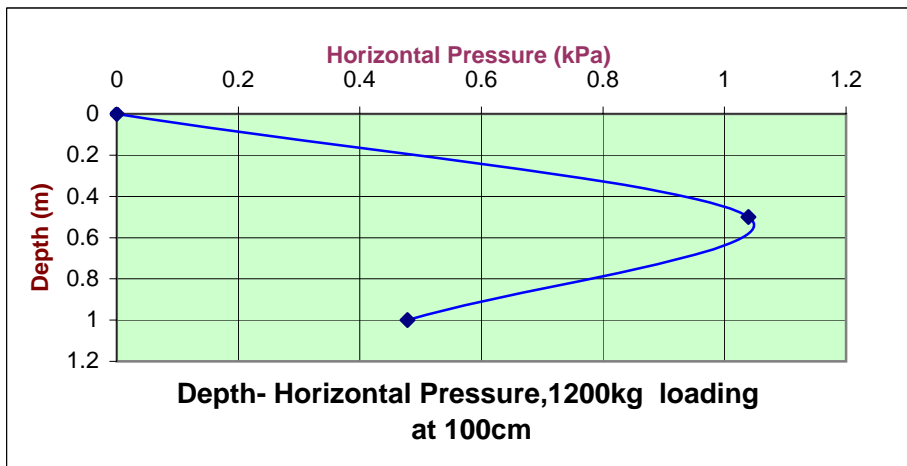
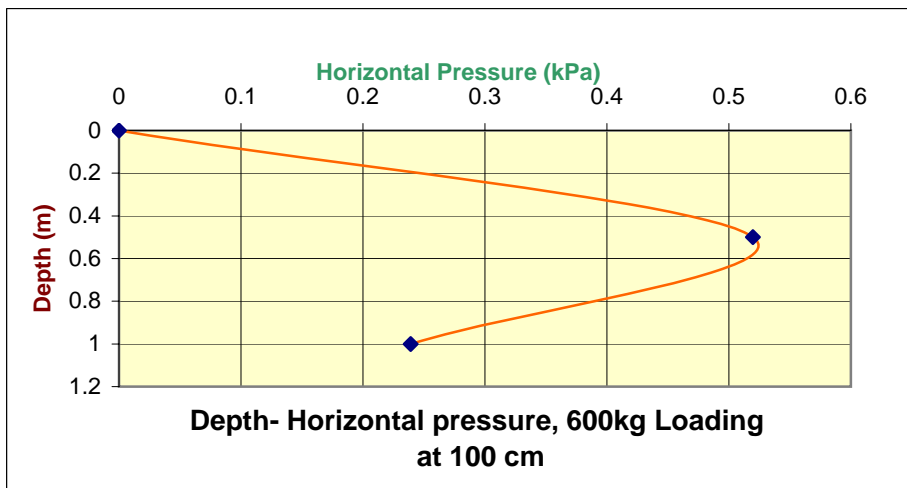
Measurements of Horizontal Pressure, Loading at 100 cm, Medium Case sand

Field Tests

Test No.19
 location: station No. 14+20m,
 20m north of culvert No.64
 Date:29/06/03
 Temp.: 28 C

Type of soil: sand
 Compaction status: Medium Compaction case
 by using steel hand tamper

Depth (m)	Roh (digit)	Calibration Factor (C)	R1h 600kg (digit)	P1h (kPa)	R2h 1200kg (digit)	P2h (kPa)	R3h 1800kg (digit)	P3h (kPa)	R4h 0.0kg (digit)
0				0		0		0	
0.50	8907	0.1299	8903	0.5196	8899	1.0392	8894	1.6887	8903
1.00	8704	0.1196	8702	0.2392	8700	0.4784	8697	0.8372	8703



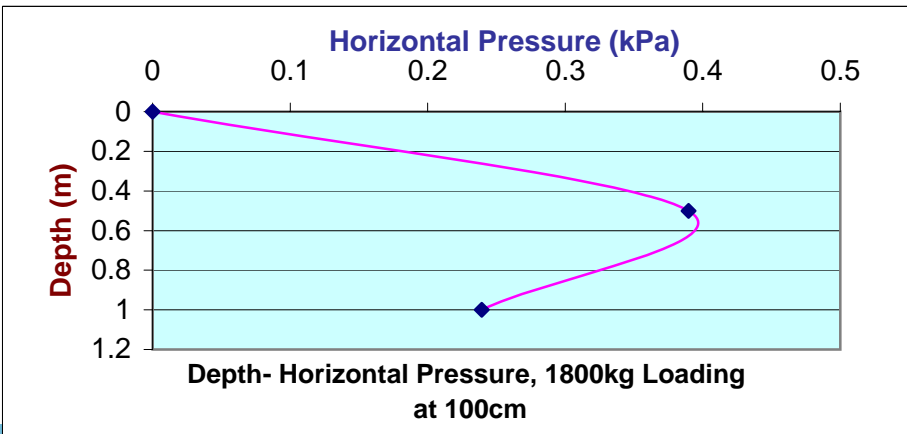
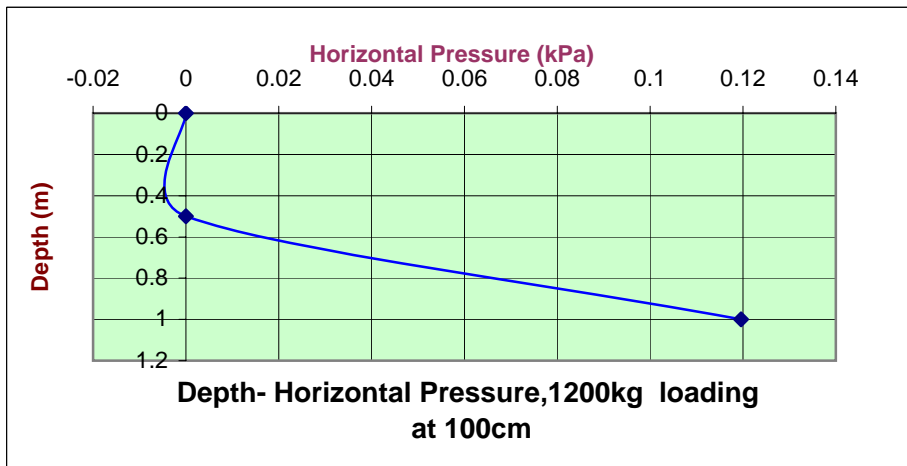
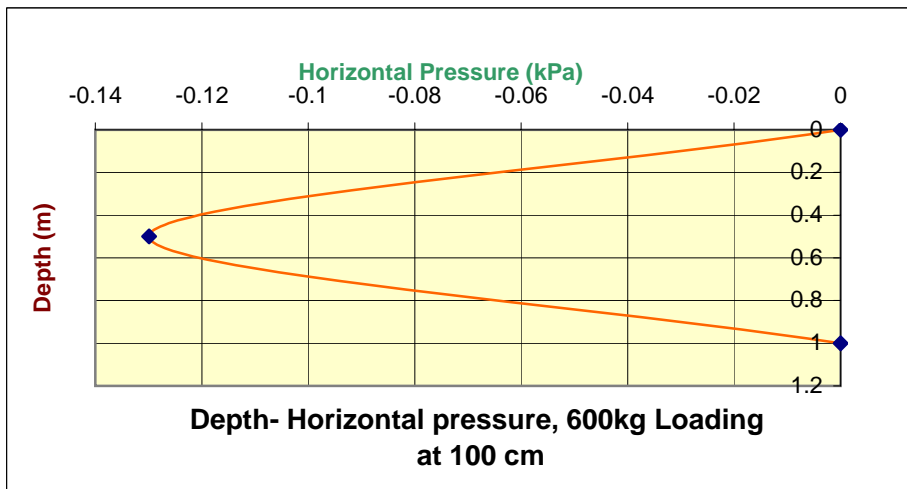
Measurements of Horizontal Pressure, Loading at 150 cm, Medium Case sand

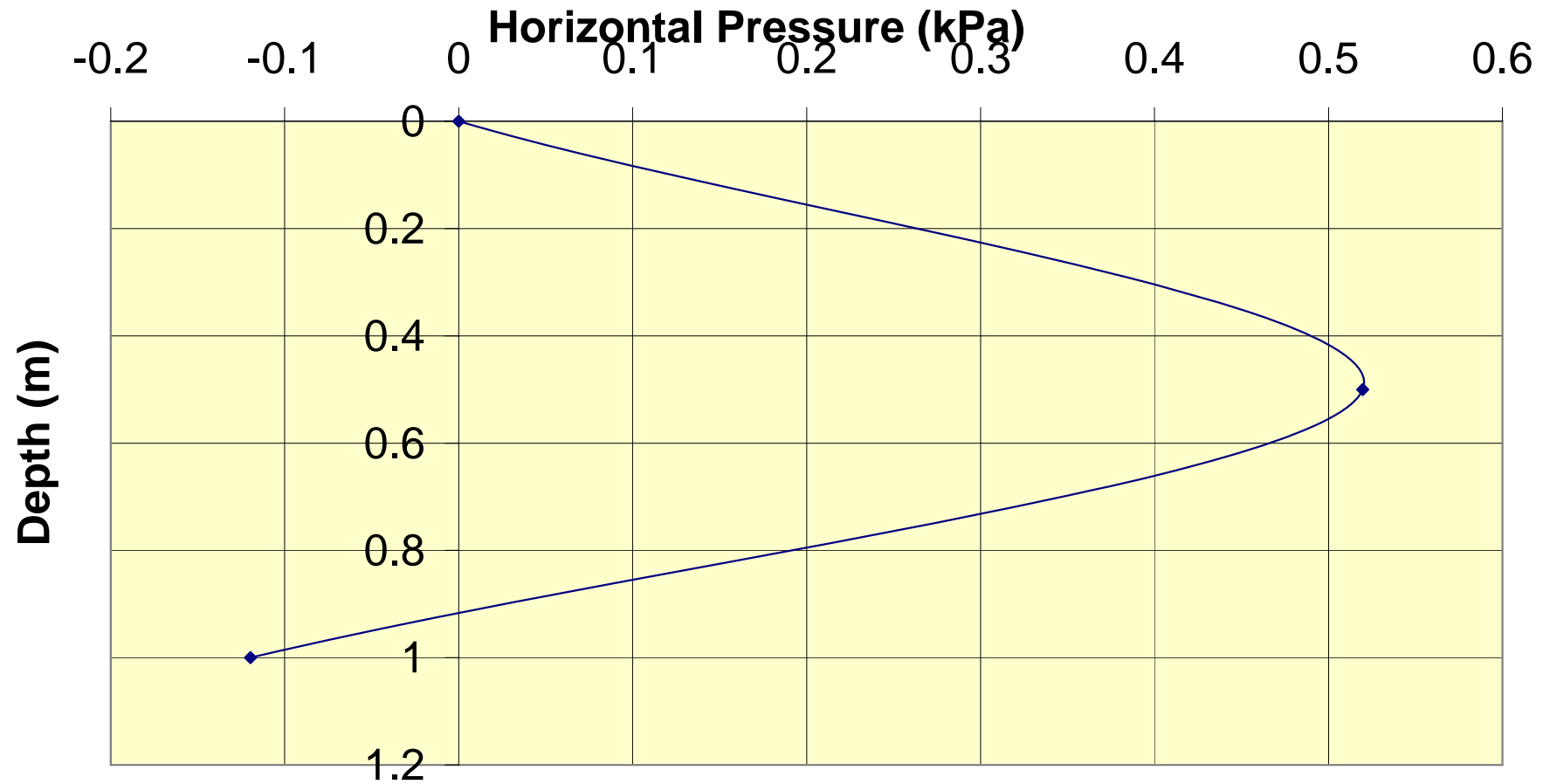
Field Tests

Test No.20
 location: station No. 14+20m,
 20m north of culvert No.64
 Date:29/06/03
 Temp.: 28 C

Type of soil: sand
 Compaction status: Medium Compaction case
 by using steel hand tamper

Depth (m)	Roh (digit)	Calibration Factor (C)	R1h 600kg (digit)	P1h (kPa)	R2h 1200kg (digit)	P2h (kPa)	R3h 1800kg (digit)	P3h (kPa)	R4h 0.0kg (digit)
0				0		0		0	
0.50	8903	0.1299	8904	-0.1299	8903	0	8900	0.3897	8904
1.00	8703	0.1196	8703	0	8702	0.1196	8701	0.2392	8703





Depth- Horizontal pressure, 10 degree slope

Measurements of Horizontal Pressure, Medium Case, Repeated Test

Field Tests

Test No.22

location: station No. 14+20m,

20m north of culvert No.64

Date:30/06/03

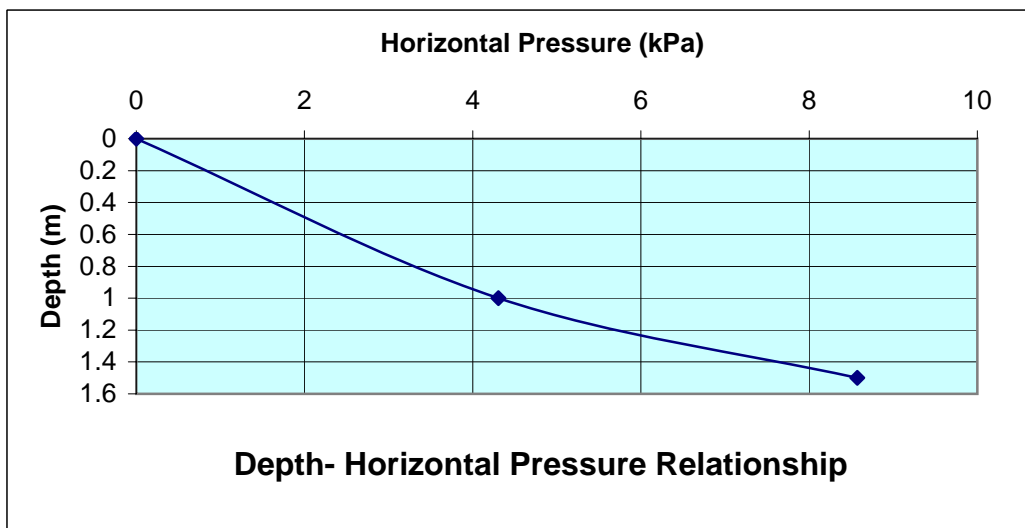
Temp.: 30 C

Type of soil: sand

Compaction status: Medium compaction by

using steel hand tamper

Depth (m)	Roh (digit)	R1h (digit)	Calibration Factor (C)	Ph (kPa)
0				0
1.00	8776	8740	0.1196	4.3056
1.50	8998	8932	0.1299	8.5734



Measurements of Horizontal Pressure, Loading at 25 cm, (Repeated Test)

Medium Compacted sand

Field Tests

Test No.23

location: station No. 14+20m,
20m north of culvert No.64

Date:30/06/03

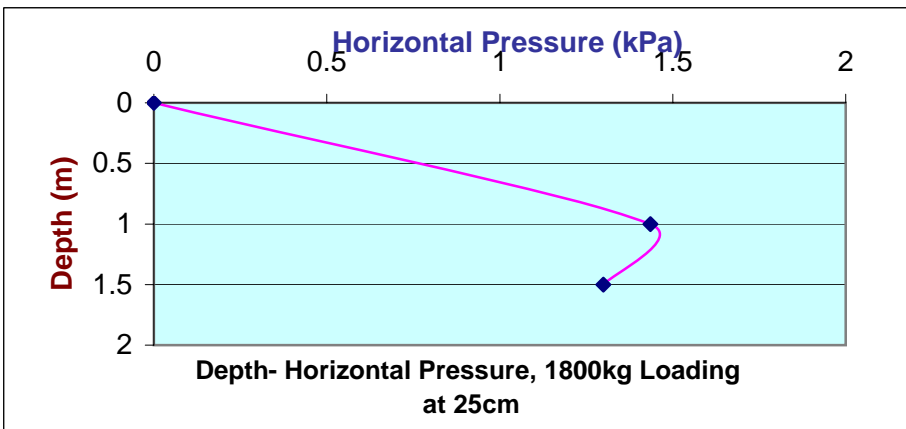
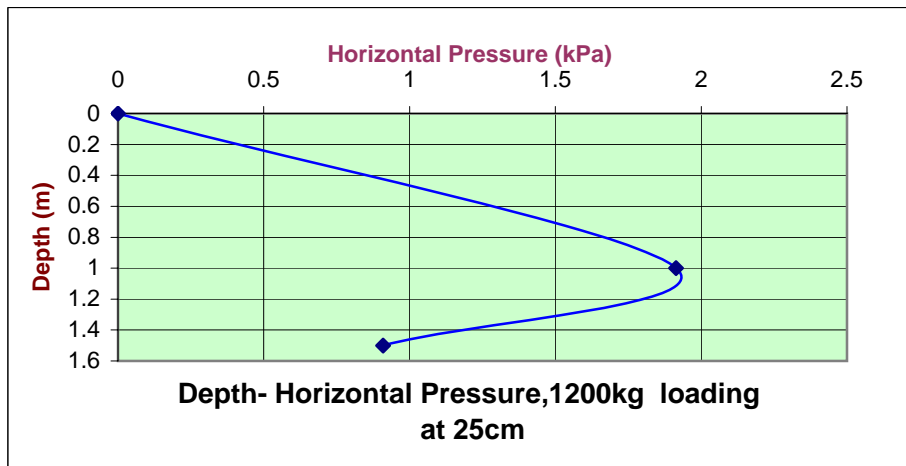
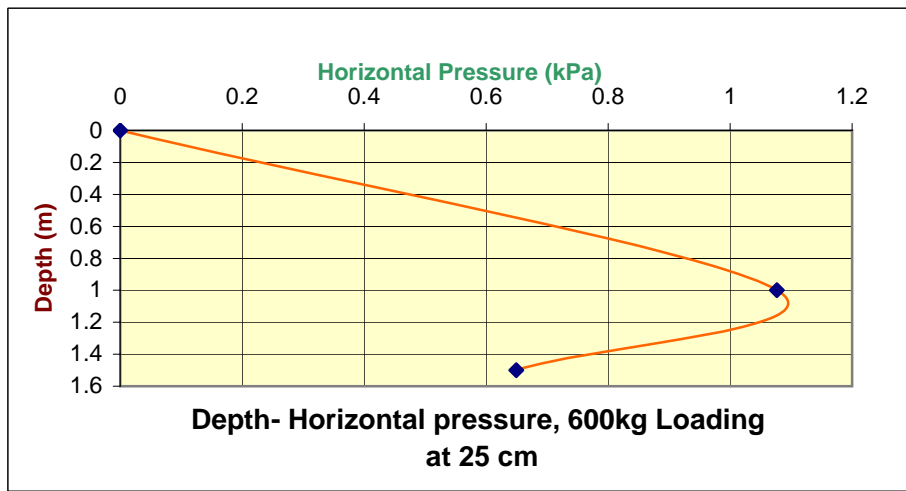
Temp.: 30 C

Type of soil: sand

Compaction status: Medium Compaction case

by using steel hand tamper

Depth (m)	Roh (digit)	Calibration Factor (C)	R1h 600kg (digit)	P1h (kPa)	R2h 1200kg (digit)	P2h (kPa)	R3h 1800kg (digit)	P3h (kPa)	R4h 0.0kg (digit)
0				0		0		0	
1.00	8740	0.1196	8731	1.0764	8724	1.9136	8728	1.4352	8741
1.50	8932	0.1299	8927	0.6495	8925	0.9093	8922	1.299	8931



Measurements of Horizontal Pressure, Loading at 50 cm, Medium Compacted sand, (Repeated Test)

Field Tests

Test No.24

location: station No. 14+20m,
20m north of culvert No.64

Date:30/06/03

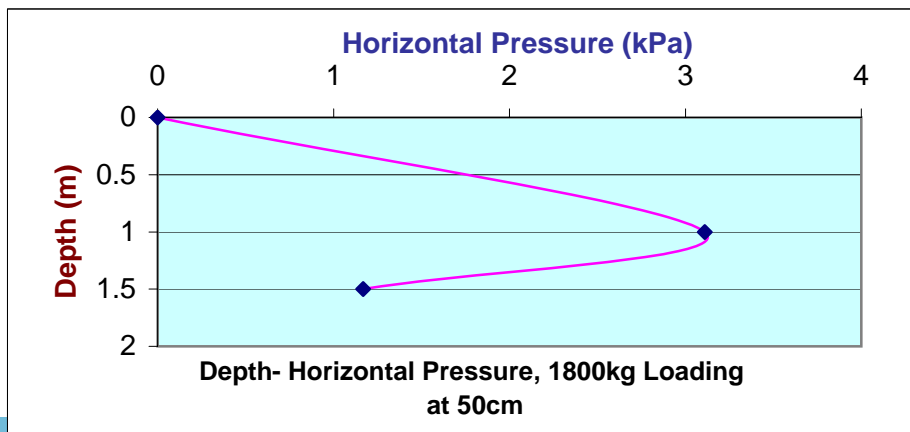
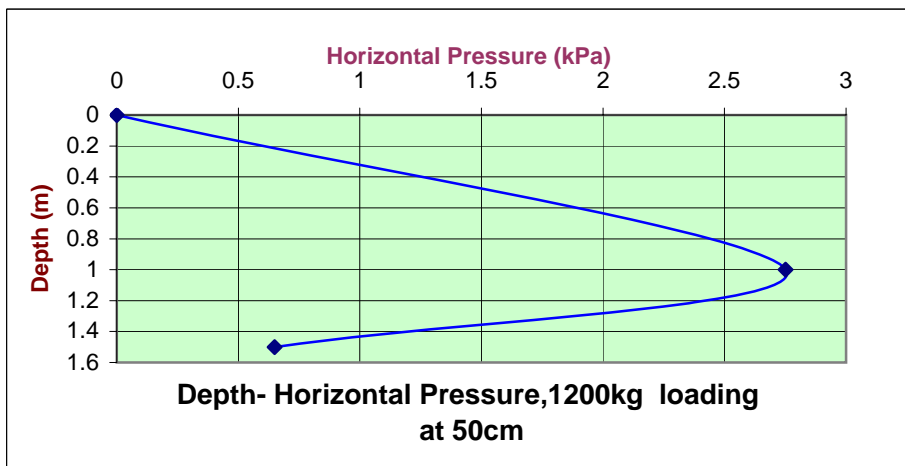
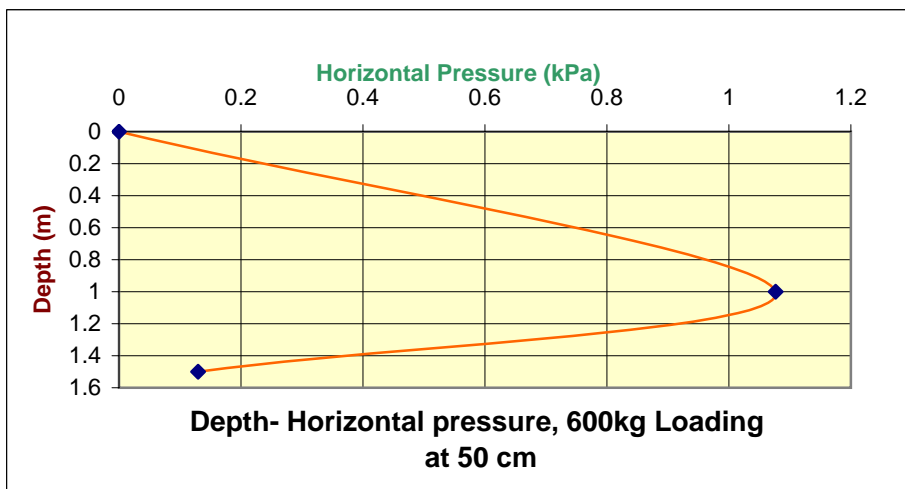
Temp.: 30 C

Type of soil: sand

Compaction status: Medium Compaction case

by using steel hand tamper

Depth (m)	Roh (digit)	Calibration Factor (C)	R1h 600kg (digit)	P1h (kPa)	R2h 1200kg (digit)	P2h (kPa)	R3h 1800kg (digit)	P3h (kPa)	R4h 0.0kg (digit)
0				0		0		0	
1.00	8741	0.1196	8732	1.0764	8718	2.7508	8715	3.1096	8734
1.50	8931	0.1299	8930	0.1299	8926	0.6495	8922	1.1691	8930



Measurements of Horizontal Pressure, Loading at 100 cm, Medium Compacted sand

Field Tests

Test No.25

location: station No. 14+20m,
20m north of culvert No.64

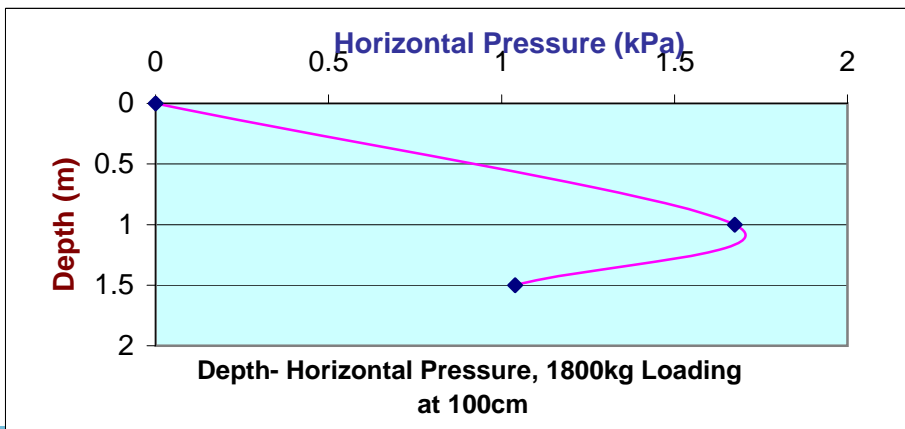
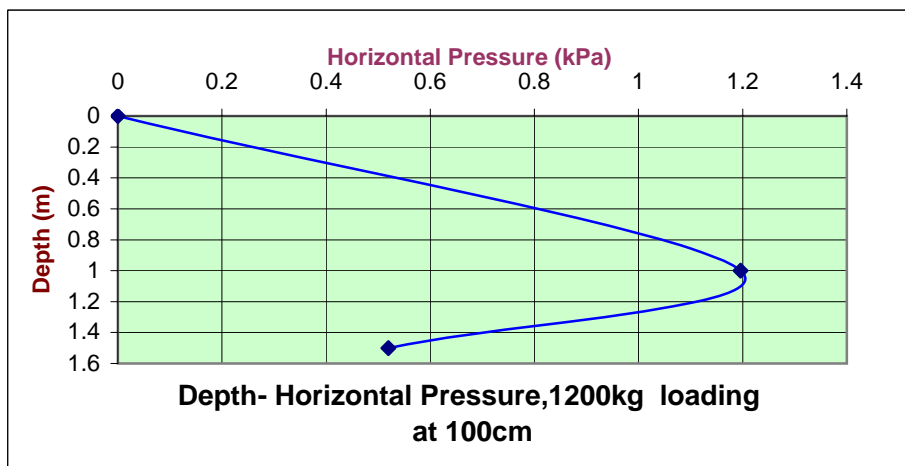
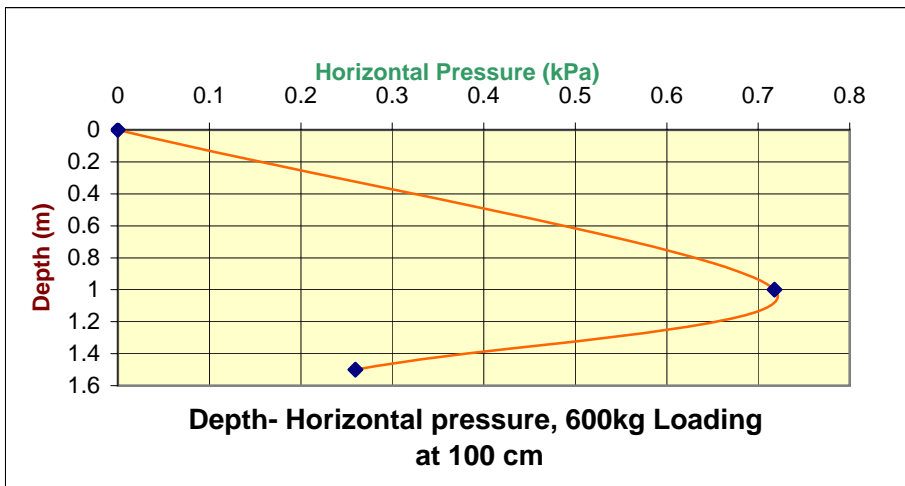
Date:30/06/03

Temp.: 30 C

Type of soil: sand

Compaction status: Medium Compaction case
by using steel hand tamper

Depth (m)	Roh (digit)	Calibration Factor (C)	R1h 600kg (digit)	P1h (kPa)	R2h 1200kg (digit)	P2h (kPa)	R3h 1800kg (digit)	P3h (kPa)	R4h 0.0kg (digit)
0				0		0		0	
1.00	8734	0.1196	8728	0.7176	8724	1.196	8720	1.6744	8728
1.50	8930	0.1299	8928	0.2598	8926	0.5196	8922	1.0392	8927



Measurements of Horizontal Pressure, Loading at 150 cm, Medium Compacted sand

Field Tests

Test No.26

location: station No. 14+20m,
20m north of culvert No.64

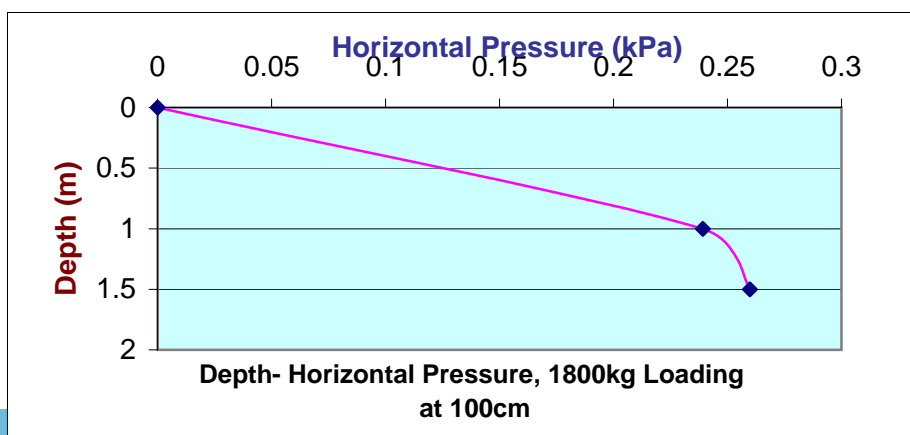
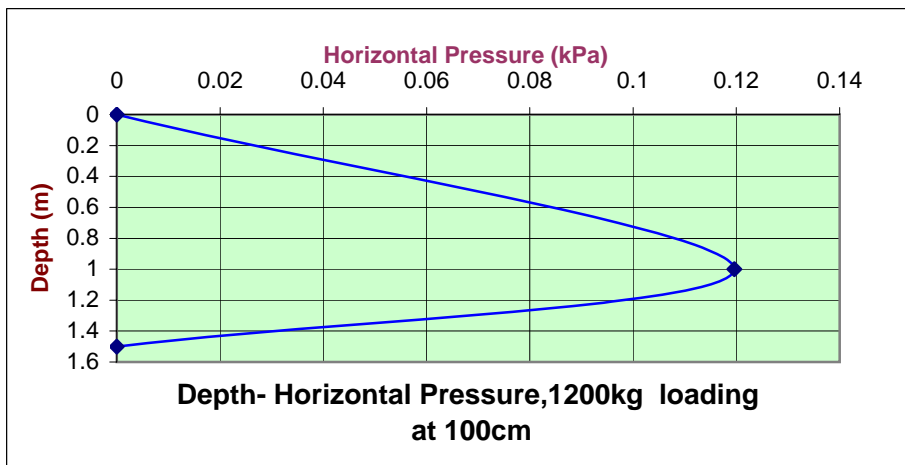
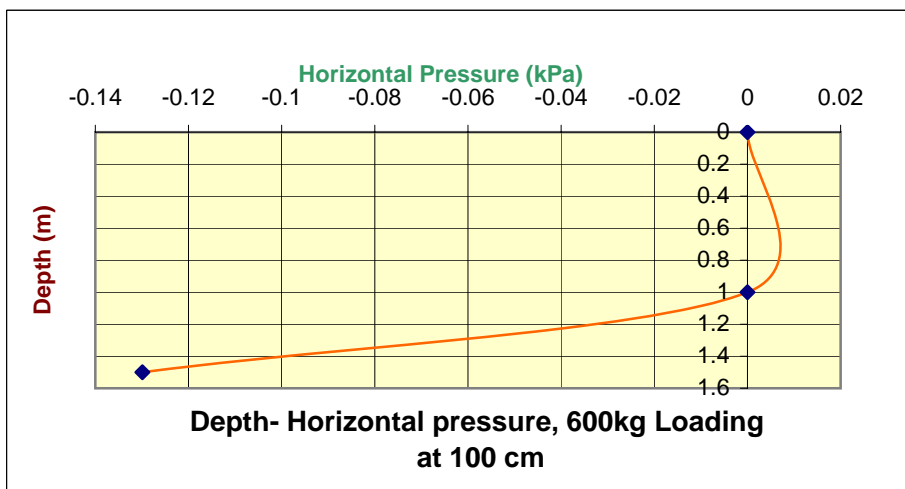
Date:30/06/03

Temp.: 30 C

Type of soil: sand

Compaction status: Medium Compaction case
by using steel hand tamper

Depth (m)	Roh (digit)	Calibration Factor (C)	R1h 600kg (digit)	P1h (kPa)	R2h 1200kg (digit)	P2h (kPa)	R3h 1800kg (digit)	P3h (kPa)	R4h 0.0kg (digit)
0				0		0		0	
1.00	8728	0.1196	8728	0	8727	0.1196	8726	0.2392	8729
1.50	8927	0.1299	8928	-0.1299	8927	0	8925	0.2598	8928



Measurements of Horizontal Pressure, Inclined Case, Medium compacted sand

Field Tests

Test No. 27

location: station No. 14+20m,
20m north of culvert No.64

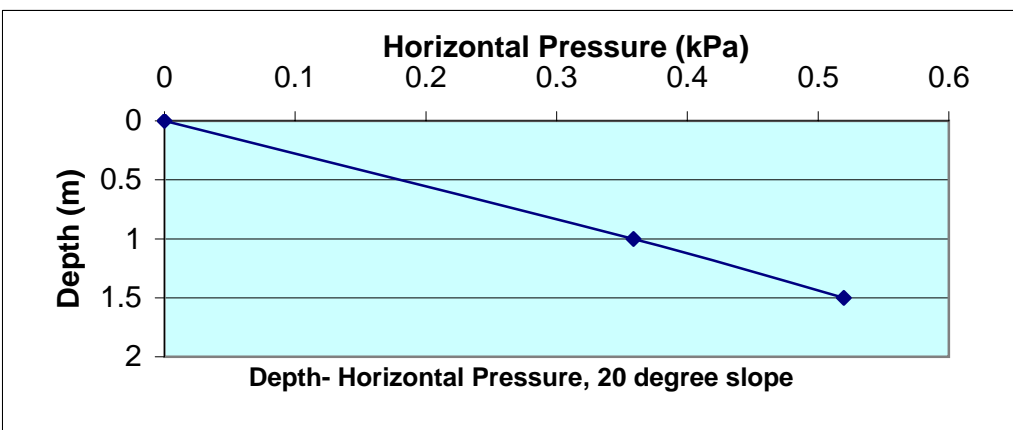
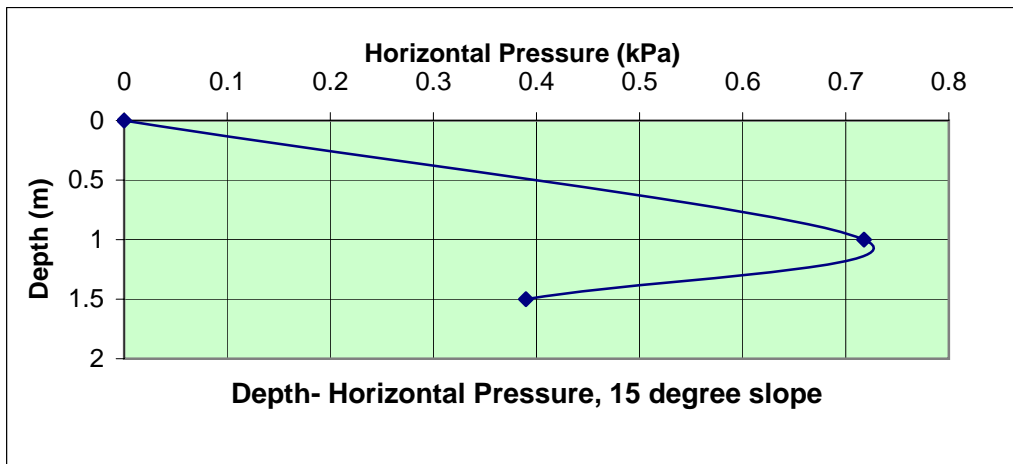
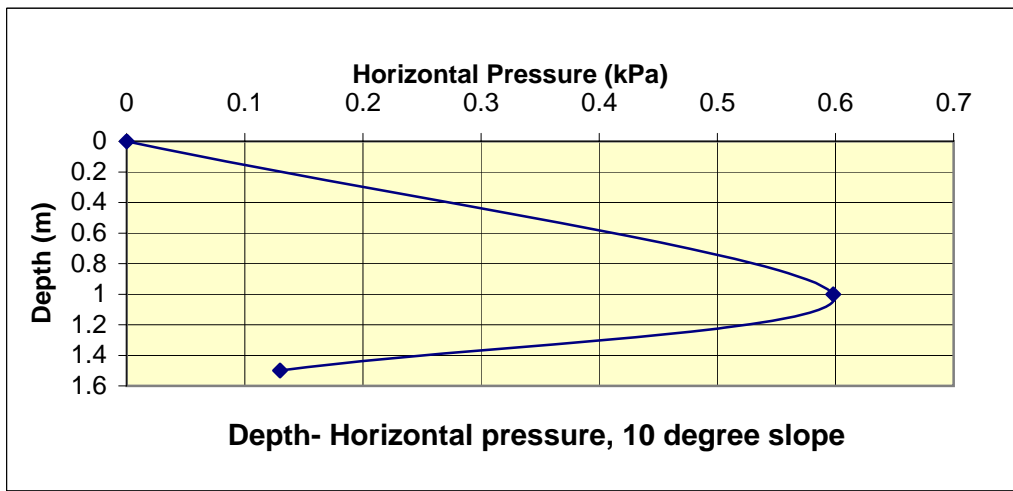
Date:30/06/03

Temp.: 30 C

Type of soil: sand

Compaction status: Medium case by using
steel hand tampe

Depth (m)	Roh (digit)	Calibration Factor (C)	R1h 10 degree (digit)	P1h (kPa)	R2h 15 degree (digit)	P2h (kPa)	R3h 20degree (digit)	P3h (kPa)
0				0		0		0
1.00	8729	0.1196	8724	0.598	8723	0.7176	8726	0.3588
1.50	8928	0.1299	8927	0.1299	8925	0.3897	8924	0.5196



Measurements of Horizontal Pressure, Medium Case, Internal Movement, Loading 25cm, Passive Case

Field Tests

Test No.28

location: station No. 14+20m,
20m north of culvert No.64

Date:30/06/03

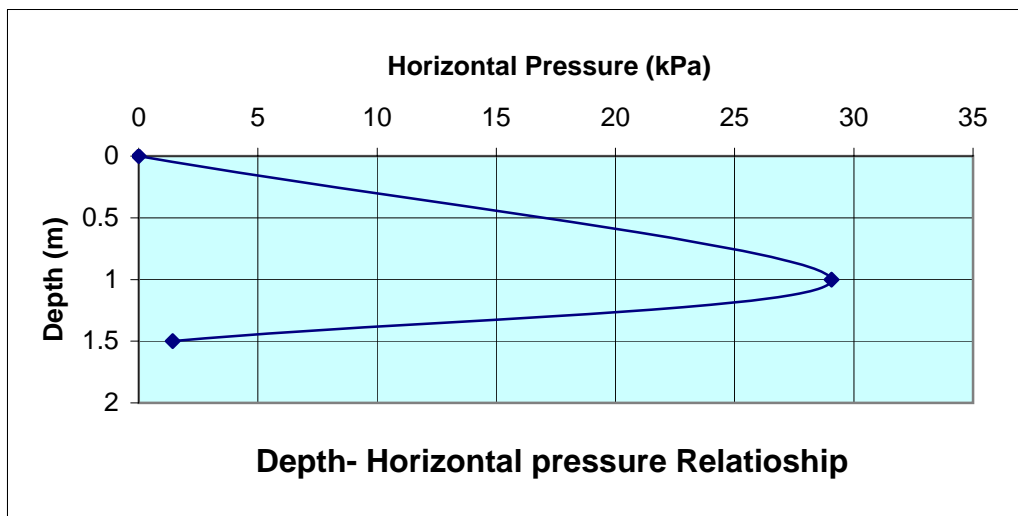
Temp.: 30 C

Type of soil: sand

Compaction status: Medium compaction by
using steel hand tamper

Depth (m)	Roh (digit)	R1h (digit)	Calibration Factor (C)	Ph (kPa)
0				0
1.00	8726	8483	0.1196	29.063
1.50	8927	8916	0.1299	1.4289

Rod (digit)	R1 (digit)	Deformation Factor ©	Deformation (mm)
5094	3799	0.01828	23.6726



APPENDIX (B)

SAND LABORATORY TEST RESULTS, FIELD STUDY

GRAIN SIZE ANALYSIS & LIMITS

CLIENT :	UNRWA م. رفيق عابد	LAB No	1811/03
PROJECT :	EH/PD/-	DATE	23/06/2003
Contract No.	PPD/BC/09/2001	Description:	Dune Sand
		Tested By	A.S

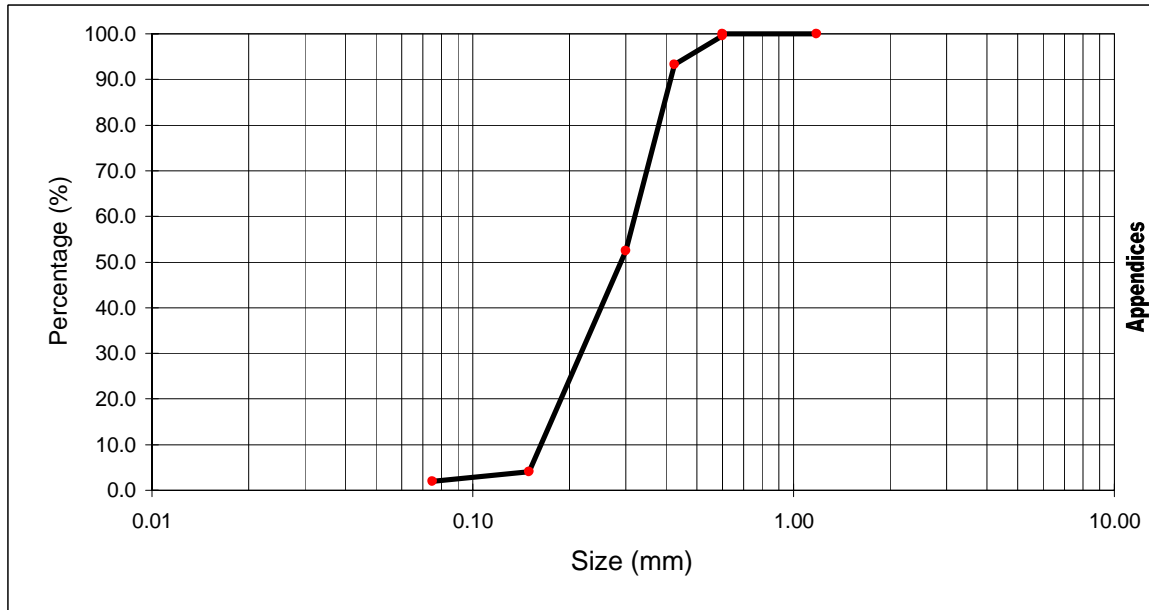
GRAIN SIZE

SIEVE SIZE (mm)	SIEVE #	SAMPLE % Passing
1.18	#16	100.0
0.600	#30	100.0
0.600	#30	99.6
0.425	#40	93.3
0.300	#50	52.4
0.150	#100	4.1
0.075	#200	2.0

ATTERBERG LIMITS

LIQUID LIMIT	NP	-
PLASTIC LIMIT	NP	-
PLASTIC INDEX	NP	-

Specific Gravity | 2.604



ملاحظات :-

هذه النتائج تخص العينات المفحوصة فقط**
لا يجوز اصدار هذا التقرير الا بموافقة خطية من المختبر**

CHECKED BY : M-El.Swaisy

Signature \

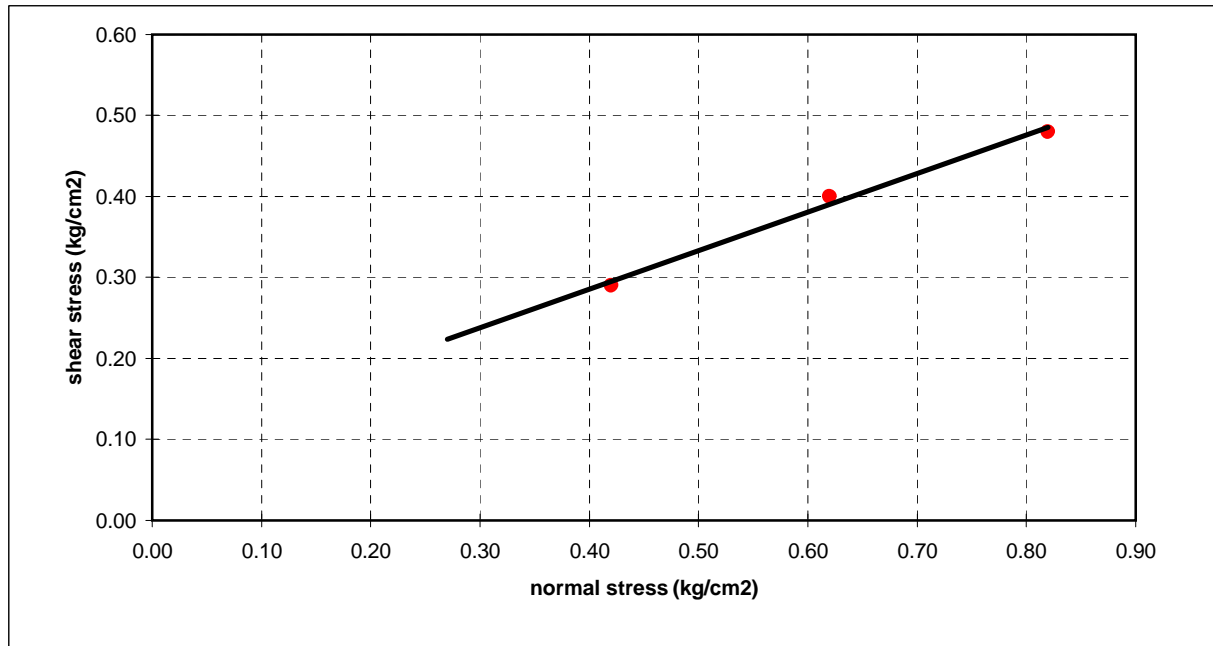
DIRECT SHEAR TEST

PROJECT:	مشروع حماية الشواطئ
CLIENT:	م. رفیق عابد / UNRWA
LOCATION:	GAZA

LAB No	1837/03
DATE	24/06/2003
TEST No :	1

Classification	Yellowish Fine Sand (SP)	
Sample Dry Density(g/cm ³)	1.50	
% water content	4.00%	
Sample Wet Density(g/cm ³)	1.56	
SPECIFIC GRAVITY(GS)	2.60	
Void Ratio (e)	73.3%	

SHEAR STRESS (Kg/cm ²)	0.29	0.40	0.48
NORMAL STRESS (Kg/cm ²)	0.42	0.62	0.82



c (Kg/cm ²)	0.10
F ⁰	25.4

Checked By : A.Hamad

Signature :

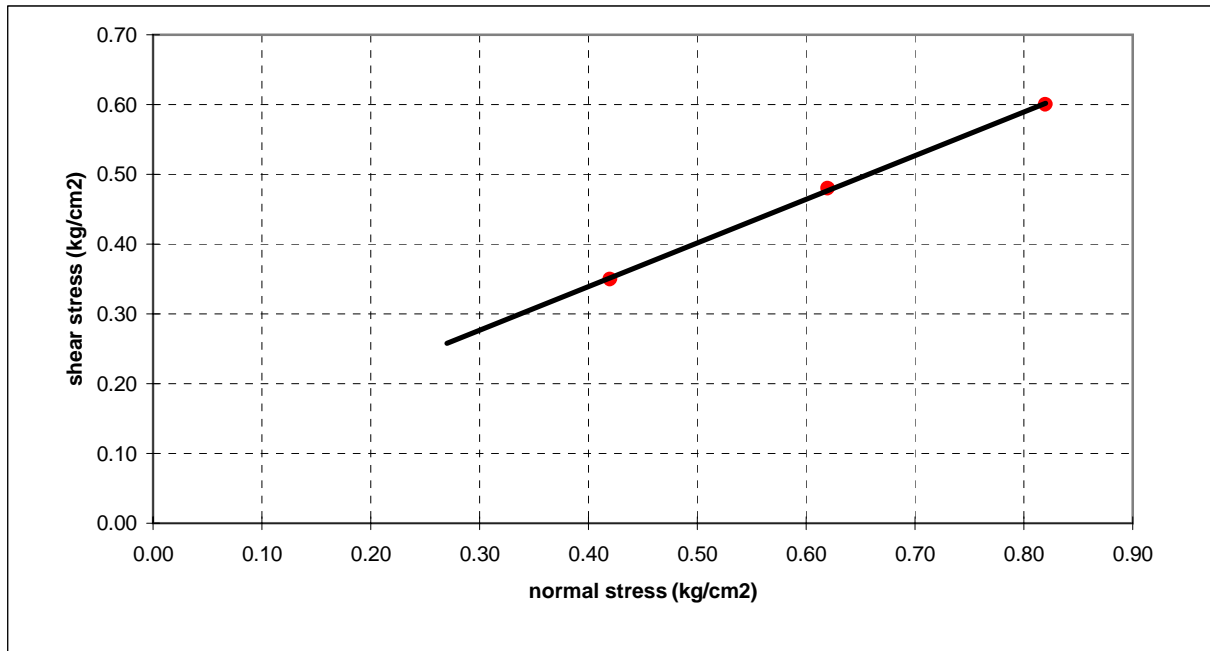
DIRECT SHEAR TEST

PROJECT:	مشروع حماية الشواطئ
CLIENT:	م. رفیق عابد / UNRWA
LOCATION:	GAZA

LAB No	1837/03
DATE	24/06/2003
TEST No :	2

Classification	Yellowish Fine Sand (SP)		
Sample Dry Density(g/cm ³)	1.63		
% water content	4.00%		
Sample Wet Density(g/cm ³)	1.70		
SPECIFIC GRAVITY(GS)	2.60		
Void Ratio (e)	59.5%		

SHEAR STRESS (Kg/cm ²)	0.35	0.48	0.60
NORMAL STRESS (Kg/cm ²)	0.42	0.62	0.82



c (Kg/cm ²)	0.08
F ⁰	32.0

Checked By : A.Hamad

Signature :

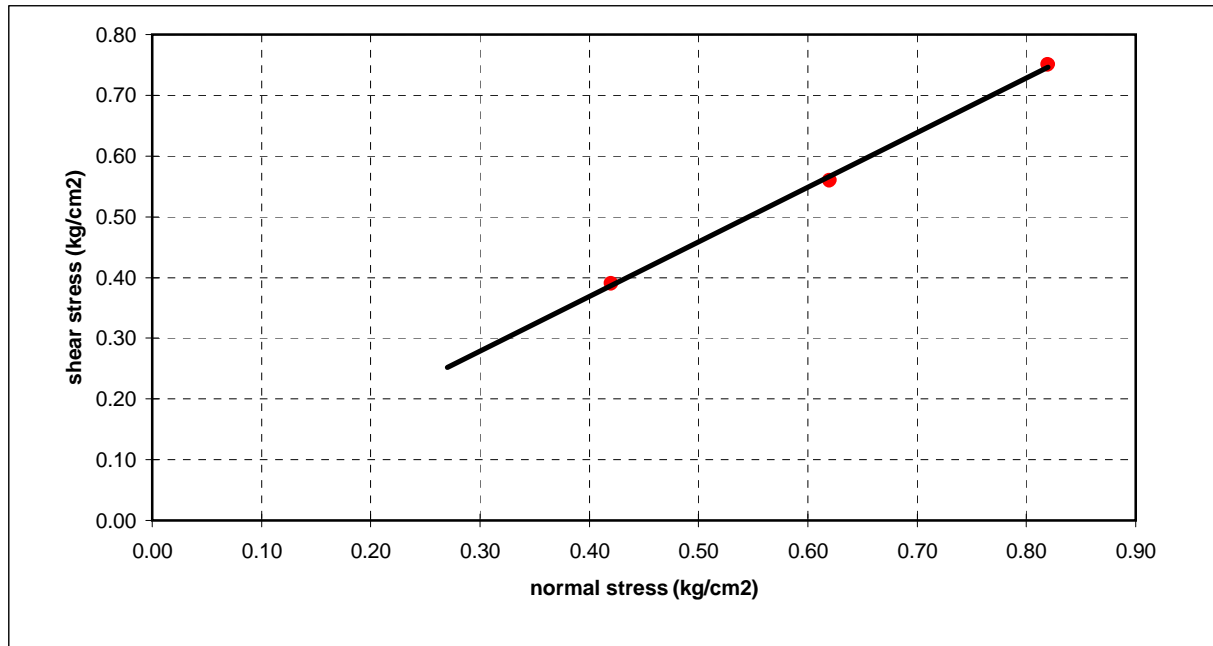
DIRECT SHEAR TEST

PROJECT:	مشروع حماية الشواطئ
CLIENT:	م. رفیق عابد / UNRWA
LOCATION:	GAZA

LAB No	1837/03
DATE	24/06/2003
TEST No :	3

Classification	Yellowish Fine Sand (SP)	
Sample Dry Density(g/cm ³)	1.75	
% water content	4.00%	
Sample Wet Density(g/cm ³)	1.82	
SPECIFIC GRAVITY(GS)	2.60	
Void Ratio (e)	48.6%	

SHEAR STRESS (Kg/cm ²)	0.39	0.56	0.75
NORMAL STRESS (Kg/cm ²)	0.42	0.62	0.82



c (Kg/cm ²)	0.00
F ⁰	42.0

Checked By : A.Hamad

Signature :

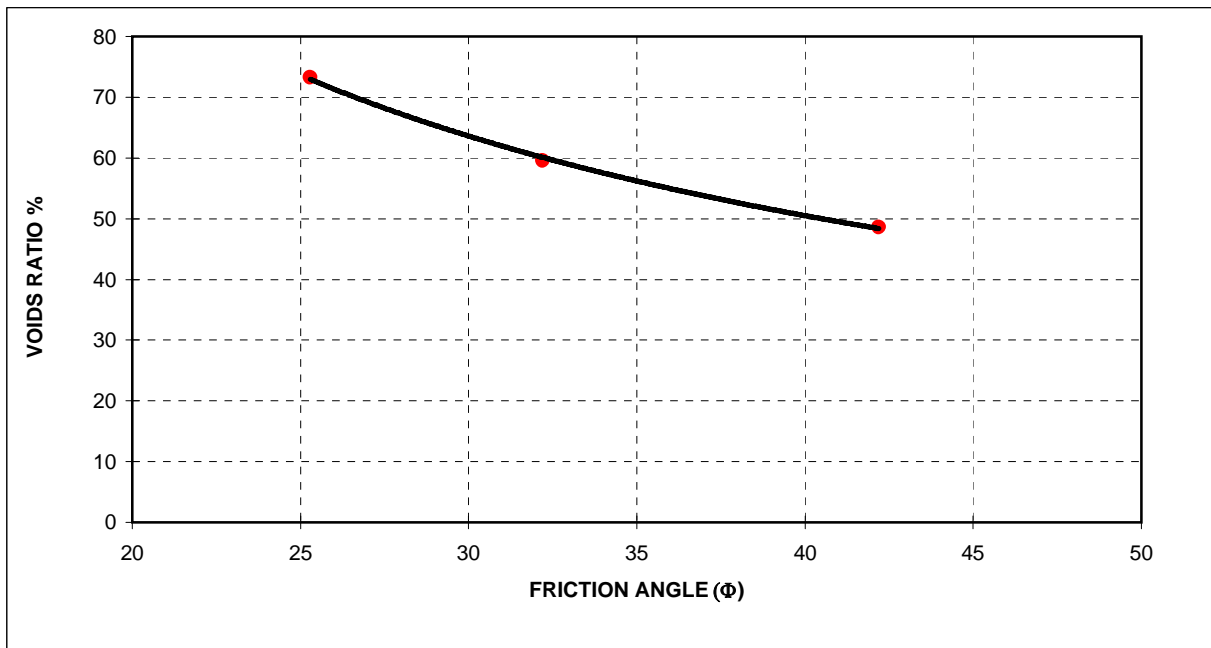
VOIDS RATIO Vs ANGLE OF INTERNAL FRICTION

PROJECT:	مشروع حماية الشواطئ
CLIENT:	م. رفیق عابد / UNRWA
LOCATION:	GAZA

LAB No	1837/03
DATE	24/06/2003
TEST	

Classification	Yellowish Fine Sand (SP)
----------------	--------------------------

VOIDS RATIO	73.30	59.50	48.60
F	25.30	32.20	42.20



Checked By : A.Hamad

Signature :

APPENDIX (C)

INSTRUMENTS CALIBRATION CERTIFICATIONS



48 Spencer Street Lebanon, NH 03766 USA

GK-401 Calibration Data Sheet

Customer: Global Drilling Suppliers, Inc. Job Number: 20809

Calibration Date: June 03, 2003 Calibration Recall June 03, 2004

Calibration Instruction: 403 QALV3 Rev: A

Serial Number: 1303 Calibration Technician Careen Macie

GK-401 Position "A" (period μ s)

Test Box Switch	GK-401 Reading	Frequency Counter	*Percent of Reading Error (< or = 0.1%)
750 Hz	1333.900	1333.181	0.054
1.5 KHz	666.900	666.591	0.046
3.0 KHz	333.500	333.295	0.061

Calibration Standards:

Control Number 011, Calibration recall date: January 13, 2004

This certifies the above named instrument has been calibrated by comparison with standards traceable to the National Institute of Standards and Technology (NIST) in compliance with ANSI/NCSL Z540-1 and is in tolerance as found.

$$\text{*Percent of Reading error} = 1 - \left(\frac{\text{Lower of the Two Readings}}{\text{Higher of the Two Readings}} \right) \times 100\%$$

This certificate shall not be reproduced, except in full, without written permission from Geokon, Inc.

401 cal rev: H

C-1



48 Spencer St. Lebanon, N.H. 03766 USA

Vibrating Wire Displacement Transducer Calibration ReportRange: 100 mmCalibration Date: June 02, 2003Serial Number: 03-9260Temperature: 23.7 °CCal. Std. Control Numbers: 373, 344, 529Technician: KOB

GK-401 Reading Position B

Actual Displacement (mm)	Gage Reading 1st Cycle	Gage Reading 2nd Cycle	Average Gage Reading	Calculated Displacement (Linear)	Error Linear (%FS)	Calculated Displacement (Polynomial)	Error Polynomial (%FS)
0.0	2524	2522	2523	-0.12	-0.12	0.01	0.01
20.0	3625	3624	3625	20.01	0.01	19.98	-0.02
40.0	4724	4723	4724	40.09	0.09	39.98	-0.02
60.0	5821	5820	5821	60.14	0.14	60.03	0.03
80.0	6909	6908	6909	80.03	0.03	80.00	0.00
100.0	7994	7993	7994	99.85	-0.15	99.99	-0.01

(mm) Linear Gage Factor (G): 0.01828 (mm/ digit) Regression Zero: 2530Polynomial Gage Factors: A: 3.44748E-08 B: 0.01791 C: -45.400(inches) Linear Gage Factor (G): 0.0007195 (inches/ digit)Polynomial Gage Factors: A: 1.35727E-09 B: 0.0007052 C: -1.7874Calculated Displacement: Linear, $D = G(R_0 - R_1)$ Polynomial, $D = AR_1^2 + BR_1 + C$

* Refer to manual for temperature correction information.

Function Test at Shipment:GK-401 Pos. B: 5062Temp(T₀): 22.9 °CDate: June 05, 2003

The above instrument was found to be in tolerance in all operating ranges.

The above named instrument has been calibrated by comparison with standards traceable to the NIST, in compliance with ANSI Z540-1.

This report shall not be reproduced except in full without written permission of Geokon Inc.



48 Spencer St. Lebanon, N.H. 03766 USA

Vibrating Wire Pressure Transducer Calibration Report

Type: S Date of Calibration: May 23, 2003
 Serial Number: 03-3620 Temperature: 23.5 °C
 Pressure Range: 350 kPa †Barometric Pressure: 1003.4 mbar
 Cal. Std. Cntrl. #(s): 511, 506, 216, 25167, 524, 529, 403, 018 Technician: FAD

Applied Pressure (kPa)	Gage Reading 1st Cycle	Gage Reading 2nd Cycle	Average Gage Reading	Calculated Pressure (Linear)	Error Linear (%FS)	Calculated Pressure (Polynomial)	Error Polynomial (%FS)
0.000	8843	8844	8844	0.353	0.10	0.247	0.07
70.00	8264	8264	8264	69.66	-0.10	69.69	-0.09
140.0	7677	7677	7677	139.9	-0.04	140.0	0.00
210.0	7092	7091	7092	209.9	-0.03	210.0	-0.01
280.0	6503	6503	6503	280.3	0.07	280.3	0.08
350.0	5920	5920	5920	350.0	0.00	349.8	-0.05

(kPa) Linear Gage Factor (G): 0.1196 (kPa/ digit) Regression Zero: 8846
 Polynomial Gage Factors: A: -1.465E-07 B: -0.1174 C: 1050.1
 Thermal Factor (K): -0.1024 (kPa/ °C)

(psi) Linear Gage Factor (G): 0.01735 (psi/ digit)
 Polynomial Gage Factors: A: -2.12412E-08 B: -0.01703 C: 152.31
 Thermal Factor (K): -0.01485 (psi/ °C)

Calculated Pressures: Linear, $P = G(R_0 - R_1) + K(T_1 - T_0) - (S_1 - S_0)**$
 Polynomial, $P = AR_1^2 + BR_1 + C + K(T_1 - T_0) - (S_1 - S_0)**$
 **Barometric compensation is not required with vented and differential pressure transducers.

Factory Zero Reading:
 GK-401 Pos. B or F(R₀): 8814 Temp(T₀): 23.1 °C †Baro(S₀): 989.9 mbar Date: June 05, 2003

*Initial zero readings must be established in the field following the procedures described in the Instruction Manual. If the Polynomial equation is used the field value of C must be calculated by plugging the initial zero reading into the polynomial equation with the value of P set to zero.

The above instrument was found to be in tolerance in all operating ranges.
 The above named instrument has been calibrated by comparison with standards traceable to the NIST, in compliance with ANSI Z540-1.
 This report shall not be reproduced except in full without written permission of Geokon Inc.



48 Spencer St. Lebanon, N.H. 03766 USA

Vibrating Wire Pressure Transducer Calibration ReportType: SDate of Calibration: May 28, 2003Serial Number: 03-3666Temperature: 23.4 °CPressure Range: 350 kPa†Barometric Pressure: 985.7 mbarCal. Std. Cntrl. #(s): 511, 506, 216, 468, 524, 529, 25167, 018Technician: YAOB

Applied Pressure (kPa)	Gage Reading 1st Cycle	Gage Reading 2nd Cycle	Average Gage Reading	Calculated Pressure (Linear)	Error Linear (%FS)	Calculated Pressure (Polynomial)	Error Polynomial (%FS)
0.000	9064	9064	9064	0.235	0.07	0.042	0.01
70.00	8528	8527	8528	69.93	-0.02	69.90	-0.03
140.0	7990	7990	7990	139.8	-0.07	139.9	-0.03
210.0	7450	7450	7450	209.9	-0.03	210.1	0.02
280.0	6910	6910	6910	280.0	0.01	280.1	0.03
350.0	6371	6370	6371	350.1	0.04	349.9	-0.04

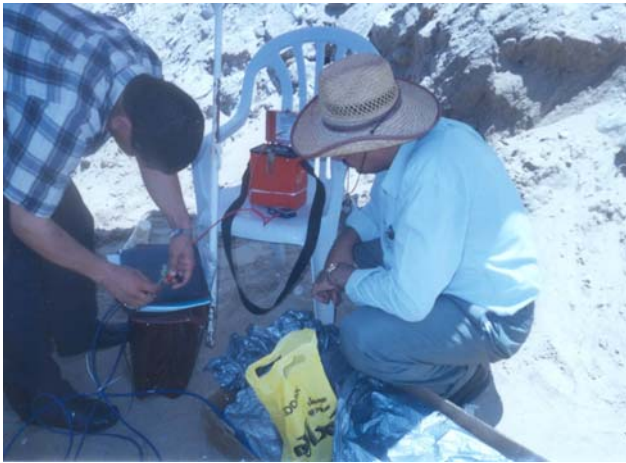
(kPa) Linear Gage Factor (G): 0.1299 (kPa/ digit) Regression Zero: 9066Polynomial Gage Factors: A: -1.998E-07 B: -0.1268 C: 1166.0Thermal Factor (K): -0.11554 (kPa/ °C)(psi) Linear Gage Factor (G): 0.01884 (psi/ digit)Polynomial Gage Factors: A: -2.89722E-08 B: -0.01839 C: 169.11Thermal Factor (K): -0.016758 (psi/ °C)Calculated Pressures: Linear, $P = G(R_0 - R_1) + K(T_1 - T_0) - (S_1 - S_0)**$ Polynomial, $P = AR_1^2 + BR_1 + C + K(T_1 - T_0) - (S_1 - S_0)**$ ***Barometric compensation is not required with vented and differential pressure transducers.***Factory Zero Reading:**GK-401 Pos. B or F(R₀): 9007 Temp(T₀): 23.2 °C †Baro(S₀): 989.9 mbar Date: June 05, 2003

*Initial zero readings must be established in the field following the procedures described in the Instruction Manual. If the Polynomial equation is used the field value of C must be calculated by plugging the initial zero reading into the polynomial equation with the value of P set to zero.

The above instrument was found to be in tolerance in all operating ranges.
 The above named instrument has been calibrated by comparison with standards traceable to the NIST, in compliance with ANSI Z540-1.
 This report shall not be reproduced except in full without written permission of Geokon Inc.

APPENDIX (D)

EXPERIMENTS PHOTOS





APPENDIX (E)

PHOTOS OF EQUIPMENT USED IN GEOTEXTILE TESTS

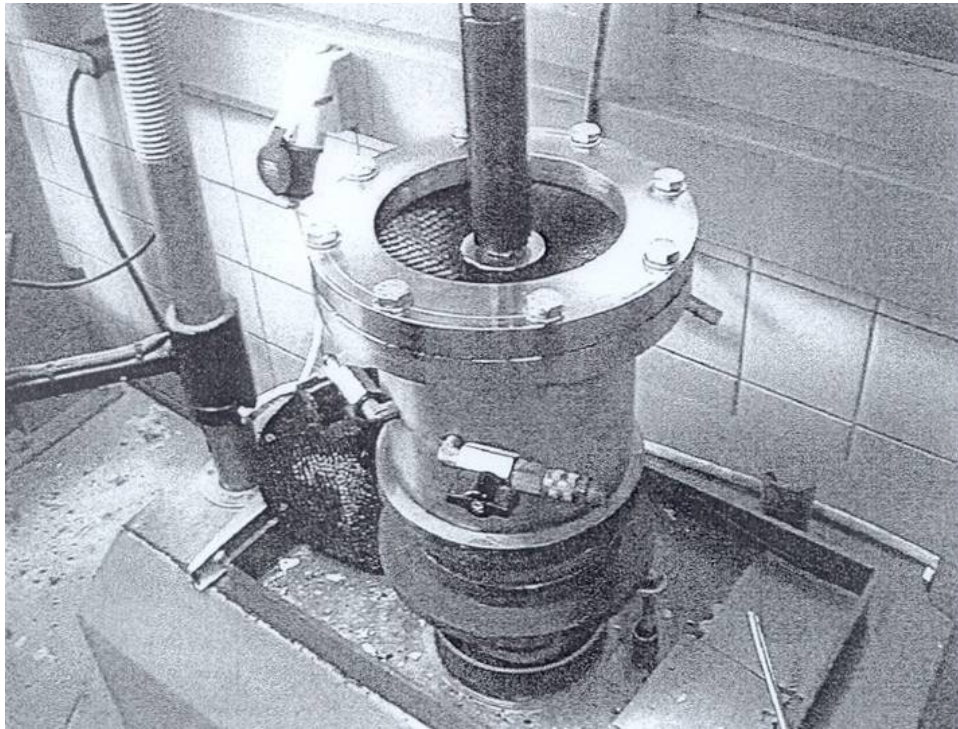


Figure E-3 Geotextile Sample Before Failure

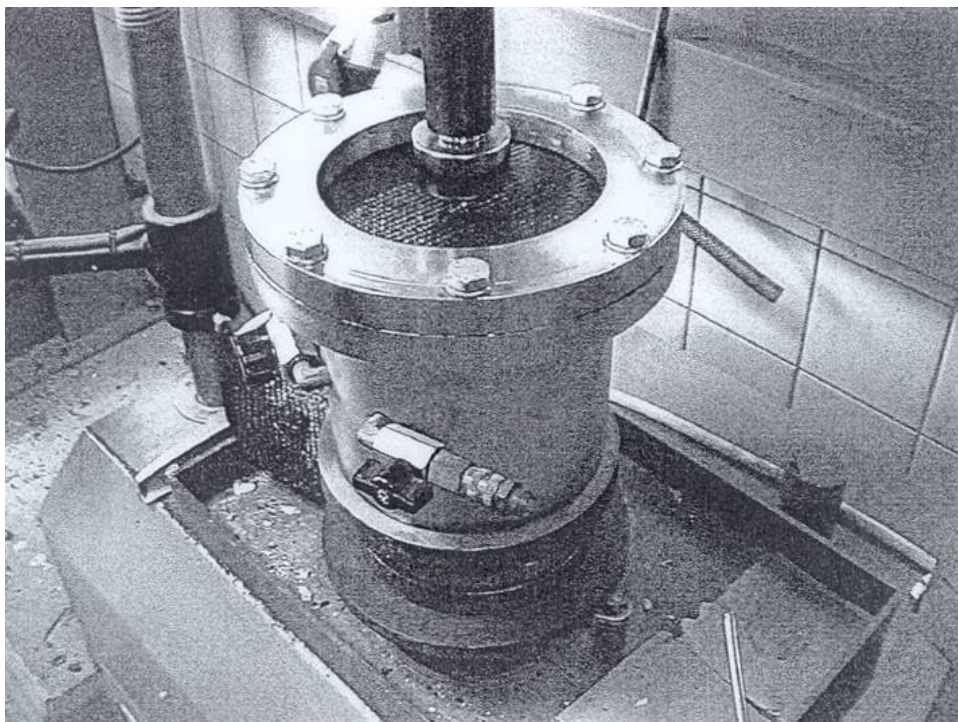


Figure E-4 Geotextile CBR Static Puncture Test

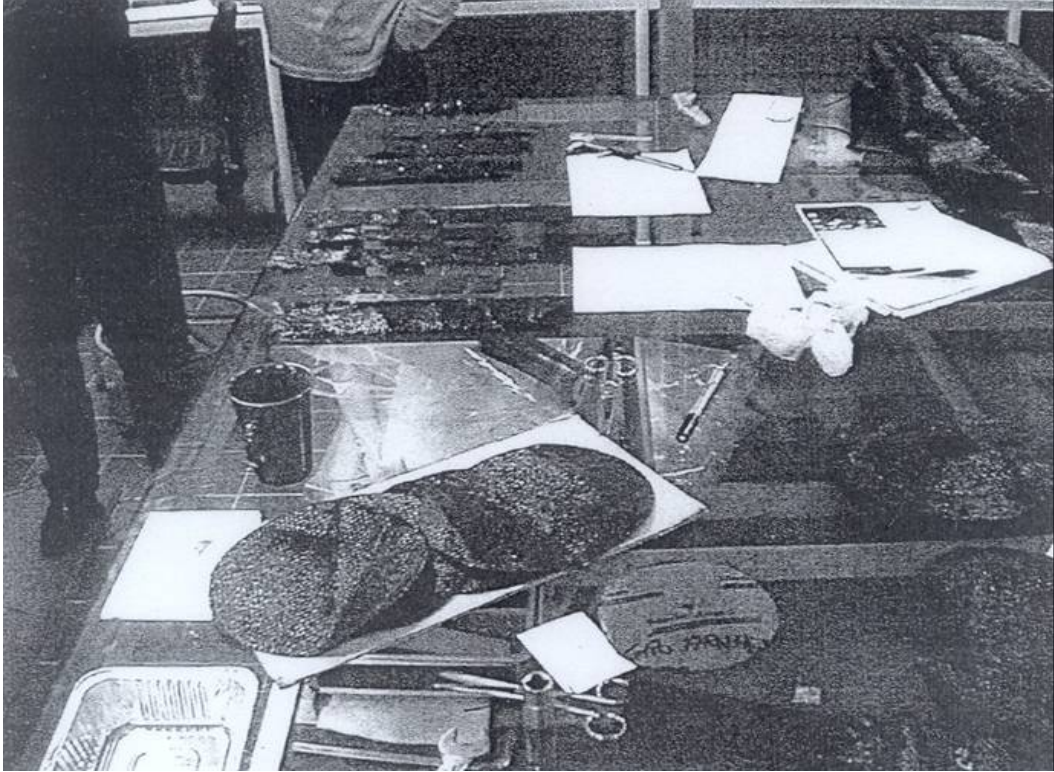


Figure E-1 Preparation of Geotextile Sample in the Laboratory

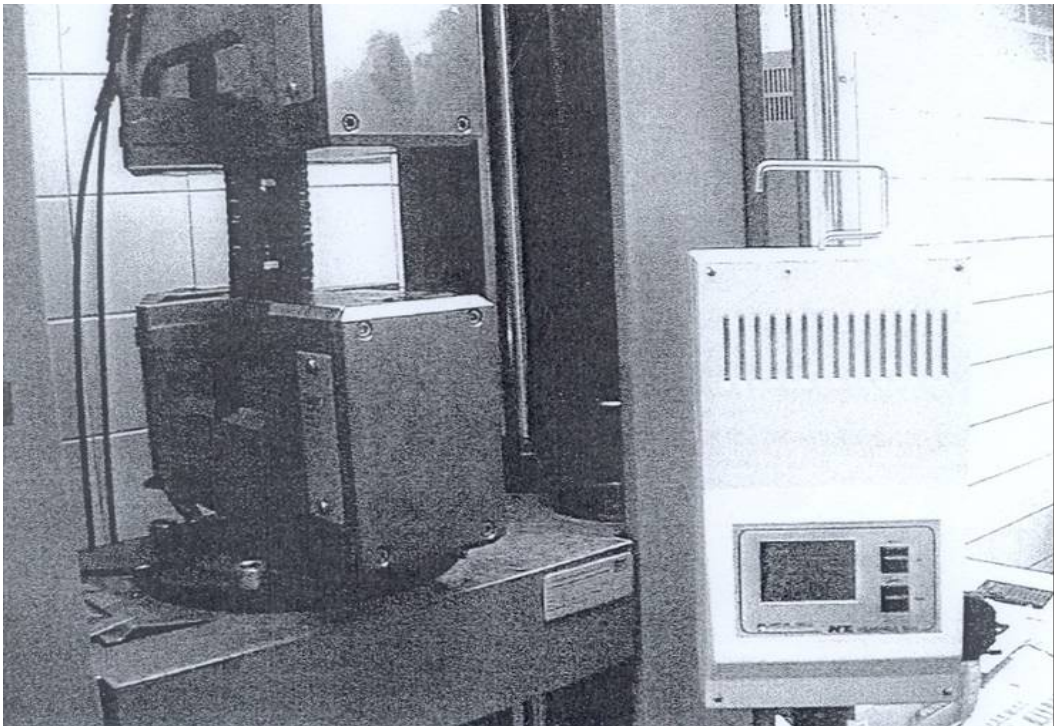


Figure E-2 Geotextile Testing of Tensile Strength

APPENDIX (F)

PROJECT IMPLEMENTATION PHOTOS



